Max-Planck-Institut
für Meteorologie

MAX-PLANCK-GESELLSCHAFT

International Max Planck Research School
on Earth System Modelling

Potentials and Side-Effects of Herbaceous Biomass Plantations for Climate Change Mitigation

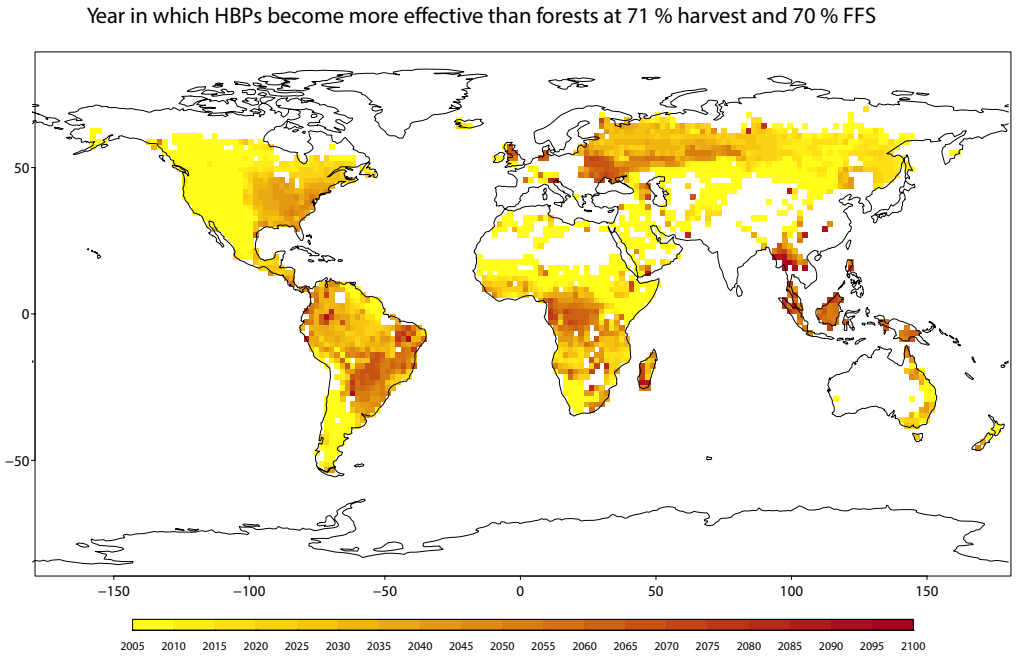

Dorothea Mayer

Hamburg 2017

Berichte zur Erdsystemforschung
Reports on Earth System Science

197
2017

Hinweis

Die Berichte zur Erdsystemforschung werden vom Max-Planck-Institut für Meteorologie in Hamburg in unregelmäßiger Abfolge herausgegeben.

Sie enthalten wissenschaftliche und technische Beiträge, inklusive Dissertationen.

Die Beiträge geben nicht notwendigerweise die Auffassung des Instituts wieder.

Die "Berichte zur Erdsystemforschung" führen die vorherigen Reihen "Reports" und "Examensarbeiten" weiter.

Notice

The Reports on Earth System Science are published by the Max Planck Institute for Meteorology in Hamburg. They appear in irregular intervals.

They contain scientific and technical contributions, including Ph. D. theses.

The Reports do not necessarily reflect the opinion of the Institute.

The "Reports on Earth System Science" continue the former "Reports" and "Examensarbeiten" of the Max Planck Institute.

Anschrift / Address

Max-Planck-Institut für Meteorologie
Bundesstrasse 53
20146 Hamburg
Deutschland

Tel./Phone: +49 (0)40 4 11 73 - 0
Fax: +49 (0)40 4 11 73 - 298

name.surname@mpimet.mpg.de
www.mpimet.mpg.de

Layout

Bettina Diallo and Norbert P. Noreiks
Communication

Copyright

Potentials and Side-Effects of Herbaceous Biomass Plantations for Climate Change Mitigation

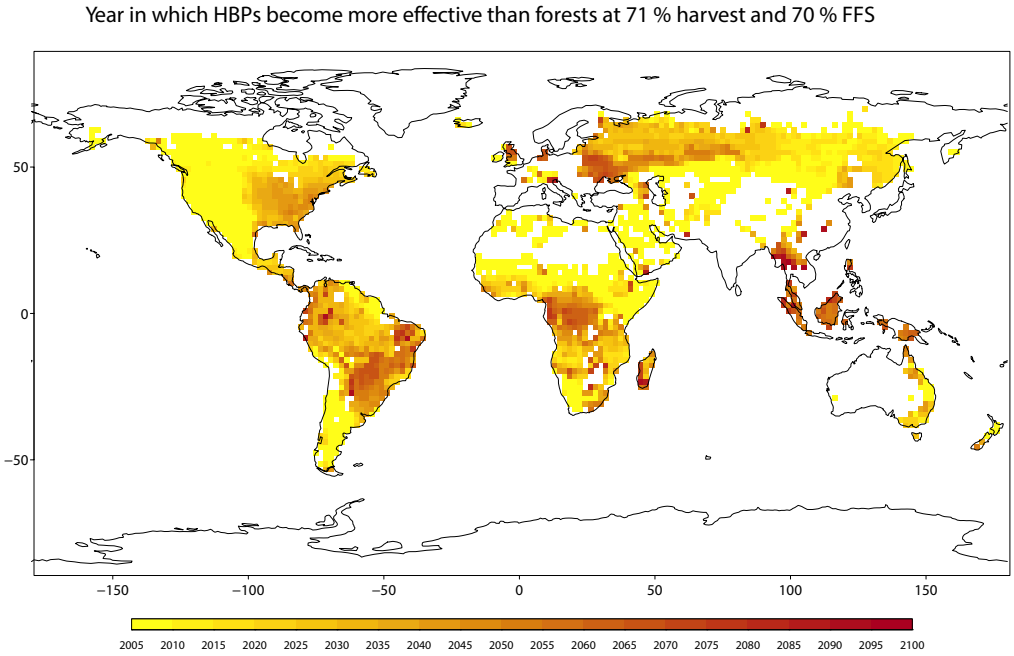

Dissertation with the aim of achieving a doctoral degree
at the Faculty of Mathematics, Informatics and Natural Sciences
Department of Earth Sciences of Universität Hamburg

submitted by

Dorothea Mayer

Hamburg 2017

Dorothea Mayer

Max-Planck-Institut für Meteorologie
Bundesstrasse 53
20146 Hamburg

Tag der Disputation: 05.07.2017

Folgende Gutachter empfehlen die Annahme der Dissertation:

Dr. Julia Pongratz
Prof. Dr. Martin Claußen

Berichte zur Erdsystemforschung / Max-Planck-Institut für Meteorologie 197
Reports on Earth System Science / Max Planck Institute for Meteorology 2017

ISSN 1614-1199

Abstract

Enhancing terrestrial carbon sinks is much discussed as a climate engineering method both in politics and science. The debate focuses mostly on its potential for carbon sequestration and fossil-fuel substitution, whereas effects such as changes in heat and water fluxes are often ignored. Furthermore, many previous studies used idealized scenarios to assess global biomass potentials without considering other ecosystem services. To implement herbaceous biomass plantations in the Max-Planck-Institute Earth System Model, I parametrized a new plant type that reflects the properties of tall, highly productive C4-grasses such as *Miscanthus* and *Panicum* and adapted the model's phenology and carbon cycle to represent the unique characteristics of these plantations. To evaluate the model, I used values found in the literature and compared the model's performance with that of herbaceous biomass plantations in the Lund-Potsdam-Jena managed Land model.

I assessed potentials and side-effects of herbaceous biomass plantations on the climate in a 'plausible' scenario: Based on the representative concentration pathway (RCP) 4.5 which assumes that large areas of agricultural lands are abandoned, I modelled the climatic consequences of using such abandoned croplands for biomass plantations, under an RCP8.5 forcing (high CO_2-emissions). As baseline, I used a scenario previously simulated by Sonntag et al. 2016 which assumes that forests naturally establish on the abandoned areas, leading to substantial carbon uptake by 2100. I compared these two options of land-use-based climate engineering with regards to sequestration potentials and side-effects. Moreover, I examined the relevance of fossil-fuel substitution and assessed the importance of going beyond pure carbon considerations by exploring biogeophysical effects and their potential to offset or enhance impacts of altered CO_2-concentrations on the local or global climate.

My 'plausible' scenario simulated an expansion of herbaceous biomass plantations to 5.6 million square kilometers. Global yields over the 95 years simulated amount to 255-330 PgC. When used for fossil-fuel substitution, they reduce CO_2-concentrations by 70-90 ppm and temperatures by 0.2-0.4°C as compared to the baseline afforestation. Replacing forests with herbaceous biomass plantations not only significantly alters plant carbon stocks but also how these carbon stocks develop over time. Forests respond to CO_2-fertilization more strongly than do herbaceous biomass plantations, so that a replacement reduces the area's sink capacity. At the end of the century, forests would store 114 PgC more than do herbaceous biomass plantations. Nevertheless, with fossil-fuel substitution, herbaceous biomass plantations are simulated to be more effective at sequestering carbon than forests. In many areas, they become more effective than forests quickly, even when considering current technological limits of biomass conversion into fossil-fuels.

Biogeochemical effects dominate the effects on the climate whereas biogeophysical effects are negligible on global and local scales. Only albedo significantly correlates over large regions with the extent of herbaceous biomass plantations. However, changes

were slight and did not affect local temperatures. Significant biogeophysical effects were identified only for components of the water cycle in individual regions such as southeast Brazil. Overall, I conclude that (1) herbaceous biomass plantations can function as a method of climate engineering when deployed globally and if they are established on abandoned croplands, (2) they have larger CO_2-reduction potential than regrowing forests when used for fossil-fuel substitution, (3) side-effects via biogeophysical pathways are small compared to the cooling resulting from carbon sequestration.

Zusammenfassung

Die Ausweitung terrestrischer Kohlenstoffsenken wird sowohl in Politik, als auch in der Wissenschaft als klimaändernde Maßnahme (climate engineering) viel diskutiert. Die Debatte konzentriert sich meistens auf deren Potential zur Kohlenstoffbindung, während Effekte wie zum Beispiel zur Veränderung von Wärmeflüssen und Wasserhaushalt oft ignoriert werden. Darüberhinaus benutzten viele frühere Studien idealisierte Szenarien, um die globalen Biomassepotentiale einzuschätzen ohne andere Leistungen globaler Ökosysteme zu berücksichtigen.
Um grasartige Biomasseplantagen in das Max-Planck-Institute Earth System Modell zu implementieren, habe ich einen neuen Pflanzentyp parametrisiert, welcher die Eigenschaften großer, hochproduktiver C4-Gräser, wie *Miscanthus* und *Panicum*, widerspiegelt und passte die Phänologie und den Kohlenstoffzyklus an die Besonderheiten dieser Plantagen an. Ich evaluierte das Modell mit Literaturwerten und verglich die Modellleistung mit jener der grasartigen Biomasseplantagen des Lund-Potsdam-Jena managed Land Modells.
Die Potentiale und Nebeneffekte grasartiger Biomasseplantagen auf das Klima schätzte ich in einem 'plausiblen' Szenario ab: Große Agrarflächen, welche nach dem Representative Concentration Pathway RCP4.5 aufgegeben werden, benutzt mein Szenario für Biomasseplantagen, wobei diese Landnutzung an die Emissionen des RCP8.5 (hohe Kohlenstoffdioxidemissionen) gekoppelt wurden. Als Vergleichsbasis benutzte ich ein von Sonntag et al. 2016 entwickeltes Szenario, in welchem die gleichen Flächen aufgeforstet werden, was bis 2100 zu erheblicher Kohlenstoffdioxidaufnahme führen würde. Ich verglich diese beiden Möglichkeiten der landnutzungsbasierten Klimabeeinflussung im Hinblick auf deren Kohlenstoffanreicherungspotentiale und möglicher Nebeneffekte. Zudem, schtzte ich den Einfluss der Substitution fossiler Energieträger durch Biomasse aus Biomasseplantagen auf die Kohlenstoffbilanz ab und untersuchte, wie wichtig es ist, über die reine Kohlenstoffkreislaufbetrachtung hinauszugehen, indem ich das Potential biogeophysikalischer Effekte analysierte, den Einfluß geänderter CO_2-Konzentrationen auf das lokale und globale Klima zu verstärken oder abzuschwächen.
Mein 'plausibles' Szenario simulierte eine Expansion grasartiger Biomasseplantagen auf 5.6 Millionen Quadratkilometer. Globale Ernten betrugen 255-330 Pg Kohlenstoff in den 95 Jahren der Simulation. Mit der Ersetzung fossiler Energieträger erzielten grasartige Biomasseplantagen eine Reduktion atmosphärischer Kohlenstoffdioxidkonzentrationen von 70-90 ppm und eine Senkung globaler Temperaturen von 0.2-0.4°C im Vergleich zum Aufforstungsszenario. Der Wechsel von Wäldern zu grasartigen Biomasseplantagen veränderte nicht nur die Pflanzenkohlenstoffbestände, sondern auch wie sich diese Kohlenstoffbestände über die Zeit entwickeln. Wälder reagieren stärker auf Kohlenstoffdioxiddüngung als grasartige Biomasseplantagen, sodass der Austausch die Kohlenstoffsenken der Flächen beeinträchtigte. Ende des Jahrhunderts enthielten Wälder 114 Pg Kohlenstoff mehr als die grasartigen Biomasseplantagen. Trotzdem waren grasartige Biomasseplantagen Dank ihrer Fähigkeit zur Substitution fossiler En-

ergieträger bessere Kohlenstofffänger als Wälder. In vielen Gegenden wurden sie schnell effektiver als Wälder, selbst unter Berücksichtigung unserer derzeitigen technologischen Beschränkungen zur Herstellung von Treibstoffen aus Biomasse.
Biogeochemische Effekte dominieren die Auswirkungen auf das globale und lokale Klima; die biogeophysikalischen Effekte sind vergleichsweise vernachlässigbar. Nur die Reflektivität der Landoberfläche (Albedo) korreliert signifikant mit der Ausdehnung der Biomasseplantagen. Dennoch waren die Änderungen so klein, dass sie die lokalen Temperaturen nicht veränderten. Signifikante Änderungen des Wasserzyklus wurden nur in einzelnen Regionen, wie dem Südosten Brasiliens, festgestellt. Insgesammt schließe ich aus meiner Arbeit, dass (1) grasartige Biomasseplantagen als klimaändernde Maßnahme verwendet werden können, sofern sie auf aufgegebenen Agrarflächen angepflanzt werden, dass (2) sie ein größeres Kohlenstoffsenkungspotenzial haben als Wälder, vorausgesetzt sie werden als Ersatz für fossile Energieträger verwendet und dass (3) Nebeneffekte über biogeophysikalische Wirkungen klein sind, im Vergleich zum Kühlungspotential der Kohlenstoffspeicherung.

Contents

Chapter 1

Introduction

Land-use and land-use change affect land carbon stocks and land surface properties (Bonan, 2008; Pongratz et al., 2009b; Brovkin et al., 2013). These changes influence the climate system. Land ecosystems can both absorb carbon dioxide via photosynthesis and release carbon dioxide via respiration, thereby driving global carbon cycles and altering carbon dioxide concentrations in the atmosphere (Lal, 2004; Arora and Boer, 2010). Land surface properties can alter wind speeds, radiation balance or latent and sensible heat fluxes (Betts, 2001; Brovkin et al., 2006; Bonan, 2008). In this thesis I analyze changes produced by one particular form of land-use change: the large-scale establishment of herbaceous biomass plantations.

Herbaceous biomass plantations consist of highly productive C4-grasses such as members of the genera *Miscanthus* and *Panicum*. Different species and varieties of these perennial grasses grow under most climatic conditions from the inner tropics to the northern temperate regions (Stewart et al., 2009; Zub and Brancourt-Hulmel, 2010; Dougherty et al., 2014). Their uses include fodder and bedding for various grazing livestock as well as feed for coal power plants or as a basis for biogas and biofuel (Frühwirth et al., 2006; McKendry, 2002a,b,c). As technologies for transforming cellulose into biofuels improve, biomass value for fossil-fuel substitution increases (Nussbaumer, 2003). Substituting fossil-fuels by biomass reduces net greenhouse gas emissions, further driving demand for biomass as countries struggle to meet both their rising energy needs and their emissions reduction targets (Clifton-Brown et al., 2004; Heaton et al., 2008). Therefore, many scenarios envisioning the future project expansions of areas used for biomass cultivation throughout the 21st century (van Vuuren et al., 2011b). However, how such large-scale changes in land-use will affect the global and regional climate remains unclear.

Global climate reacts to changes in the Earth's orbit, volcanism, rock weathering as well as changes in carbon dioxide (CO_2) concentrations (Hartmann et al., 2013; Masson-Delmotte et al., 2013). Changes in Earth's orbit and rock weathering act over millenia and are negligible on human timescales. Volcanism acts quickly but its effects usually decline within a few years. Changes in CO_2-concentrations act on timescales of decades

to centuries. Throughout the past century, CO_2-concentrations rose and continue to rise as a result of human activities (Subak et al., 1993; Hartmann et al., 2013; Betts et al., 2016). Three activities have mainly contributed to this rise: fossil-fuel burning, cement production and land-use change (Hartmann et al., 2013). Land-use change emits CO_2 when land-cover types with low carbon densities such as crops or pastures replace carbon rich natural ecosystems such as forests (Pongratz et al., 2009b).
Regional climate additionally reacts to changes in land surface properties (Pongratz et al., 2009a). Topography and vegetation height and density affect wind speeds. Albedo determines the radiation balance at the surface and in the canopy, altering sensible heat fluxes. Evapotranspiration drives latent heat fluxes, cooling the surface and immediate surroundings but warming the atmosphere by increasing concentrations of water vapor, a potent greenhouse gas (Bonan, 2008).
This thesis analyzes the global and regional effects of large-scale herbaceous biomass plantations on the climate. I model the large-scale replacement of crops by biomass plantations using a plausible rather than idealized scenario, in the global Max-Planck Institute Earth System Model (MPI-ESM). The representative concentration pathway RCP 4.5, developed for the coupled model intercomparison project (CMIP), projects large-scale abandonment of agricultural areas as food production intensifies on the most productive soils, diets shift to products with lower carbon footprints and costs of carbon emissions rise (Thomson et al., 2011). I model the climatic consequences of using these abandoned croplands for herbaceous biomass plantations, under an RCP 8.5 emissions forcing (Meinshausen et al., 2011; Riahi et al., 2011). I choose this hybrid between RCP 4.5 and RCP 8.5 for three reasons. First, RCP 8.5 projects the highest increase in anthropogenic greenhouse gas emissions of all RCP scenarios. The high CO_2-concentrations ensure that the reduction produced by drawing-down carbon from the atmosphere is maximized, which helps identify the scope of achievable CO_2-reduction. Second, the land-use projections of RCP 8.5 assume an increase in areas used for food production to feed a rapidly growing population. The remaining forest lands might be used for biomass plantations but this would create an undesirable signal from deforestation. The land-use of the RCP 4.5 provides the large areas necessary for my study in the abandoned croplands. Third, this study builds on a study by Sonntag et al. 2016 in which the same basic scenario setup is used but with the original RCP4.5 land-use left intact. This allows a direct comparison between the effects of afforestation and biomass plantations using the same areas alternatively for afforestation and for biomass plantations. I ask what the net effects of such large-scale changes would be on the regional and global climate.

1.1 Motivation

1.1.1 Increasing carbon dioxide emissions drive climate change

The discovery of fossil-fuels as an energy source spawned an era of unprecedented wealth and comfort for a larger proportion of the global population than ever before. Fossil-fuels release their energy when they are burned. Burning off fossil-fuels in turn emits carbon dioxide (CO_2) as a by-product. The growing demand for energy and associated CO_2-emissions have rapidly increased global CO_2-concentrations in the atmosphere from roughly 280 ppm in pre-industrial times to currently 400 ppm (Subak et al., 1993; Hartmann et al., 2013; Betts et al., 2016).
CO_2, along with other greenhouse gases, such as water vapor and methane, traps heat and energy from the sun or radiated back from Earth and prevents it from escaping into space. This phenomenon warms the troposphere naturally and is necessary to make Earth habitable for humans and most other species. In the past few million years CO_2-concentrations were relatively constant oscillating between 200 and 300 ppm. These oscillations caused changes in global average annual temperatures and all available data indicate that the recent rapid increase in CO_2-concentrations has triggered additional warming (Hartmann et al., 2013). In 2015 average global temperatures were approximately 1°C higher than a century ago (Hansen et al., 2016).
This rapid increase in global temperatures is the most noticeable symptom of global climate change. Higher temperatures increase evaporation from the oceans and evapotranspiration from land ecosystems and change latent and sensible heat fluxes. Recent studies suggest that the atmospheric alterations even change global wind patterns such as jet streams (Seidel et al., 2008).
How these diverse phenomena will affect global weather systems is still unclear. Recent findings suggest they could lead to increased droughts in some areas and flooding in others. Changing weather patterns affect ecosystems on multiple levels and have already led to substantial migrations of various species, while others, unable to either adapt or migrate, have gone extinct (Thomas et al., 2006; Pimm and Joppa, 2015).
Humans depend on ecosystems for their sustenance. Ecosystems provide oxygen, food, raw materials for buildings, and various other appliances and filter pollutants from both air and water. Yet, both land and marine ecosystems are now threatened by rapid climate change. If humans fail to stabilize global CO_2-concentrations, they risk jeopardizing food security and water supplies and losing various other ecosystem services.

1.1.2 Bioenergy: a possible solution?

Using biomass for energy production has been suggested as a climate engineering technique to both reduce CO_2-concentrations in the atmosphere and decrease emissions from fossil sources (Adler et al., 2007). But the many biogeochemical and biogeophysical feedbacks between ecosystems and the atmosphere, many of which are poorly understood, complicate projections about the net effects of large-scale land-use change.

Biomass can substitute fossil-fuels by various means: sugar and oil-rich plants such as sugarcane or oil-seed can be fermented to ethanol or biodiesel to substitute petrol, cellulose and biodegradable waste can be digested to biogas to substitute natural gas and any kind of biomass can be burned to substitute coal. In all cases except the use of biodegradable waste, large areas of farm or forest-land must be dedicated to producing biomass. While merely replacing fossil-fuels by biomass would reduce emissions from fossil sources, the associated large-scale land-use change could increase emissions temporarily. These additional emissions would then first have to be sequestered, before the biomass plantations could truly be effective. Furthermore, land-use change affects other land surface properties especially if diverse natural habitats or conventional agricultural crops and pastures are replaced by dedicated bioenergy crops.

Bioenergy crops differ from other plants. Because of their quick growth and high productivity, they transpire more, altering local water cycles and heat fluxes (Hickman et al., 2010). They regrow from the roots after harvesting, changing carbon and nutrient cycles (Jørgensen, 1997). Biomass grasses affect surface albedo outside the tropics because of their long growing season and the timing of the harvest, in late winter or early spring. The 3 - 4 m high stems dry over the winter masking snow in colder regions (Miller et al., 2015). Any simulation assessing the effects of biomass plantations on the Earth system should account for their physiology.

Several previous studies assess various aspects of large-scale biomass plantations. Studies focusing on economic potentials find that policy incentives aiming at land-based climate mitigation strategies may jeopardize food security as biomass plantations compete for land with food crops (Beringer et al., 2011; Popp et al., 2012; Humpenöder et al., 2014). Conversely, if biomass plantations displace natural ecosystems, these ecosystems emit additional carbon dioxide to the atmosphere, postponing the 'break-even point' at which biomass plantations start sequestering carbon (Melillo et al., 2009; Hughes et al., 2010; Dass, 2013). Regardless, most studies agree that biomass plantations may benefit the climate by substituting fossil-fuels and thus preventing emissions (Clifton-Brown et al., 2004). However, opinions diverge on the scales of this substitution and on how biomass plantations may affect non-carbon related aspects of the climate system. If biomass crops such as wheat replace tropical forests, they increase albedo which should lead to a cooling but decreases in evapotranspiration increase surface temperatures (Hallgren et al., 2012, 2013). If biomass plantations replace temperate or boreal forests, albedo and evapotranspiration both cool the

climate (Georgescu et al., 2011; Hallgren et al., 2013). How these interactions between albedo, evapotranspiration and surface heat fluxes influence local temperatures is still debated.
Beyond their effects on climate, biomass plantations also affect their environment. Evapotranspiration can lead to changes in terrestrial hydrological cycles, changing percolation and runoff (Vanloocke et al., 2010; Le et al., 2011). In addition, both herbaceous and woody biomass plantations would push ecosystems even further away from the natural state than crops currently do (Heck et al., 2016). Such changes impact the surrounding ecosystems and can lead to additional feedbacks to the climate system.

1.1.3 Research questions

All previous studies leave gaps in our understanding of the influences of different land-use types on the climate. None of them compares how herbaceous biomass plantations would affect the climate, if they were established not at the expense of forests or agricultural areas, but on areas that might be abandoned for economic or demographic reasons. No study analyzes biomass plantations in a global land-use scenario, including its feedbacks on the climate, using a global, fully-coupled model. The representative concentration pathway RCP4.5 projects that large areas of agricultural land will be abandoned within the coming century. I intend to compare the effects of two different land-use types planted on these areas and thus close one of the gaps in our understanding of the earth system.
My study aims at presenting a comprehensive picture of potentials and effects of large-scale herbaceous biomass plantations on the climate. In this study I will analyze the consequences of large-scale implementations of herbaceous biomass plantations on the climate in order to resolve the following questions:

- How do different land-uses influence the regional and global climate when implemented on a large scale?
- How large are the effects of fossil-fuel substitution that can be consistently accounted for in a coupled model?
- How do biogeophysical properties of herbaceous biomass plantations affect the climate on local and global scales?

This thesis describes the implementation and evaluation of herbaceous biomass plantations in the Max-Planck-Institute Earth System Model (chapter 2), as well as the results from four fully coupled model simulations with herbaceous biomass plantations using different settings (chapter 3). I compare these simulations with an afforestation baseline simulation described in Sonntag et al. 2016 and the two RCPs from which the hybrid scenario was constructed, RCP4.5 and RCP8.5 (chapters 3 and 5). I also

analyze a simulation designed to isolate biogeophysical effects, to understand how biogeophysical feedbacks of land-use change might affect the Earth system (chapter 4).

1.2 Background

1.2.1 The Earth System

The Earth System contains six basic elements: the atmosphere, the hydrosphere, the cryosphere, the lithosphere, the pedosphere and the biosphere. Each element exchanges matter and energy with the other elements. The atmosphere is composed of the gasses surrounding the Earth. The hydrosphere encompasses all water bodies such as oceans, lakes and rivers but also underground reservoirs of water such as aquifers. The cryosphere contains all perennial bodies of ice. The lithosphere contains all rocks. The pedosphere encompasses all soils and the biosphere encompasses all living organisms.
Energy enters the atmosphere in the form of sunlight and radiates back into space as heat. Sunlight is absorbed by the oceans and the land which can either radiate it back or transfer it as heat to deeper layers. The biosphere uses sunlight to drive various biological processes, the most important of which is photosynthesis conducted by plants and some microorganisms. This process drives the uptake of carbon into the biosphere that is the major source of energy for life on Earth.

1.2.1.1 Global carbon cycle

Carbon cycles through all components of the Earth System (figure 1.1). In the atmosphere, it forms simple gasses such as carbon dioxide or methane. In the ocean, these gasses dissolve in the water, react with ions or are taken up by microorganisms. On land, carbon dioxide is incorporated by plants into living tissues. Both on land and in the ocean, carbon can be mineralized to form sediments, rocks or fossil resources, such as oil, gas or coal. Carbon-containing gasses escape back into the atmosphere through natural processes such as volcanism, wildfires, decaying of organic matter or by humans altering land-use, burning organic matter or fossil-fuels. The processes driving the various fluxes operate at timescales between years and millions of years (Ciais et al., 2013).

Gasses dissolve in ocean water and are released constantly. Currently more carbon flows towards the ocean with a net flux of 2.3±0.7 PgC/a (Hartmann et al., 2013). In the ocean, carbon dioxide reacts with water to form carbonic acid and bicarbonate. This reaction is reversible and can release carbon dioxide to the atmosphere as well as bind it. Carbon dioxide can also be absorbed by phytoplankton via photosynthesis and released via respiration or stored in the organic tissues of microorganisms, plants and animals, which eventually die and sink to the bottom forming sediment layers.

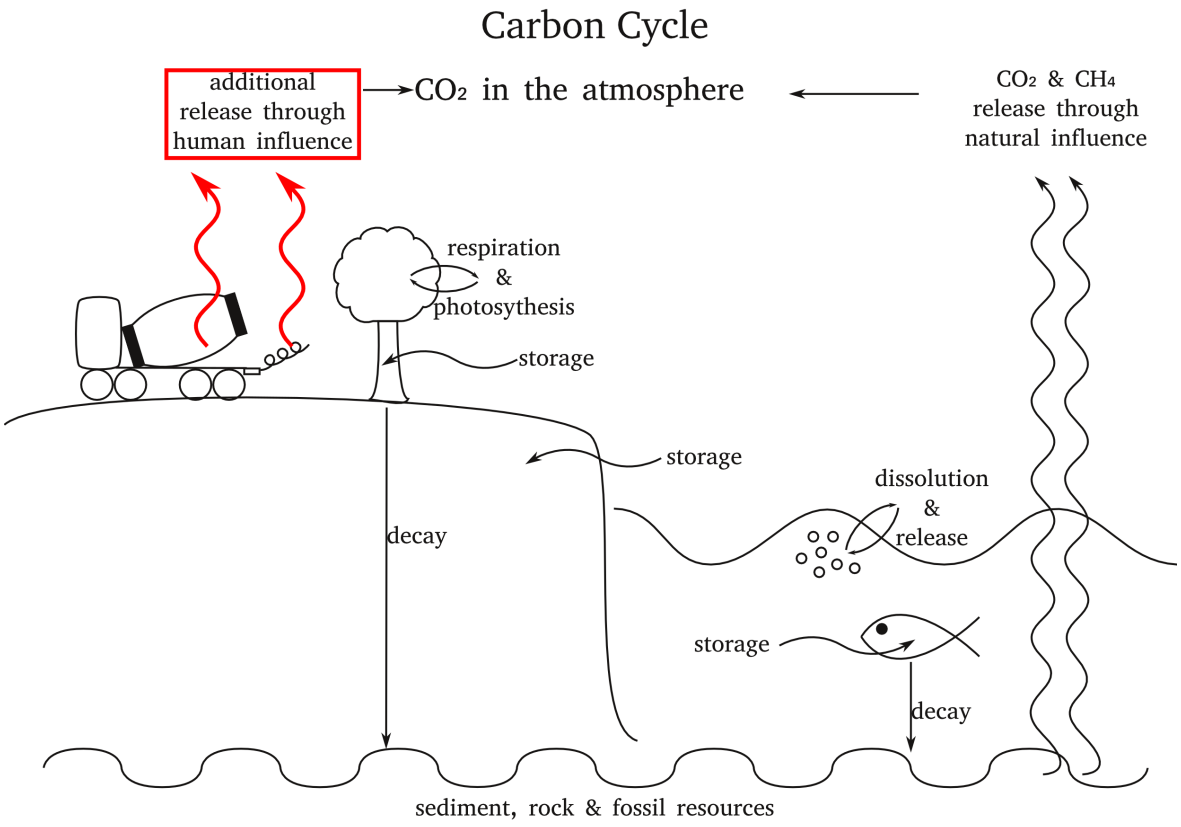

Figure 1.1: Simplified representation of the global carbon cycle, human disturbance is highlighted in red.

Microorganisms can also use bicarbonate to form calcareous shells, releasing carbon dioxide in the process.
Carbon enters the land ecosystems mainly through photosynthesis in land plants and microorganisms (123 PgC/a), although a small amount is bound chemically through rock weathering (0.3 PgC/a, Hartmann et al. 2013). A variety of processes release carbon from the land biosphere. Natural processes include respiration, wildfires and freshwater outgassing. Carbon stored in living organisms enters the soils through roots or when organisms die. In the soils, microorganisms mineralize organic carbon compounds. Both organic and inorganic carbon compounds can be washed out of soils to rivers and the ocean where it accumulates as sediments. Over time, sediments compress to stone, locking carbon in the lithosphere. This carbon can be released through volcanic activity back into the atmosphere.
Under a stable climate, the various carbon compounds and fluxes reach equilibrium where fluxes between pools compensate each other. This equilibrium can be perturbed by natural processes, such as volcanism, or by human activities. Humans upset this balance by altering existing fluxes and introducing additional fluxes. Human activities contribute to the release of carbon from land ecosystems through biomass burning, wood harvest, land-use change, crop production and animal husbandry. In addition, humans alter sedimentation rates by diverting or damming rivers or releasing waste products into freshwater and marine ecosystems. Most importantly, the massive burning of fossil-fuels releases large quantities of carbon dioxide from the lithosphere directly into the atmosphere. This steady input of carbon into the atmosphere alters the climate and influences all other parts of the carbon cycle.
Most plants follow one of two alternative photosynthetic pathways. The C3-pathway binds carbon dioxide in a compound containing 3 carbon atoms at the beginning of the Calvin cycle which produces primary sugars. The C4-pathway binds carbon dioxide in a compound containing 4 carbon atoms which temporarily stores carbon and transports it to the photosynthetically active cells. There, they release carbon dioxide, artificially increasing its concentration. This increases photosynthetic and water-use efficiencies compared to C3-plants. Most C4-plants are grasses (Ehleringer and Cerling, 2002).
Rising carbon dioxide affects C3-plants more than C4-plants. C3-plants are directly dependent on atmospheric carbon dioxide concentrations for their photosynthetic efficiency, while C4-plants artificially regulate the carbon dioxide concentrations in their cells to suit their needs. Thus, when carbon dioxide concentrations increase in the atmosphere, C3-plants respond by increasing their productivity and water-use efficiency. C4-plants respond similarly, but to a lesser degree (Ghannoum et al., 2000). In both C3- and C4-plants photosynthetic efficiency correlates with water use efficiency. Therefore, changing one parameter affects other land-atmosphere interactions.

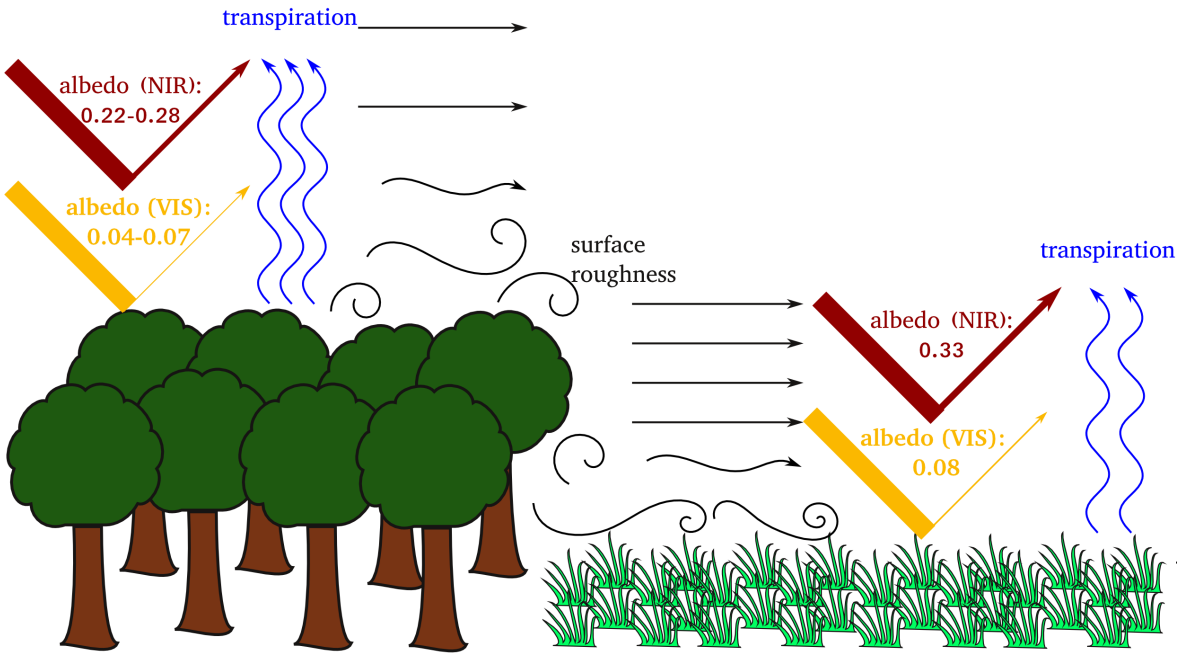

Figure 1.2: Simplified representation of the land-atmosphere interactions. Values for albedo as simulated by JSBACH.

1.2.1.2 Land-atmosphere interactions: plants influence the climate system beyond the carbon cycle

The land surface exchanges energy and water with the atmosphere (figure 1.2). These exchanges depend on the surface type. Surfaces absorb, scatter or reflect sunlight, depending on their reflectivity (albedo) and orientation, directing energy fluxes. Surface roughness slows, channels or diverts airflow, altering wind speeds and directions. Water evaporates, cooling surfaces and transporting heat back into the atmosphere.
Vegetation dominates these exchanges in all but the most barren regions. Surface properties in different regions depend largely on the plant types growing there. Plant types differ in leaf color, texture, orientation and area as well as density and clumping patterns. These properties determine surface roughness and thus influence air flows and wind speeds and directions in the canopy (Vautard et al., 2010). Forests impact surface roughness more than grasses because of their greater height and complex canopies. Thus, forests affect a larger volume of air than grasses and to a greater extent thanks to their more heterogeneous canopies.

Trees also affect albedo, especially in winter when dark branches mask snow while grasses are completely covered by snow producing a homogenous, highly reflective surface. In spring, summer and autumn, canopy structures and densities scatter light. Leaf color, texture and orientation determine albedo and thus light distribution, diffusion and reflection. Leaf absorption and reflectance differs between wavelengths. Leaves reflect far more in the near infrared (NIR) spectrum than in the visible range

(VIS) because the latter drives photosynthesis (Rechid et al., 2009; Schaaf et al., 2002).
Plants influence how water cycles through ecosystems. Canopies intercept precipitation, reducing the amount of water input to soils as some water evaporates directly from the surfaces of leaves. Canopy interception also increases the duration of water input to soils as moisture drips from the leaves long after precipitation has stopped. Roots loosen soils, increasing the soils' capabilities to absorb water. Dense canopies shade soils, cooling them and reducing evaporation from their surface. Simultaneously, extensive root systems absorb water and transport it to the canopies which transpire and transfer it back to the atmosphere. Thus, canopies increase the overall surface area through which water is exchanged with the atmosphere.
Transpiration correlates with the leaf area index of the canopy. Leaf area index expresses total leaf area of the canopy per unit ground area. Leaf area determines the number of stomata which in turn regulate transpiration. Therefore more extensive canopies with higher leaf area index lead to higher transpiration. C4-grasses alter this relationship by increasing their water-use efficiency. This allows them to close or partially close their stomata during hot or dry conditions without losing their capacity to photosynthesize.
Climate change affects all land-atmosphere interactions. Increasing temperatures could lead to increased transpiration while increased carbon dioxide levels could increase water-use efficiency and therefore decrease transpiration, especially under drought conditions. Climate change also affects plant distributions and therefore all aspects related to canopies and root systems. These shifts are particularly conspicuous when forests invade grasslands or grasslands outcompete forests in a certain area.
Humans influence land-atmosphere interactions through land management and land-use change. As with natural ecosystem shifts, land-use change involves changes in the composition and types of plants growing in an area. However, unlike shifts due to climate change, humans adjust land-use according to their needs rather than according to the plants and ecosystems best suited for the local climate. Thus plants and ecosystems fostered by humans often grow under suboptimal conditions or are less well adapted to the environment they grow in, than other plants or ecosystems might be. Thus, human induced changes to ecosystems can feed back into the climate both through land-use change and through the choice of plants favored by land managers.
Urbanization is a special case of land-use change. Urbanization seals soils for roads and buildings and significantly alters energy and water fluxes in and around affected areas. However, in the year 2000 cities only covered 0.5% of the land surface and this fraction is expected to rise to approximately 1.2% of the land surface (Seto et al., 2012). This area is not considered in the CMIP5 version of the MPI-ESM.
Historically, the most extensive land-use change was the conversion of forests and natural grasslands to croplands and pastures (Houghton and Nassikas, 2017). In recent years, while deforestation still dominates in the tropics, other areas are abandoned either because their productivity declined, or because of policies promoting

afforestation and restoration of natural ecosystems. Some areas are also converted to biomass plantations.

1.2.2 Biomass substitutes for fossil-fuels

Fossil-fuels produce energy depending on the type of fuel. Coal burns in power plants generating electricity and heat. Oil burns in the engines of motorized vehicles generating motion. Gas can be used for either of these purposes. Each of these fuels can be substituted by biomass.
Two types of biomass are currently used for energy: organic residues and dedicated crops (Cherubini, 2010). Organic residues can stem from plants or animals. Plant residues can come from harvest byproducts, such as straw from food or feed crops or branches from harvested trees that would otherwise remain on fields or in forests and decay. Plant residue can also come from waste products such as discarded wooden furniture or beams transformed into pellets or any other type of organic waste. Animal residues usually stem from excrement or animal fats, byproducts of animal husbandry and meat production. Dedicated crops are divided into three types: oil-rich, starch- and sugar-rich and lignocellulosic feedstock. Oil-rich seeds directly yield vegetable oils that are converted into biofuels. Starch is broken down into sugar which is converted into ethanol, another biofuel that can substitute mineral oil. Cellulose-rich crops such as trees or grasses can be directly used in conventional coal plants for co-firing. Alternatively, they can be converted to biofuels via the Fischer-Tropsch-process (van Vliet et al., 2009).
Both types of biomass have advantages and drawbacks. Using organic residues reduces wastes and emissions from landfills. In addition, they occur as by-products of conventional industries. Therefore, their production is economical and does not require additional land dedicated to their cultivation. However, their availability is limited by the processes that generate them. Their main drawback is that these waste products often were returned to the land, especially in agriculture and forestry, which contributed to nutrient recycling and carbon input into soils. Dedicated crops often yield more energy than waste products. They are bred specifically for their purpose, decreasing conversion losses. However, dedicated crops block land which could otherwise be used for food or timber production. Their production often involves large quantities of fertilizer, pesticides or other energy-inputs, decreasing their economic and mitigation potentials. In the case of woody biomass plantations, long rotation times can further reduce financial gains.
Lignocellulosic feedstocks outperform other dedicated crops because of their versatility, higher productivity and their ability to grow on marginal or degraded lands unsuitable for food crops. In addition, land-use efficiency increases by 50% for lignocellulosic biofuels compared to sugar- or starch-derived bioethanol (Valles et al., 2014). In particular, herbaceous biomass plantations, such as *Miscanthus* or *Panicum* plantations,

combine high productivity with rapid rotation times, ensuring stable incomes for producers. In addition, these perennial grasses need little to no fertilizer because of their ability to recycle nutrients. Outside the tropics, their stems remain on the fields over the winter, protecting soils from erosion and allowing nutrients to leech back into the soils. This process dries the stems and reduces nitrogen content, increasing the quality of harvested material. Energy inputs are minimized in herbaceous biomass plantations because of their perennial nature. The roots survive and regrow after each harvest. Thus, a single planting event is followed by up to twenty years of harvests (Dufossé et al., 2014).

1.2.3 Biomass in global climate policy

Historically, biomass provided the vast majority of humanity's energy. Fires fueled by wood, peat or dung heated homes and cooked meals. Charcoal burners transformed wood into charcoal for the use of smiths, glass makers and other artisans. During the industrial revolution, fossil-fuels replaced most of this biomass as primary energy source, particularly in industrialized nations. While this generated wealth for oil-rich countries, others became dependent on oil imports.
In 1931, the Brazilian government started encouraging the use of sugarcane-derived ethanol as an additive to gasoline to reduce their dependency on oil imports (Nass et al., 2007). During the oil crisis of the 1970s, many oil importing countries became aware of their own vulnerability and dependence on this finite resource and began searching for alternative energy sources, one of which was biomass. The amount of energy derived from biomass slowly increased from then on (Gennari et al., 2015). Currently, biomass provides 14% of humanity's primary energy. About 75% of biomass provides energy for heating and cooking in developing countries, while the remaining 25% of biomass provides electricity, heat and liquid and gaseous fuels for industrialized nations (Parikka, 2004). For instance, bioethanol use for fuel supplied 2.5% of all transport fuels in 2012 (Nass et al., 2007; Valles et al., 2014). However, total energy produced, approximately 40 EJ/a in 2004, only amounted to 38% of estimated potentials of 100 EJ/a (Parikka, 2004).
As climate change gradually became a more pressing issue, renewable energies found their way into numerous policies meant to limit CO_2-emissions. In an agreement in 2003, the European Union (EU) targeted a share of biofuels in gasoline of 2% until 2005, 5.75% until 2010 and, in 2007, extended their target to 10% until 2020 (Schlegel et al., 2007; Söderberg and Eckerberg, 2013). In 2007, the United States of America (USA) targeted a production of 80 Gl/a of bioethanol from non-grain sources until 2022 (Gelfand et al., 2013). Interestingly, the policy specifically mentions non-grain sources, showing how states strive to balance food security and energy production.
In 2015, the United Nations Climate Change Conference (COP21) negotiated the Paris Agreement which formulates the intent of all member states to limit global average temperature increase to less than 2°C. This target requires substantial decreases of

CO_2-emissions from fossil sources. The Paris Agreement also acknowledges the importance of food security, further enhancing the significance of non-grain sources for biofuels.
Apart from the conflict between food and fuel, biomass production for fossil-fuel substitution may have other consequences on local scales which could make them less attractive to local decision makers. Any change in land-use changes land-atmosphere interactions which ultimately determine local climate, water availability and overall human well-being. Any measures to mitigate climate change will only be implemented if people benefit from them.
In spite of all efforts, studies show that global efforts will likely fail to achieve the 2°C target unless they aggressively reduce their emissions and additionally invest in technologies to mitigate climate change (Gasser et al., 2015). Countries can reduce emissions by further developing and deploying renewable energies. Lignocellulosic biomass, as the most versatile renewable energy, could be deployed on much larger scales than they currently are and thereby substitute larger amounts of fossil-fuels. The impacts of such large-scale changes on the climate may not be as straightforward as they appear. Understanding the multiple feedbacks and possible side-effects of such changes may prevent potentially harmful incentives. A safe way of exploring the effects of land-use policies on the climate is by simulating them in an Earth System Model.

1.2.4 Modeling biomass in an Earth System Model

Earth System Models simulate the various aspects and feedbacks of the Earth System. Their goal is to represent as many exchanges of matter and energy between the different components of the Earth System as possible. Models further understanding of the Earth System and the complex interplay between its parts. Models allow projections into the future and help decision makers envision what different policies might entail.
A fully coupled Earth System Model is particularly useful when attempting to model the effects of large-scale land-use change on the climate. When fully coupled, Earth System Models represent not only land-atmosphere interactions but also the reactions of the ocean. Since the ocean serves as both a large heat and carbon sink and the main source of rainwater on Earth, it can react dynamically and non-linearly to changes in the atmosphere as well as feed its reactions back into the atmosphere from where it can influence the land. Two exchanges are particularly important in this context: carbon and water.
Carbon outgassing from the ocean could potentially offset reductions in fossil-fuel use. During the past century, the ocean has absorbed approximately 48% of anthropogenic emissions (Sabine et al., 2004). These accumulations depend partly on the photosynthetic activities of phytoplankton and partly on the partial pressure difference at the ocean-atmosphere interface. If this pressure difference changes, the ocean could release some of the carbon dioxide it has accumulated partly or totally offsetting any

land-based efforts to reduce greenhouse gas emissions.
Water continuously evaporates from the ocean's surface. The amount depends on the amount of energy available. As temperatures rise, more energy is available and hence more water evaporates from the ocean's surface. More water vapor in the atmosphere leads to more rainfall both on the ocean and on land. Plants rely on precipitation for their existence. Precipitation determines where certain plant types can grow. Changing precipitation regimes can shift the optimal ranges for ecosystems and thus lead to changes in vegetation coverage and type. Thus, increases in precipitation may trigger increases in photosynthetic activity of land-plants that were formerly water limited, enhancing the natural land carbon sink. Such feedbacks from the ocean to the land must be taken into account to determine the full effects of any land-use policy on the climate.

Chapter 2

Implementation of Herbaceous Biomass Plantations into a Global Earth-System Model

2.1 Introduction

Any modeling study begins with adjusting the model to represent the processes under scrutiny. The land component JSBACH of the Max Planck Institute Earth System Model (MPI-ESM) does not contain herbaceous biomass plantations. Therefore, I developed a model for this plant type and included it in the model.
Several previous studies have tried to model herbaceous biomass plantations. Most of these studies used regional models (Clifton-Brown et al., 2004; Vanloocke et al., 2010; Georgescu et al., 2011; Le et al., 2011) or dynamic global vegetation models that do not represent the atmosphere and ocean (Melillo et al., 2009; Beringer et al., 2011; Dass, 2013; Humpenöder et al., 2014; Heck et al., 2016). Hughes et al. 2010 use the C4-grass plant functional type of their vegetation model as an approximation for *Miscanthus*. However, *Miscanthus* and other grasses used for bioenergy production differ greatly from common C4-grasses. For instance, C4-grasses in Hughes et al. 2010 have a leaf area index of 3 m^2/m^2, while *Miscanthus* reportedly can reach levels exceeding 9 m^2/m^2 (Heaton et al., 2008). Leaf area index determines leaf surface area which influences evapotranspiration, surface albedo and roughness, energy fluxes and canopy structure. A generic C4-grass plant functional type, therefore, cannot adequately represent *Miscanthus* if the study aims to examine the effects of herbaceous biomass plantations on the climate.
I model herbaceous biomass plantations using all available literature values to parametrize and evaluate the model. Importantly, values found in the literature, obtained through field measurements, underline the unique characteristics of biomass grasses. I assess the model using available literature values for yields and water use

efficiency, the only variables available for *Miscanthus* and *Panicum* that are not used as input parameters by the model. Yields are emphasized since more data is available for them than for water use efficiency and from a wider variety of climatic zones.
Apart from describing the implementation of herbaceous biomass plantations, this chapter also describes the modification of the land-use scenario. The land-use scenario modifies the original representative concentration pathway, RCP4.5 land-use. In the original RCP4.5 land-use, large areas of agricultural lands are abandoned. These areas then revert to natural lands, such as forests and grasslands. In the modified scenario, all areas which would have reverted to forests are reclaimed for herbaceous biomass plantations. JSBACH models land-use change in its transition scheme. A transition describes a shift from one land-use type to another in a given area. The transition scheme of JSBACH describes the ensemble of all changes between the different land-use types present in a given area. In this chapter, I describe how I modified the transitions scheme to include herbaceous biomass plantations.
Several steps are necessary in order to simulate herbaceous biomass plantations in JSBACH. First, I characterized herbaceous biomass plantations as a separate plant functional type within JSBACH. Second, I adapted the phenology scheme of JSBACH to account for the unique annual cycle of herbaceous biomass plantations. Third, I developed a harvest scheme that enabled carbon storage and simulated 'burning' in a coal power plant. Lastly, I modified the transition scheme of JSBACH to include herbaceous biomass plantations.

2.2 Materials and Methods

2.2.1 The Max Planck Institute Earth System Model, MPI-ESM

The global earth system model MPI-ESM couples the atmospheric general circulation model ECHAM6 (Stevens et al., 2013) with the ocean circulation model MPIOM (Jungclaus et al., 2013). MPIOM includes the ocean biochemistry model HAMOCC5 (Ilyina et al., 2013). ECHAM6 contains the land surface and vegetation model JSBACH (Reick et al., 2013; Schneck et al., 2013). The version used for the original CMIP5 experiments as described by Giorgetta et al. 2013, was modified to represent herbaceous biomass plantations.
In all simulations the atmosphere and the land are resolved with a T63 grid (approximately 1.875×1.875 Gaussian grid), whereas the ocean and ocean biochemistry are resolved with a GR15 grid (approximately 1.5×1.5 horizontal resolution). Vertical resolution consists of 47 layers for the atmosphere (from the surface to 0.01 hPa) and 40 layers for the ocean.
The MPI-ESM includes closed carbon and water cycles. Carbon, water and energy are exchanged between model components via the OASIS coupler (Giorgetta et al.,

2013). Atmospheric carbon dioxide concentrations can be either prescribed or driven by anthropogenic emissions. Emission driven simulations allow carbon dioxide concentrations to adjust in response to feedbacks from the land or ocean.

2.2.2 JSBACH

JSBACH simulates physical and biochemical processes of the land surface. Vegetation is represented by plant functional types (PFTs) organized in a tile-structure. The number of tiles varies depending on initial settings. Surface properties and carbon fluxes are calculated for each tile separately. Tiles are grouped into land-cover types between which land-use transitions occur. Land-use transitions are implemented in accordance with the harmonized land-use scheme developed by Hurtt et al. 2011 (Reick et al., 2013). In addition, natural vegetation types can shift dynamically in response to climatic stimuli (Brovkin et al., 2009).
The land carbon cycle is represented by a series of pools. Carbon enters the plant carbon pools via photosynthesis and leaves via respiration and litter production. Litter pools decompose into the humus pool. Carbon in the litter and humus pools is slowly mineralized and returns to the atmosphere. Whenever the area of a given plant functional type changes due to land-use transitions or dynamic vegetation shifts, the carbon contained in its pools is reallocated to account for the change (Pongratz et al., 2009b; Schneck et al., 2013).

2.2.3 Herbaceous biomass plantations

Miscanthus and *Panicum* naturally grow in a large variety of tropical, subtropical and temperate climates. In plantations, these frost-tolerant C4 grasses can grow far beyond their natural range (Zub and Brancourt-Hulmel, 2010). These perennial plants grow as long as conditions are favorable which can be all year for wet tropical regions. When conditions cease to be favorable (winter, dry season), above-ground biomass dies while roots survive, allowing them to regrow from the roots as soon as conditions improve (Frühwirth et al., 2006; Hansen et al., 2004).
Outside the tropics, farmers harvest herbaceous biomass plantations in late winter/early spring, before the start of the growing season (Frühwirth et al., 2006). During the winter, nutrients leech from the above-ground biomass and return to the soil, reducing the need for fertilizer (Cadoux et al., 2012). There are no reports on how *Miscanthus* and *Panicum* are managed in the tropics.

2.2.4 Literature review and model evaluation

2.2.4.1 Yield data

Due to their economic potential, many studies have analyzed yield potentials of herbaceous biomass plantations. They focus on different species of the genera *Miscanthus* and *Panicum*. All studies used for model evaluation are listed in table 2.1 along with the mean yields they report. Citations were checked to prevent the same data from being used twice.
For the evaluation, studies were grouped by country or, for larger countries, by state, region or province. Yields were averaged over all available yields and all reported treatments, such as planting density, cultivar choice, fertilization or irrigation input. Averages over several years and larger areas reduce biases resulting from local conditions (soil, microclimate) or specific weather conditions (drought, rainy growing season). Averages over different cultivars, species and genera reduce biases resulting from species-specific growing preferences. Averages over different treatments reduce biases resulting from the choice of cultivation techniques.

Table 2.1: All studies used for the evaluation of the model and the mean yields they report

Study	**Country, State/Province**	**Genus**	**Average Yields Reported [t/ha]**
Acaroğlu and Aksoy 1998	Turkey	*Miscanthus*	27.7
Acaroğlu and Şemi Aksoy 2005	Turkey	*Miscanthus*	12.6
Adler et al. 2006	USA, Pennsylvania	*Panicum*	5.6
Andrea et al. 2014	Brazil, Parana State	*Panicum*	10.0
Angelini et al. 2009	Italy	*Miscanthus*	28.7
Aravindhakshan et al. 2010	USA, Oklahoma	*Miscanthus*	13.1
Arundale 2012	USA, Georgia	*Miscanthus*	4.5
	USA, Illinois	*Miscanthus*	23.0
	USA, Kentucky	*Miscanthus*	16.0
	USA, Louisiana	*Miscanthus*	9.0
	USA, Michigan	*Miscanthus*	25.0
	USA, Mississippi	*Miscanthus*	19.5
	USA, New Jersey	*Miscanthus*	7.0
	USA, Oklahoma	*Miscanthus*	6.0
	USA, South Dakota	*Miscanthus*	5.0
	Canada, Ontario	*Miscanthus*	6.5
Brosse et al. 2012	Spain	*Miscanthus*	24.0
	Greece	*Miscanthus*	35.0
	Italy	*Miscanthus*	31.0
	Canada, Quebec	*Miscanthus*	10.5
	USA, Illinois	*Miscanthus*	34.0
Christian et al. 2005	United Kingdom	*Miscanthus*	15.5
Christian et al. 2008	United Kingdom	*Miscanthus*	17.8

Table 2.1: All studies used for the evaluation of the model and the mean yields they report

Chung and Kim 2012	Switzerland	*Miscanthus*	16.0
	Austria	*Miscanthus*	22.0
	Italy	*Miscanthus*	25.0
	Germany	*Miscanthus*	17.5
	United Kingdom	*Miscanthus*	15.5
Clifton-Brown et al. 2001	Portugal	*Miscanthus*	26.9
	United Kingdom	*Miscanthus*	12.1
	Germany	*Miscanthus*	17.0
	Denmark	*Miscanthus*	11.5
	Sweden	*Miscanthus*	16.1
Clifton-Brown et al. 2004	Ireland	*Miscanthus*	12.0
Clifton-Brown et al. 2007	Ireland	*Miscanthus*	11.2
Cosentino et al. 2007	Italy	*Miscanthus*	14.8
Danalatos et al. 2007	Greece	*Miscanthus*	30.5
Fales et al. 2008	USA, Iowa	*Panicum*	5.1
Gauder et al. 2012	Germany	*Miscanthus*	12.0
Heaton et al. 2008	USA, Illinois	*Miscanthus*	29.6
	USA, Illinois	*Panicum*	11.5
Himken et al. 1997	Germany	*Miscanthus*	17.5
Hong et al. 2011	Germany	*Miscanthus*	25.5
	Italy	*Miscanthus*	23.5
	France	*Miscanthus*	38.8
	China, Fujian Province	*Miscanthus*	3.2
Jørgensen 1997	Denmark	*Miscanthus*	7.7

Table 2.1: All studies used for the evaluation of the model and the mean yields they report

Kering et al. 2012	USA, Oklahoma	*Miscanthus*	4.7
	USA, Oklahoma	*Panicum*	17.8
Larsen et al. 2014	Denmark	*Miscanthus*	9.3
Lemus et al. 2002	USA, Iowa	*Panicum*	10.0
Lemus 2004	USA, Kentucky	*Panicum*	16.1
	USA, Mississippi	*Panicum*	13.2
	USA, Tennessee	*Panicum*	15.4
	USA, Virginia	*Panicum*	14.8
	USA, West Virginia	*Panicum*	14.1
Lewandowski et al. 2000	Denmark	*Miscanthus*	11.0
	Germany	*Miscanthus*	15.3
Lim et al. 2014	South Korea	*Miscanthus*	24.9
Lima et al. 2014	Brazil (country average)	*Panicum*	30
Liu and Sang 2013	China, Gansu Province	*Miscanthus*	22.5
Mooney et al. 2009	USA, Tennessee	*Panicum*	13.1
Mulkey et al. 2006	USA, South Dakota	*Panicum*	4.3
Mulkey et al. 2008	USA, South Dakota	*Panicum*	4.7
Palmer et al. 2014	USA, North Carolina	*Miscanthus*	17.8
	USA, North Carolina	*Panicum*	20.5
Sanderson et al. 1999	USA, Texas	*Panicum*	13.2
Sanderson 2008	USA, Alabama	*Panicum*	20.7
	USA, Pennsylvania	*Panicum*	6.4
Schwarz 1993	Austria	*Miscanthus*	22.0
Sharma et al. 2003	Italy	*Panicum*	7.3
Siregar et al. 1985	Indonesia, Java	*Panicum*	31.9

Table 2.1: All studies used for the evaluation of the model and the mean yields they report

Sladden et al. 1991	USA, Alabama	*Panicum*	12.3
Stewart et al. 2009	Japan, Akita Prefecture	*Miscanthus*	2.3
	Japan, Hyogo Prefecture	*Miscanthus*	3.6
	Japan, Miyagi Prefecture	*Miscanthus*	5.4
	Japan, Nagano Prefecture	*Miscanthus*	3.0
	Japan, Saitama Prefecture	*Miscanthus*	9.9
	Japan, Tochigi Prefecture	*Miscanthus*	8.9
Virgilio et al. 2007	Italy	*Panicum*	9.7
Yu et al. 2013	China, Hubei Province	*Miscanthus*	2.5
Average over all areas			14.93

2.2.4.2 Water use efficiency

In spite of the importance of irrigation for biomass production of *Miscanthus* (Ercoli et al., 1999), only two studies analyzed the water-use efficiency of herbaceous biomass plantations (Clifton-Brown and Lewandowski, 2000; Hickman et al., 2010). The two studies use different methods for estimating water use efficiency which complicates model evaluation.
Clifton-Brown and Lewandowski (2000) measure in a greenhouse under controlled conditions. They exclude soil evaporation by subtracting measurements from pots containing bare soil and by applying paraffin coatings to all pots. While their study allows them to cleanly separate plant water use efficiency compared to total plant biomass and compared to harvestable material, whether their results are applicable to field trials remains unclear.
Hickman et al. (2010) calculate evapotranspiration based on field measurements of heat fluxes. Consequently, they cannot separate transpiration from evaporation and estimate water use efficiency based on total evapotranspiration. Further, they use only harvested biomass in their calculations, since the perennial roots remain in the ground after harvest.

2.2.5 General model concept for herbaceous biomass plantations

The phenology and carbon cycles of JSBACH were adapted to reflect highly productive, tall grasses such as *Miscanthus* or *Panicum*. Few studies analyze the physiological constraints of these genera and most of these focus merely on temperature constraints and frost tolerance (Naidu and Long, 2004) or on irrigation and fertilization requirements or plant densities for maximizing yields (Danalatos et al., 2007; Christian et al., 2008; Larsen et al., 2014). Since JSBACH has no irrigation or fertilization option, temperature and precipitation become the major constraints of the model. The model follows the following basic assumptions:

- Whenever the biomass grasses can grow they will grow
- Leaves are produced up to the maximum limit of leaf area index (LAI)
- If conditions are not favorable, leaves die but are not shed, instead they remain attached to the stem
- Outside the tropics, plants remain standing on the fields throughout the winter and are harvested before the new growing season (standard harvesting technique, Frühwirth et al., 2006).

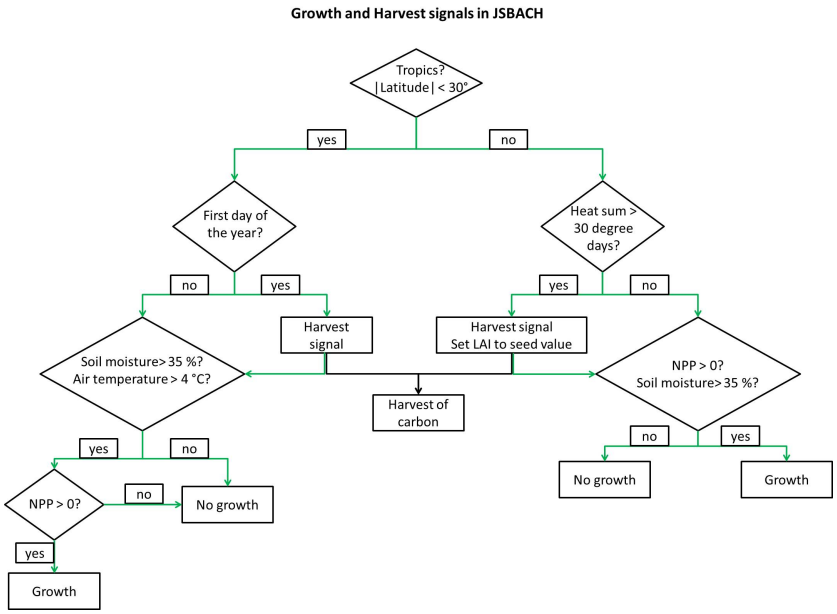

Figure 2.1: Growth and harvest signals for the phenology of herbaceous biomass plantations as implemented in JSBACH. Green arrows show the signal chain controlling phenology, black arrows show where the harvest signal is passed to the carbon (see text for details).

The idea that leaves are not shed is not supported by the literature data, which suggests that plants suffer partial biomass loss through the winter (Heaton et al., 2008). This assumption was added for two reasons: first, to avoid large-scale carbon loss induced by rapid shedding during bad weather spells (the default for JSBACH) and second, because it is unclear whether the reduction in LAI affects surface albedo, as it would in JSBACH.
Herbaceous biomass plantations were developed as new plant functional types (PFT) in JSBACH. The model distinguishes between tropical and extra-tropical herbaceous biomass plantations. JSBACH demands a number of input variables to characterize the new PFTs. For the few parameters where literature values are available, these were chosen. The rest were considered to be similar to the values of C4 crops, pastures and grasses (see table in the Appendix for details).

2.2.6 Phenology of herbaceous biomass plantations

The phenology in JSBACH describes the changes in leaf area index (LAI) throughout the year. Leaf area index responds to a variety of physiological constraints such as temperature or soil moisture. Leaf area index in turn influences other model components such as surface albedo and the size of the plant carbon pools. This part of the model had to be adapted to reflect the unique annual cycles and management techniques used in the cultivation of HBPs.
In JSBACH maximum leaf area index of herbaceous biomass plantations is 9 m^2/m^2,

a value consistent with field measurements (Heaton et al., 2008; Le et al., 2011). JSBACH defines the tropics as the region between 30 °S and 30 °N. In a fist step the phenology model distinguishes between these two regions (figure 2.1).

2.2.6.1 Tropics

In the tropics, herbaceous biomass plantations grow throughout the year as long as net primary production (NPP) is positive, air temperature is above 4 °C and soil moisture is above the wilting point (35%, figure 2.1). Leaf area index increases to its maximum limit of 9 m^2/m^2. The model assumes that farmers harvest different parts of their fields at different times and thus assure a continual supply of biomass throughout the year. In consequence, average LAI throughout any gridcell remains constant except in times of adversity. However, the carbon harvest is triggered at the start of every year.

2.2.6.2 Extra-tropics

Outside the tropics the seasonal cycle constrains plant growth and harvest. Growth begins in spring when the beginning of the growing season is triggered by the heat sum exceeding 30 degree days. The heat sum sums all temperatures exceeding 4 °C. From this date onward, plants grow whenever air temperatures exceed 4 °C and soil moisture is above the wilting point (35%). LAI increases to its maximum and remains at this level until the harvest in the following spring. Harvest is triggered by the beginning of the growing season.
Heat summation starts on January 1^{st} in the northern hemisphere and July 2^{nd} in the southern hemisphere (July 1^{st} in leap years). JSBACH computes a weighted running mean of the air temperature, termed "pseudo soil temperature", for heat summation.

2.2.7 Carbon dynamics of herbaceous biomass plantations and harvesting scheme

Carbon accumulates in the plant carbon pools throughout the growing season, depending only on photosynthesis and respiration. The phenological cycle triggers the harvest and passes the signal to the carbon. In the tropics, harvest of the carbon occurs on January, 1^{st}. Outside the tropics, harvest occurs at the beginning of the growing season. In both cases, reported yields correspond to the harvest fraction of the carbon accumulated in the previous year. Harvested carbon is passed to a separate harvest pool that can then be used for fossil fuel substitution.
Plant carbon in JSBACH is not divided into above- and belowground carbon. Thus roots, shoots, and leaves cannot be adequately modeled. Two carbon pools that differ in their turnover rates contain total plant carbon. These pools represent living tissues and reserves such as sugars or starch, respectively. Since these pools cannot be

attributed to specific plant organs, the amount of harvestable material must be determined independently. The fraction of harvestable carbon is determined using root to shoot ratios found in the literature. These root to shoot ratios range from 0.4 to 0.8 (Meyer et al., 2010). Root to shoot ratios are the ratio of root biomass relative to the shoot biomass and need to be transformed into ratios of total biomass.
If x is the root to shoot ratio, r the ratio of roots compared to the total plant and s the ratio of shoots compared to the total plant, then the following equations apply:

$$r + s = 1 \tag{2.1}$$

$$x = \frac{r}{s} \tag{2.2}$$

Thus the shoot ratio can be determined by replacing r from equation (2.2) in equation (2.1):

$$s = \frac{1}{x + 1} \tag{2.3}$$

Using the extreme root to shoot values reported in Meyer et al. (2010), I calculate a shoot fraction of 0.55 for a root to shoot ratio of 0.8 and a shoot fraction of 0.71 for a root to shoot ratio of 0.4. These values are considered to be the extremes of harvestable material the plants can produce.
I therefore distinguish two cultivation scenarios:

- **Maximum harvest scenario:** farmers intensively cultivate the fields to maximize above-ground biomass production and minimize plant investments in roots (harvest fraction: 0.71).

- **Minimum management input scenario:** farmers minimize their investments in their biomass plantations, forcing plants to invest heavily in root production and reduce above-ground biomass production (harvest fraction: 0.55).

The model considers all above-ground biomass to be harvestable carbon. This is a plausible assumption for herbaceous biomass plantations since harvest equipment cuts stems close to the ground. Below-ground biomass is passed to the litter pool after each harvest. Without proper distinction between plant organs, JSBACH cannot simulate root survival consistently.
Harvested biomass can be used to complement energy from other sources or to replace energy from other sources. If biomass is used to complement energy from other sources, carbon dioxide emitted by their combustion adds to overall anthropogenic emissions. If biomass is burnt instead of fossil fuels, carbon dioxide emissions are reduced by the amount emitted from biomass combustion. Therefore, assessing the effects of biomass plantations on the climate must include biomass use. I distinguish two extreme scenarios for biomass use:

- **High energy demand:** all available energy sources are used, including biomass plantations. Emissions from biomass combustion are added to overall anthropogenic emissions (0% substitution). In JSBACH, harvested carbon is transferred into a separate harvest pool that is depleted at a regular rate over the course of one year. If the carbon in the pool drops below a threshold, the pool is completely depleted. This depletion reflects the assumption that energy providers would use an equal amount of biomass each day but not store less than a minimum amount.

- **Fossil fuel substitution:** all available biomass substitutes the maximum possible amount of fossil fuels. Emissions from fossil-fuels are reduced by the amount emitted by biomass combustion (100% substitution). To reduce model complexity, carbon from biomass plantations is instead stored away in a separate long-term storage pool. This carbon then no longer interacts with the rest of the carbon cycle anymore. In the high energy demand scenario, the harvest pool is depleted at a constant rate. I assumed that society would use the available biomass slowly throughout the year until, after 365 days the supplies would be exhausted and barns would be emptied in anticipation of the next harvest. The depletion rate (τ) therefore is:

  $$\tau = C_h/365 \tag{2.4}$$

  Where C_h is the amount of carbon in the harvest pool. The depletion rate is subtracted from the harvest pool and returned to the atmosphere on a daily basis. If the next years harvest is delayed, for example because of cold weather, the harvest pool is emptied and remains empty until the harvest event refills it.

2.2.8 Land-use transition scheme

The transition scheme of JSBACH describes all human induced changes in land cover types. The standard land-use transition scheme of JSBACH currently does not account for biomass separately. JSBACH treats biomass for biofuel production like standard crops. One of the main challenges of this thesis was, therefore, to incorporate herbaceous biomass plantations as a separate land-use type in JSBACH. This was necessary to ensure the consistency of the underlying land-use scenario.

2.2.8.1 Land-use scenario

The land-use scenario chosen here is the Representative Concentration Pathway RCP4.5. In this scenario, large areas of agricultural lands are abandoned until the end of the century due to an intensification of agricultural methods on the most fertile soils. In the original scenario, these abandoned lands revert to their natural state, either forests or grasslands. Here, the abandoned lands that originally revert to forests are

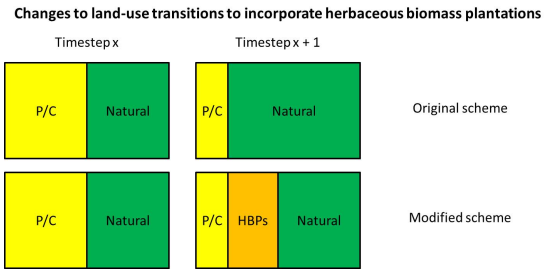

Figure 2.2: Incorporation of herbaceous biomass plantations into the modified transition scheme of RCP4.5.

covered with herbaceous biomass plantations. I use only the areas reverting to forests for two reasons: first, the majority of abandoned lands revert to forests in the original scenario and second, use of these areas allows a direct comparison between forests and herbaceous biomass plantations for the reduction of carbon dioxide concentrations (figure 2.2).

2.2.8.2 Conceptual formulation

The original land-use scheme of JSBACH accounts for four land-cover types: forests, grasses, pastures and crops. Theoretically, all of these types can lose area to any of the other types or gain area from any of the other types at every timestep. However, the land-use scheme is primarily concerned with transitions between agricultural areas and natural lands and between pastures and crops. Climate driven transitions between natural ecosystems are calculated by the dynamical vegetation scheme.
I added herbaceous biomass plantations as a fifth land-cover type. Herbaceous biomass plantations can exchange area with crops and pastures but not with forests or grasslands. The goal was to minimize the interactions with the other land-use types so as to disturb the underlying land-use scheme as little as possible. Gains to herbaceous biomass plantations should be limited to those areas that would have reverted to forests and losses should be limited to those areas that would have been reclaimed from forests if herbaceous biomass plantations hadn't been established instead.
There are two reasons why only areas that would have reverted to forests are used: first, because part of the goal of this study was to assess the mitigation potential of herbaceous biomass plantations as compared to that of forests and second, because the transition scheme uses the so-called 'pasture rule' to determine the transitions between natural areas and pastures. The underlying assumption is that farmers would preferentially use grasslands as pastures whenever they are available (Reick et al., 2013). Transitions between pastures and grasslands would be perturbed by the conversion to herbaceous biomass plantations and could potentially lead to a radically different land-use distribution.
The original land-use scheme of JSBACH uses a four-by-four transition matrix. Each element in the transition matrix describes the fraction of the area of a given land-use

type that is transferred from that land-use type to another. The details are described in Reick et al. 2013. I modified this transition matrix to include herbaceous biomass plantations. This new five-by-five transition matrix describes all previous exchanges plus the new exchanges between herbaceous biomass plantations and other types. Since exchanges between crops, pastures, and grasses are unaltered and exchanges between natural lands and herbaceous biomass plantations should not happen, the matrix can be represented as:

$$\tilde{T} = \begin{pmatrix} T_{C\to C} & T_{P\to C} & T_{G\to C} & \tilde{T}_{F\to C} & \tilde{T}_{H\to C} \\ T_{C\to P} & T_{P\to P} & T_{G\to P} & \tilde{T}_{F\to P} & \tilde{T}_{H\to P} \\ T_{C\to G} & T_{P\to G} & T_{G\to G} & 0 & 0 \\ \tilde{T}_{C\to F} & \tilde{T}_{P\to F} & 0 & \tilde{T}_{F\to F} & 0 \\ \tilde{T}_{C\to H} & \tilde{T}_{P\to H} & 0 & 0 & \tilde{T}_{H\to H} \end{pmatrix} \tag{2.5}$$

Where $\tilde{T}$, $T_{i\to j}$ is the fraction of area that is transferred from cover type i to cover type j which remains unaltered by the new transition scheme and $\tilde{T}_{i\to j}$ describes a transition element that is altered by the new transition scheme. The land-use types are abbreviated as C for crops, P for pastures, G for grasses, F for forests and H for herbaceous biomass plantations.
This matrix can be solved for three separate cases:

- Crops and pastures contract to the benefit of natural lands: agricultural areas are abandoned and herbaceous biomass plantations are established on all areas that would have reverted to forests
- Crops and pastures expand in the presence of herbaceous biomass plantations: areas covered with herbaceous biomass plantations are reclaimed first, to preserve the original amount of forests
- Crops and pastures expand in the absence of herbaceous biomass plantations: forests are transformed into agricultural areas

2.3 Evaluation of model performance

2.3.1 Herbaceous biomass plantations as modeled by JSBACH

JSBACH models carbon dynamics and leaf area index of herbaceous biomass plantations differently in the tropics than outside the tropics (figure 2.3). Outside the tropics, LAI drops once a year, at the beginning of the growing season when plants are harvested. This drop coincides with a drop in the carbon pool when plant carbon passes into the harvest pool. But whereas LAI decreases for crops and, to a lesser extent,

for grasses at the end of the growing season, LAI remains high for herbaceous biomass plantations because stems remain standing on the fields over the winter. Plants can continue to assimilate carbon as long as conditions for photosynthesis are favorable. This coincides with observations (Frühwirth et al., 2006).
In the tropics LAI remains high throughout the year. This is consistent with LAI development in crops and grasses. Carbon is harvested once a year and passed to the harvest pools. In simulations without fossil-fuel substitution (FFS 0%), the harvest pool slowly depletes as biomass is 'burnt' and carbon dioxide is released to the atmosphere. In simulations with fossil-fuel substitution (FFS 100%), the pool retains all carbon and new carbon is added at every harvest event. This simulates avoided emissions from fossil-fuels that remain in the ground because they are replaced by biomass. Throughout this section, all carbon pools are depicted in g/m^2 to allow comparisons between modeled and observed data. I assumed that plant carbon would constitute 50% of dry matter which is similar to estimates from Cannell 2003 who assumed that 1 t of dry biomass could substitute 0.5 t of coal.

2.3.2 Global offline simulations

2.3.2.1 Model setup for the idealized scenarios

In order to evaluate the model, idealized scenarios were simulated with JSBACH in its stand-alone mode. The land surface was initialized as a single tile containing herbaceous biomass plantations in all gridcells. Two 10-year simulations were performed, each with one of the management schemes (55% and 71% harvest). The first year was discarded because the harvest event produced no harvest in most areas because plants had not developed their full potential. Model results were compared to available literature data to asses how well JSBACH can reproduce observed yield patterns and water use efficiency.
Simulations were driven by prescribed present-day climate derived from measurements. The NPP and GPP of these idealized simulations were compared to results from the Lund-Potsdam-Jena managed Land (LPJmL) model obtained from Vera Heck at the Potsdam Institute for Climate Impact Research. LPJmL previously implemented biomass plantations in their model and evaluated their findings (Beringer et al., 2011).

2.3.2.2 Results of idealized scenarios

Annual gross primary production of herbaceous biomass plantations averages 313±7 Pg/a and annual net primary production averages 153±4 Pg/a under a stable climate in JSBACH offline simulations, independently of the harvesting scheme used. Primary production for herbaceous biomass plantations is much larger than that for natural vegetation and for current vegetation because of the high productivity of

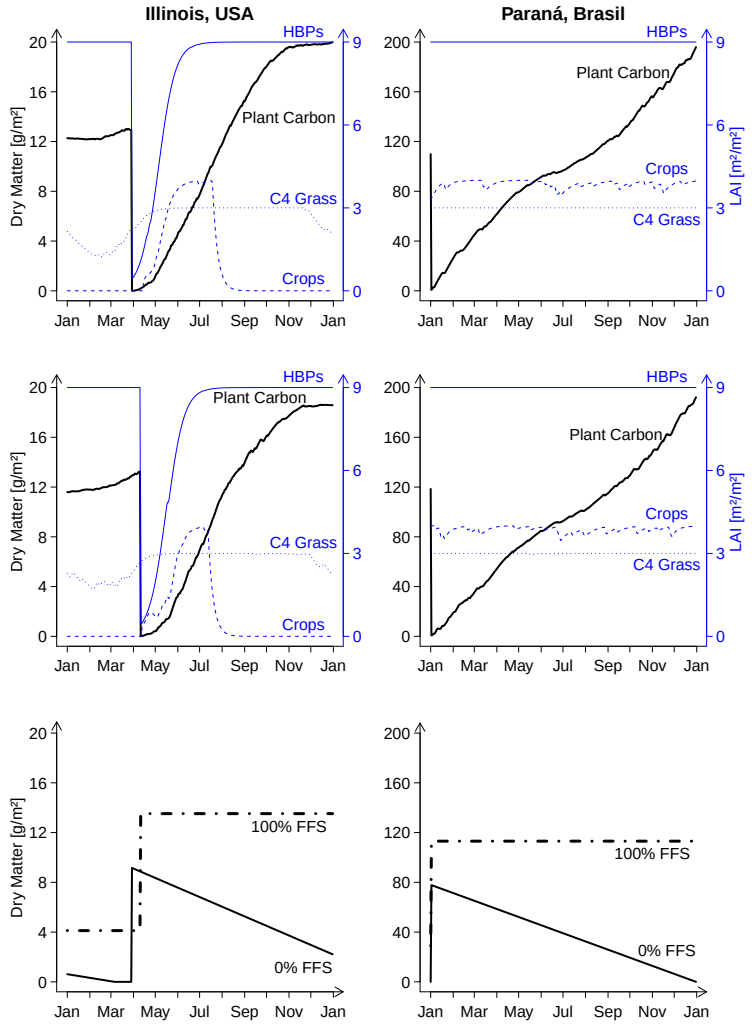

Figure 2.3: Annual cycles of leaf area index (LAI in blue) and carbon (dry matter contains 50% carbon, in black) of herbaceous biomass plantations compared to crops and grasses (LAI only) in the same simulation for a temperate region in North America (Illinois, USA) and a tropical region in South America (Paraná, Brazil) as modeled by JSBACH. The top graphs show a simulation without fossil fuel substitution (FFS 0%), the middle graphs show a simulation with fossil fuel substitution (FFS 100%), the bottom graphs show the development of the harvest pool in each of these simulations. Harvest of carbon occurs simultaneously with the drop in LAI outside the tropics, while it occurs on January, 1st in the tropics.

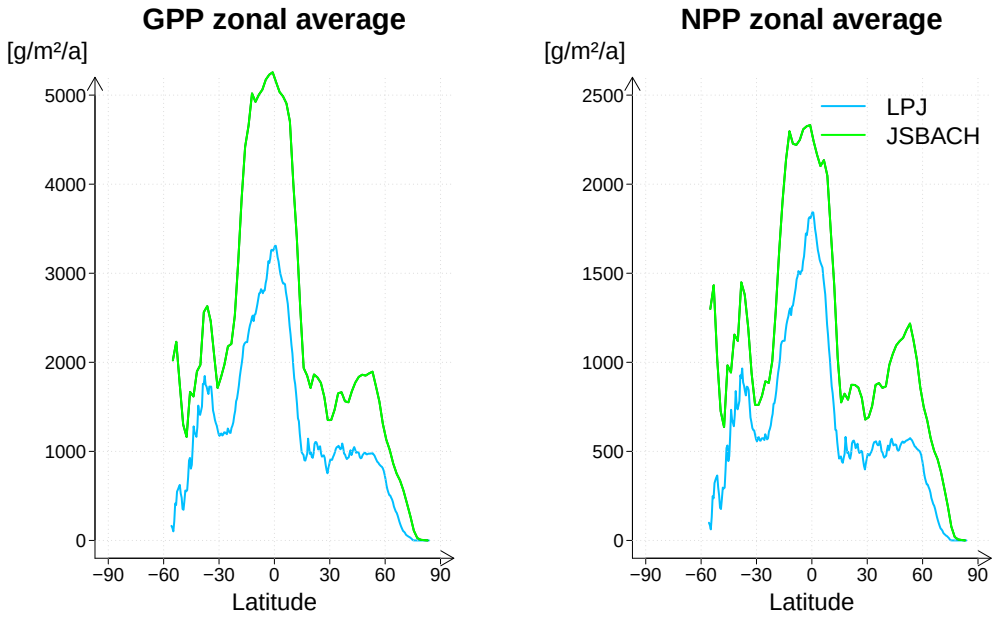

Figure 2.4: Zonal averages of GPP (left) and NPP (right) in JSBACH and LPJmL. Data from LPJmL was generated by Vera Heck at the Potsdam Institute for Climate Impact Research.

the modeled grasses in almost all environments. Several publications analyzed the high productivity of *Miscanthus* and conclude that the extraordinary cold tolerance of this C4-grass combined with high photosynthetic activity and its ability to grow well in adversity may explain this observation (Beale et al., 1996; Naidu and Long, 2004; Dohleman et al., 2009; Dohleman and Long, 2009).

Primary production peaks in the tropics, declines towards 30° latitude with a second peak in the temperate regions before declining further towards the poles (figures 2.4 and 2.5). JSBACH reproduces the global patterns found in LPJ but produces more biomass than LPJ. However, JSBACH produces more than LPJ in all other vegetation as well, so the pattern agrees with previous findings (Dalmonech and Zaehle, 2013).

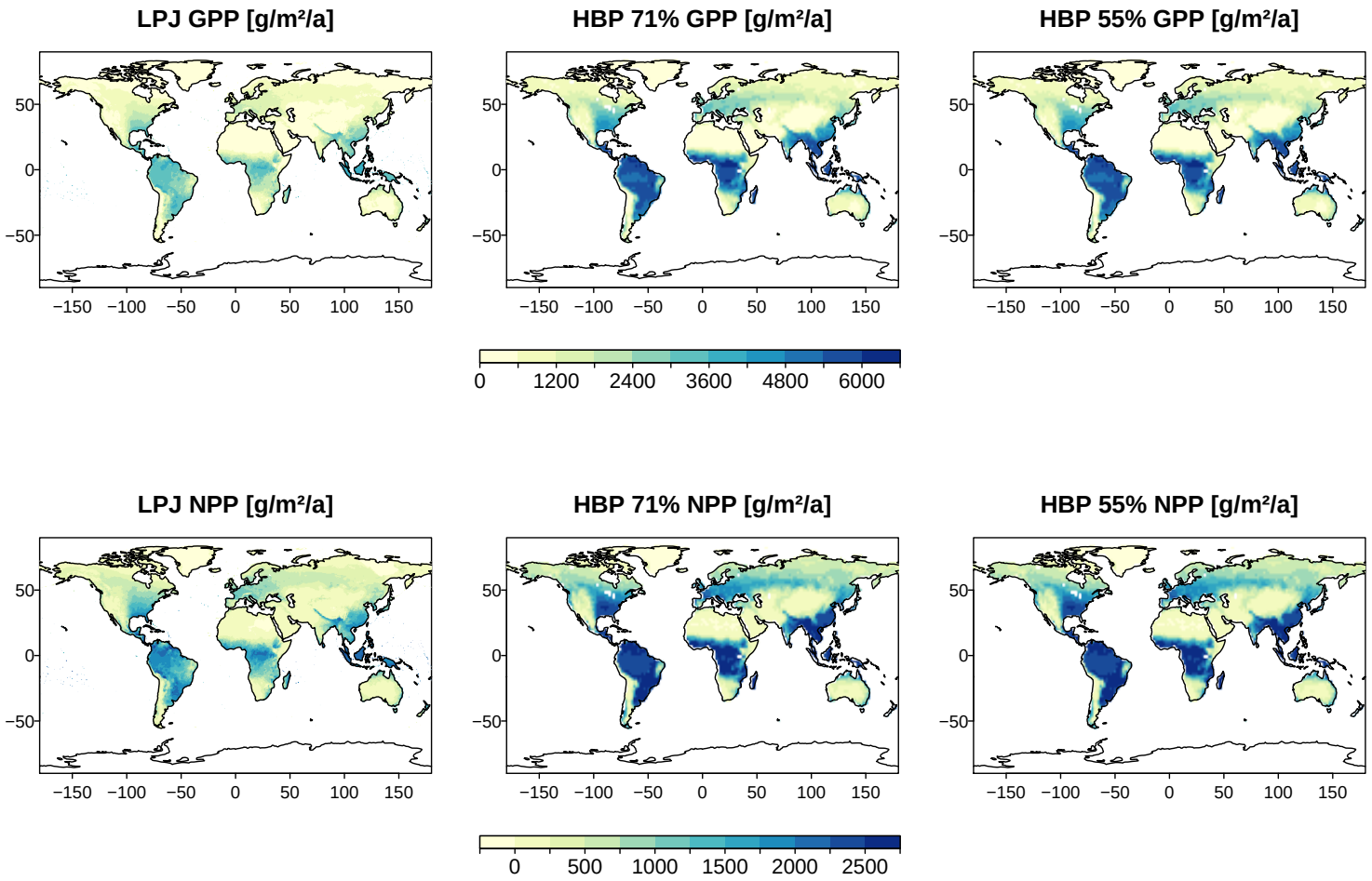

Figure 2.5: Gross (top) and net (bottom) primary production of herbaceous biomass plantations in LPJ (left), and two simulations with JSBACH (center: 71% harvest; right: 55% harvest). Data from LPJ was generated by Vera Heck at the Potsdam Institute for Climate Impact Research.

2.3.3 Comparison of modeled yields with literature values

Modeled yields average 970 g(dry matter)/m^2/a (9.7 t/ha/a) for the 55% harvest scheme and 1260 g(dry matter)/m^2/a (12.6 t/ha/a) for the 71% harvest scheme. This is slightly lower than the average measured yields of 1493 g(dry matter)/m^2/a (14.9 t/ha/a) found in the literature. Maximum modeled yields reach 2140 g(dry matter)/m^2/a (21.4 t/ha/a) for the 55% harvest scheme and 2760 g(dry matter)/m^2/a (27.6 t/ha/a) for the 71% harvest scheme. These maximum modeled yields are much lower than the maximum yields in the literature of 4900 g(dry matter)/m^2/a (49.0 t/ha/a) achieved on one plot in France (Clifton-Brown et al., 2004). However, JSBACH averages over all land gridcells which includes deserts and other areas with sparse plant growth, thus lower peak yields than those from actual fields are expected. Thus, maximum and minimum measurements found in the literature diverge much more than modeled yields between years (figure 2.8).
In the model, regional patterns differ widely (figures 2.6 and 2.7). Yields are highest in the tropics which agrees well with the few literature values available for this area. In Europe (figure 2.9) and North America, where most of the literature data was gathered, model values agree with literature data but in Asia the model seems to significantly overestimate average yields. However, in this region literature data is derived from freshly planted fields (Hong et al., 2011; Yu et al., 2013), wild grasslands (Stewart et al., 2009) or estimated from very small plots (Liu and Sang, 2013).

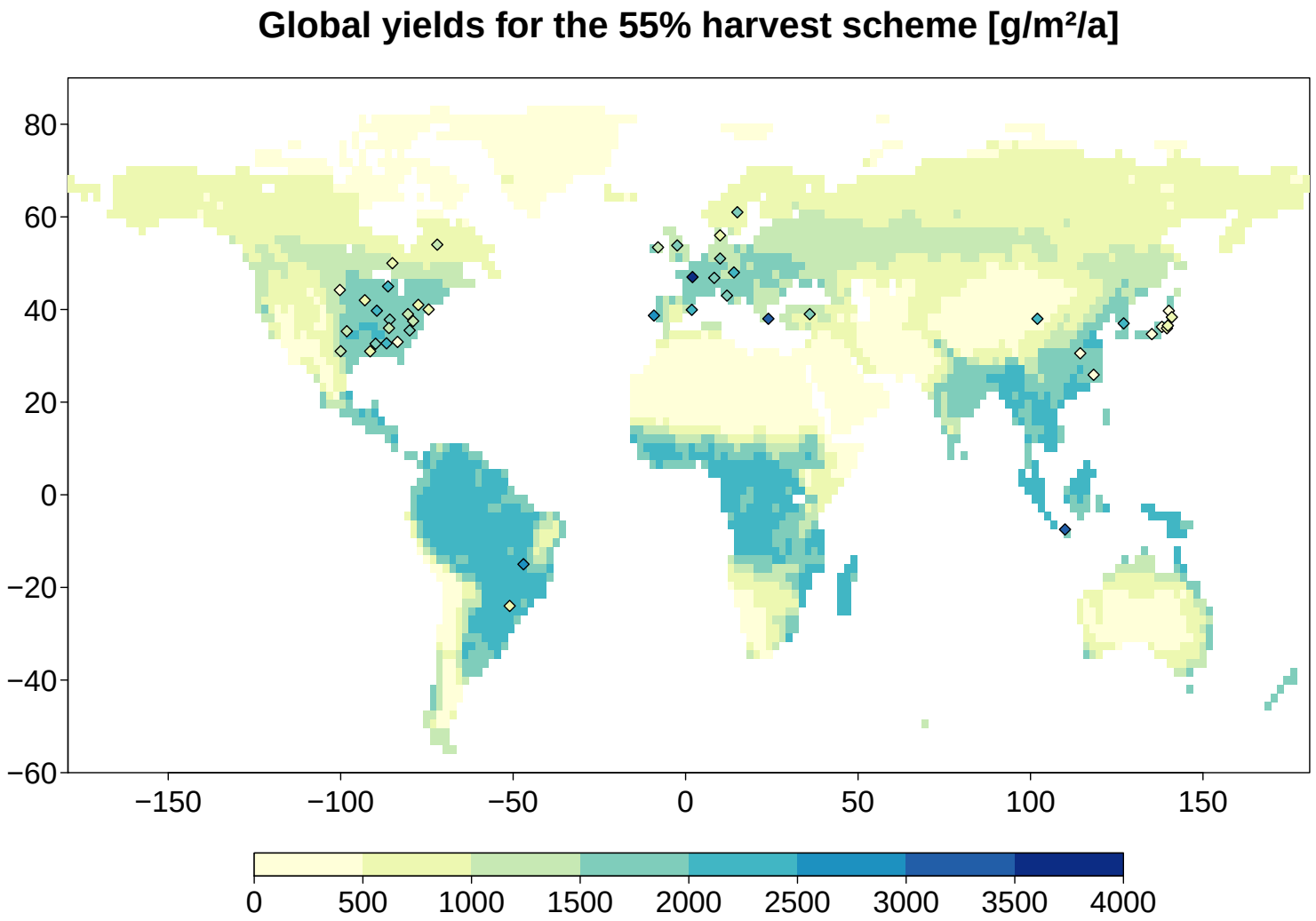

Figure 2.6: Modeled yields in the 55% harvest scheme (map) and average measured yields from literature values (diamonds), in g(dry matter)/m^2/a.

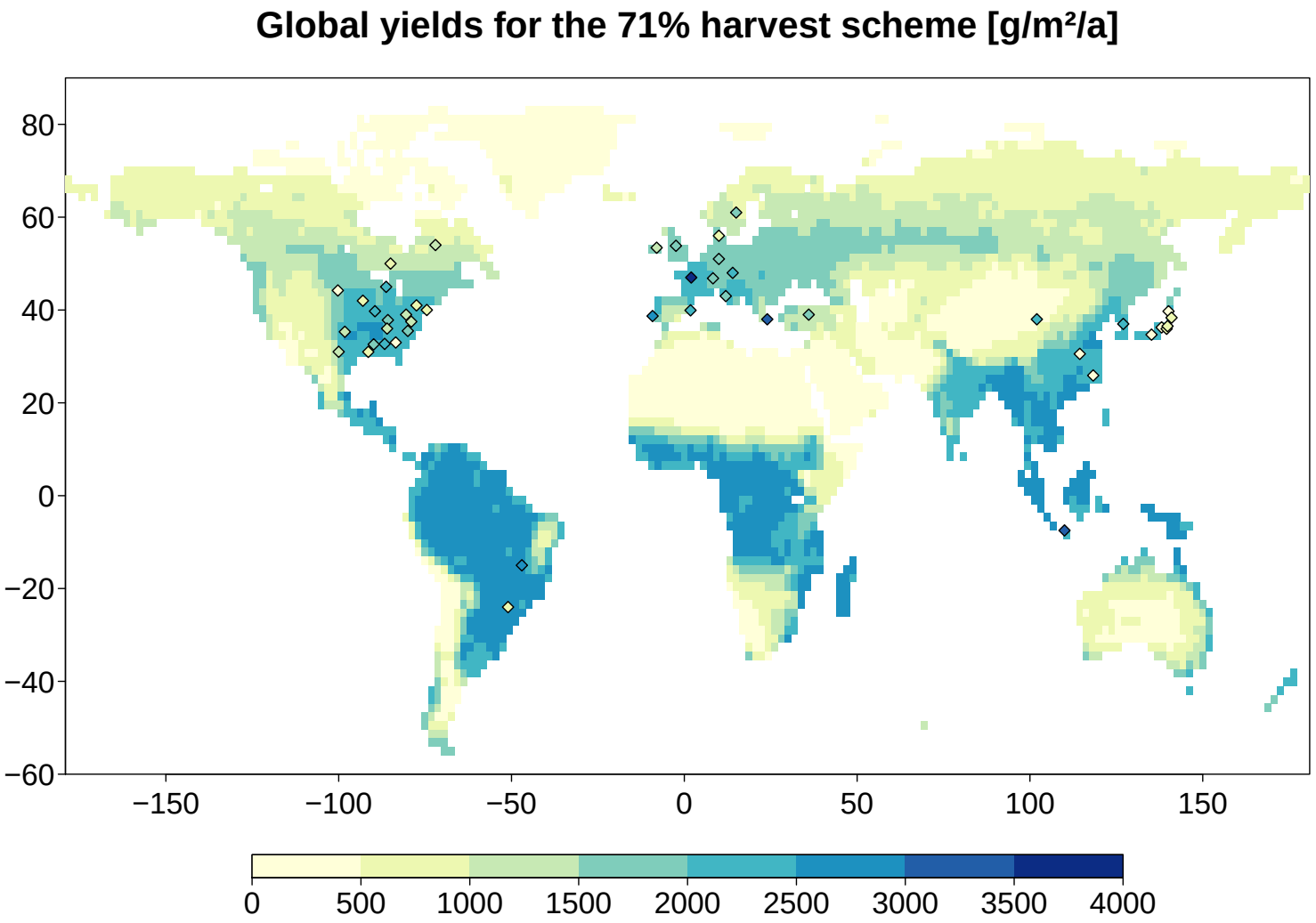

Figure 2.7: Modeled yields in the 71% harvest scheme (map) and average measured yields from literature values (diamonds), in g(dry matter)/m^2/a.

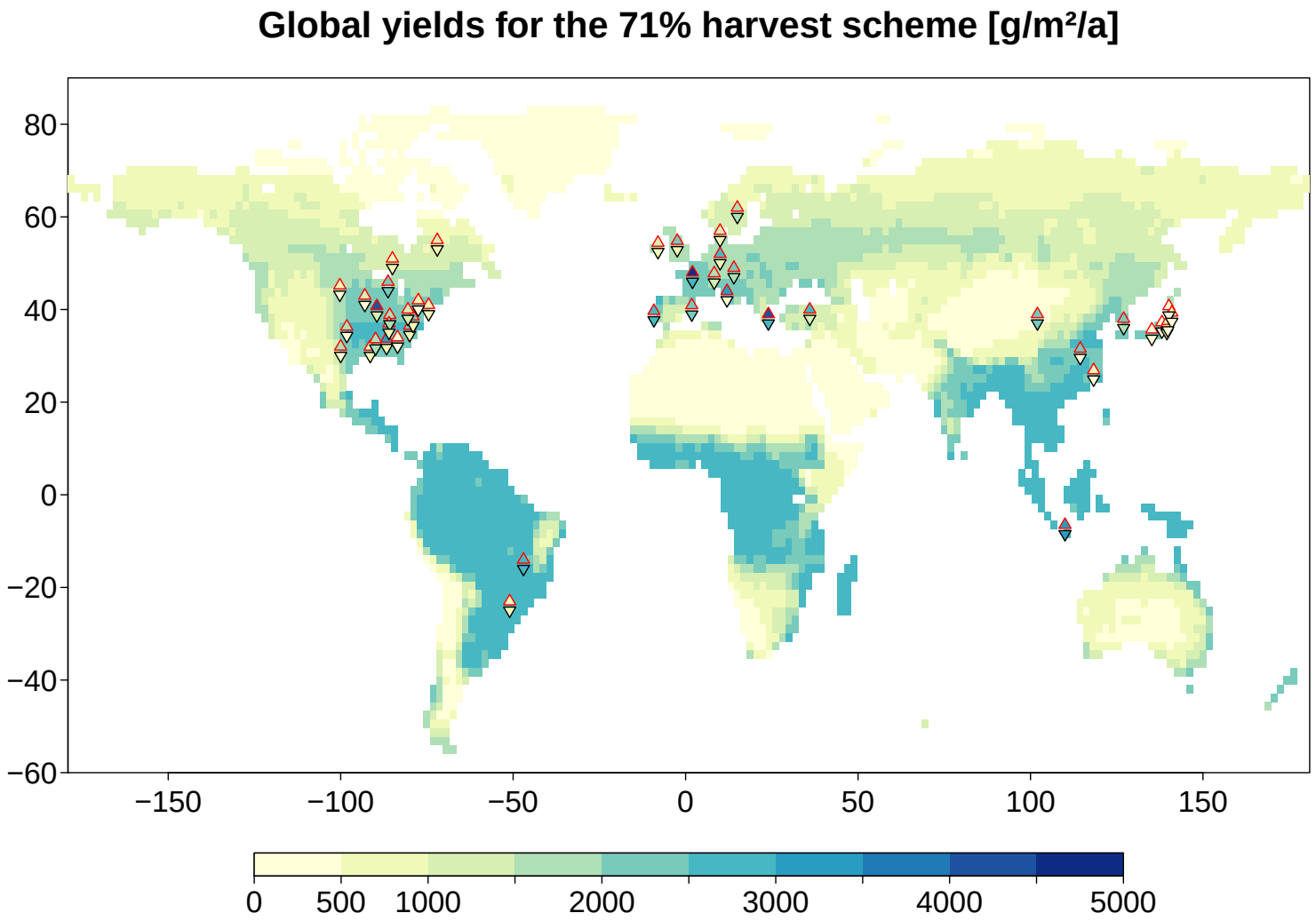

Figure 2.8: Modeled yields in the 71% harvest scheme (map) and minimum (black border) and maximum (red border) measured yields from literature values (diamonds), in g(dry matter)/m^2/a.

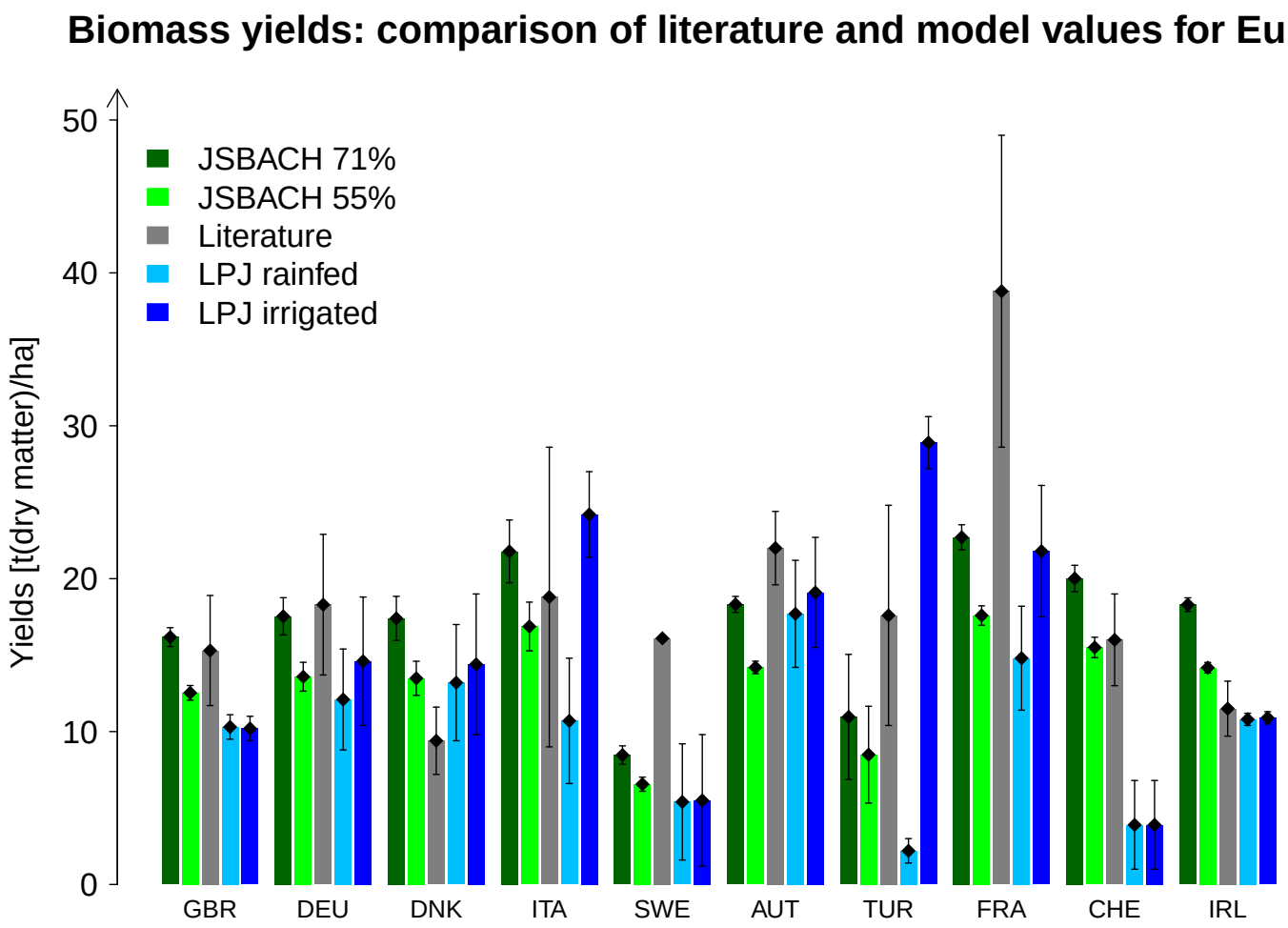

Figure 2.9: Comparison of literature and modeled yields of herbaceous biomass plantations for European countries. JSBACH 71%: yields modeled with JSBACH using the 71% harvest scheme; JSBACH 55%: yields modeled with JSBACH using the 55% harvest scheme; LPJ rainfed: yields modeled with LPJmL using precipitation as the only water source (Vera Heck personal communication); LPJ irrigated: yields modeled with LPJmL using the model's inbuilt irrigation scheme; GBR: United Kingdom (island of Great Britain); DEU: Germany; DNK: Denmark; ITA: Italy; SWE: Sweden; AUT: Austria; TUR: Turkey; FRA: France; CHE: Switzerland; IRL: Ireland

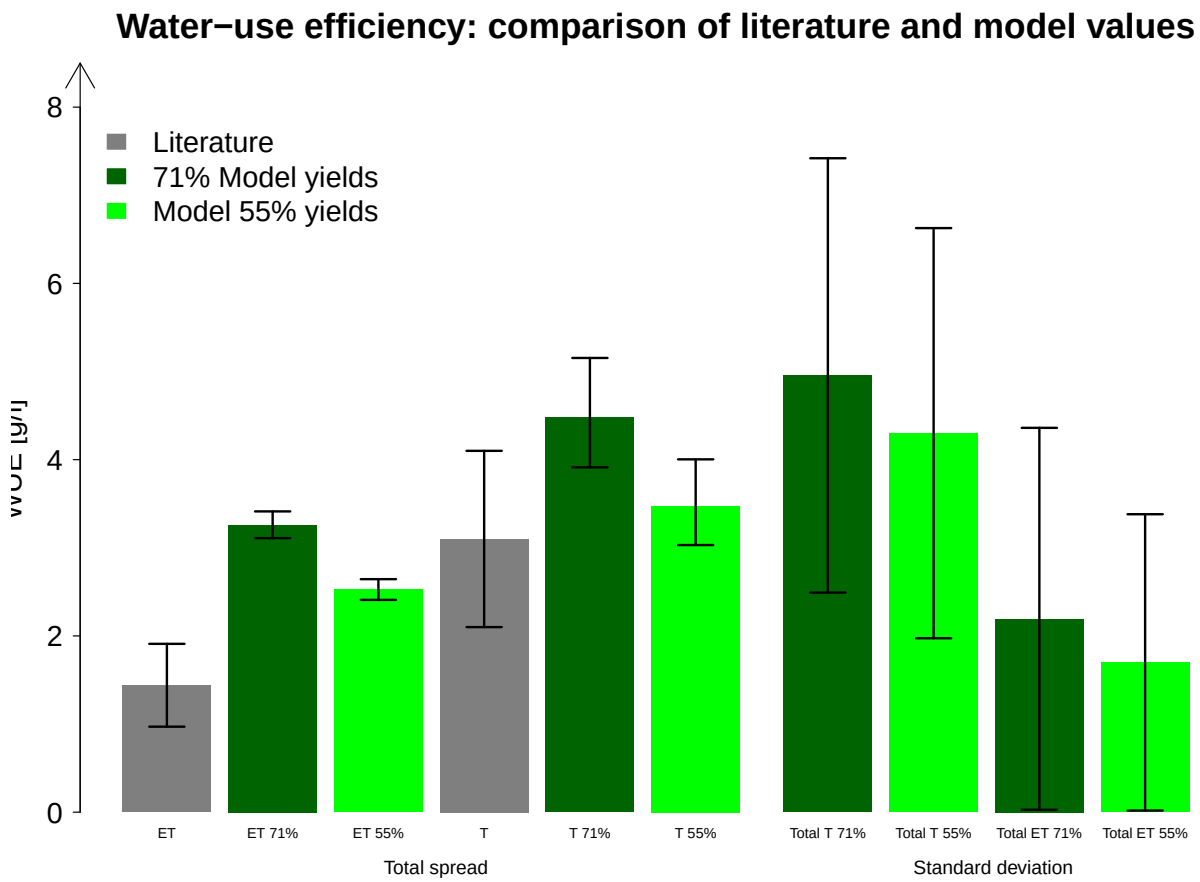

Figure 2.10: Left: Water-use efficiency (WUE) of herbaceous biomass plantations in the literature and the two model simulations (55/71%: 55% or 71% of total biomass harvested), all WUE-values were calculated using aboveground biomass (yields) only. ET: WUE calculated using evapotranspiration, literature values were taken from Hickman et al. 2010, model values were calculated using the exact gridcell containing the site used in the literature; T: WUE calculated using transpiration, literature values were taken from Clifton-Brown and Lewandowski 2000, model values were calculated using a gridcell with temperature and humidity similar to that in the greenhouse used in the study and high annual precipitation. Error bars show maximums and minimums for both measured and modeled values because the literature only reports total range. Right: WUE of herbaceous biomass plantations in the two model simulations for all gridcells. T: WUE calculated using transpiration (WUEs larger than 10 were considered unrealistic and discarded); ET: WUE calculated using evapotranspiration. Error bars show standard deviation of the model.

2.3.4 Comparison of water use efficiency with literature values

Simulated water use efficiency (figure 2.10) for transpiration only agree with measurements from the greenhouse used in Clifton-Brown and Lewandowski 2000 but do not agree with field measurements from Hickman et al. 2010. Water use efficiency is higher in the simulations with higher yields because yields were used to determine water use efficiency in both the model and measurements.

2.4 Discussion

2.4.1 Comparison of modeled yields with literature values

JSBACH reproduces the literature's values, even though it seems to regionally over- or underestimate yields when compared to literature values. Discrepancies between modeled and observed yields seem to arise from a combination of model properties and observation biases.
JSBACH represents vegetation in a very simplified way and many processes cannot be adequately modeled. Processes related to the specific dynamics within *Miscanthus* and *Panicum* (Switchgrass) plants such as root survival and low yields during establishment years are not included in the representation of the new plant functional type. Agricultural practices such as irrigation and fertilization that also influence yields equally cannot be accounted for under the current model setup. Additionally, JSBACH assumes that environments within gridcells are uniform. However in reality, each gridcell spans an area containing a large variety of local conditions. Variabilities of climate, soil conditions and topography within this area cannot be captured. Lastly, because the simulations were idealized with herbaceous biomass plantations as the only plant cover, they cannot capture potential competitions for water or other resources between plantations and adjacent other land-use types.
Studies reporting observations however, are often politically or economically motivated. They face many challenges associated with data collection. These studies are limited in several ways:

- **Plot size:** most plots are small, usually no more than one hectare. Local conditions, such as microclimate, nutrient and water availability, elevation and topography can significantly influence yields. Furthermore, yield biases on small plots can result from nearby ecosystems influencing the field through competition for water, light or nutrients and through lateral flows within the soil that transport nutrients into or out of the field. The significance of these 'edge-effects' diminishes with increasing plot size (Talbot et al., 1995; Kuemmel, 2003). Some studies avoid these biases by sampling only the central areas (Lemus, 2004) of plots while others report yields for the entire plots.

- **Timespan:** most studies started recently, yield reports over longer timespans are rare. Timespan is crucial as yields tend to be lower in the first two to three years (Larsen et al., 2014).
- **Geographical location:** the vast majority of studies were conducted in Europe and North America; studies located in other parts of the world were also mainly confined to the northern hemisphere. Thus, the tropics and southern hemisphere are comparatively undersampled.
- **Soil conditions:** some studies used prime farmland while others specifically investigated the plants' potentials when grown on degraded soils.
- **Treatment:** studies diverge widely in terms of irrigation, fertilization and planting densities, factors that can influence yields significantly, especially in the first few years after planting (Miguez et al., 2008).
- **Cultivars:** *Miscanthus* and *Panicum* comprise many different species and numerous cultivars. While some studies based their research on existing knowledge of the most productive cultivars in their region, others explored the suitability of various cultivars for previously unassessed regions (Yu et al., 2013). Therefore, some cultivars are suboptimal for the area, soils or climates they are planted in, leading to yield reductions.
- **Data quality:** some studies reported overall averages, others reported ranges, and a few reported individual values for different years and different plots.
- **Data type:** one study reported biomass estimates of *Miscanthus sinensis* yields for wild grasslands in Japan where plants were in competition with other grasses (Stewart et al., 2009).

One of the goals during model development was to estimate yields of herbaceous biomass plantations established on abandoned agricultural fields to prevent competition with food crops. Since farmers abandon their least productive soils first, biomass plantations will mainly occupy less productive areas. Therefore, JSBACH should not represent peak yields on prime farmland under optimal management conditions but rather more conservative estimates consistent with less productive farmland. Additionally, although JSBACH cannot adequately represent increased emissions due to land management (e.g. energy production for irrigation, tractors, fertilizer and pesticide production and use...) nor estimate carbon losses due to transport or processing, the model can compensate by keeping yield estimates conservative. However, most studies assume that yields will likely increase as a result of a combination of improvement and spreading of management techniques, selective breeding and genetic engineering. Furthermore, improvement in conversion technologies could reduce carbon losses during processing. Thus, adapting modeled yields to the lowest values found in the literature would lead to gross underestimates of biomass productivity.

This study strives to balance between the potentials for over- and underestimation of yields while accounting for the many measurement uncertainties and differences between model and literature values. The longest record of *Miscanthus* yields comes from Larsen et al. 2014, who report yields of different cultivars on two fields in Denmark under different management treatments between 1993 and 2012. In their study, yields stabilized after several years between 8 and 10 t(dry matter)/ha/a . While this study is not representative for the entire Earth, other important studies also consistently find yields between 8 and 12 t(dry matter)/ha/a dry matter (Clifton-Brown et al., 2001; Heaton et al., 2008; Arundale, 2012). This range coincides with what the agricultural advice book, Frühwirth et al. 2006, issued by the Austrian government, tells farmers to expect as long-term yields. Average modeled yields of 9 to 12 t(dry matter)/ha/a fall within this range. In addition, in those areas where data is more abundant, modeled yields correspond well with literature values. I conclude that JSBACH can represent literature values sufficiently well for the rest of this study, although caution is advised, especially in those areas where observations are scarce.

2.4.2 Comparison of water-use efficiency

Comparing water use efficiency estimates with the literature values is challenging. Only two literature values were available for water-use efficiency. The first was a field study (Hickman et al., 2010), while the second study measured water use under controlled conditions in a green-house (Clifton-Brown and Lewandowski, 2000). The field study is limited for the same reasons that the yields obtained from field studies are limited (see above). Finding a gridcell that exactly matches the conditions in the green-house was impossible, though I strove to stay as close to the ideal conditions as possible. Additionally, the metrics used to calculate water-use efficiency in the two studies are difficult to compare. While the field study cannot distinguish between evaporation and transpiration and instead measures evapotranspiration, the greenhouse study takes precautions to cleanly separate evaporation and transpiration and reports water-use efficiency based on transpiration. Also, the field study cannot prevent water from seeping into the study area through lateral flows, so that total water entering the system cannot be fully controlled, while the greenhouse study uses sealed pots preventing any uncontrolled water from entering or leaving the systems. On the other hand, the greenhouse study may overestimate both evaporation and transpiration because they measure the two variables in separate pots. Therefore, all water present in each pot is available for one mechanism only, whereas in the field study the two mechanism 'compete' with each other.
JSBACH has its own range of inaccuracies when calculating water-use efficiency. JSBACH uses a bucket model to simulate soil water. Although the scheme accounts for the heterogeneous field capacity distribution within a gridcell, many aspects of soil depths and texture are only approximated. Importantly, vegetation does not determine local soil properties and individual soils are not associated with any particular plant

type. Different plant types within the same gridcell compete for water resources, even when they would grow separately in reality.
In spite of all the difficulties in comparing the two, JSBACH agrees with the literature values for the greenhouse study but slightly exceeds the values for the field study. However, the model shows a large variability of water use efficiency over the entire Earth. It is likely that in nature such a large variability on the global scale would translate into considerable variability on local scales. Thus, more emphasis should be placed on the more idealized greenhouse study. Overall, the discrepancies are small. I conclude that water use efficiency in the model does not differ from the values found in the literature.

2.5 Conclusion

This chapter describes the implementation of herbaceous biomass plantations in JSBACH. I integrated herbaceous biomass plantations into JSBACH as a new plant functional type using the specific properties of *Miscanthus* and *Panicum* found in the literature whenever possible. Furthermore, I adjusted the leaf area index and carbon schemes of JSBACH to represent properties and annual harvest cycles typical for these plants. Lastly, I adapted the land-use scheme to allocate abandoned agricultural areas to herbaceous biomass plantations. This chapter describes in detail all the changes made to JSBACH to incorporate herbaceous biomass plantations and to simulate both idealized scenarios and a plausible scenario based on the land-use of RCP4.5.
This chapter evaluates the implementation of herbaceous biomass plantations using an idealized scenario in which the whole world is covered in herbaceous biomass plantations and compares them to various literature values for yields and water-use efficiency as well as to results from the LPJ-model. Although some uncertainties remain, on the whole, JSBACH can reproduce the literature values well enough for the rest of this study.
JSBACH can now represent herbaceous biomass plantations. These results can be used to introduce herbaceous biomass plantations into a more plausible scenario and assess their effect on the Earth System.

Chapter 3

Effects of Herbaceous Biomass Plantations on the Global Climate and Land Carbon Stocks: More Effective than Afforestation

3.1 Introduction

Herbaceous biomass plantations are often viewed as a climate engineering method because of their ability to replace fossil-fuels and thereby reduce emissions from fossil sources (Cannell, 2003). However, their deployment demands large areas of land, which leads to competition with other land-uses such as food production or forestry. Additionally, the conversion of any areas to herbaceous biomass plantations alters land carbon pools and land carbon dynamics. In this chapter, I explore the ability of herbaceous biomass plantations to affect the climate and carbon dynamics in a plausible scenario which preserves both food production and natural ecosystems, while minimizing losses from land conversion.

Biomass plantations can provide substantial amounts of energy and mitigate anthropogenic climate change simultaneously (Clifton-Brown et al., 2004; Beringer et al., 2011; Popp et al., 2012). The potentials for both energy production and climate mitigation are controversial and some argue that if biomass plantations displaced natural lands, the added emissions would exceed the mitigation potentials (Hughes et al., 2010; Dass, 2013; Searchinger et al., 2008). On the other hand, preserving natural ecosystems limits area extent available for cultivation of biomass plantations due to the need to preserve food security.

Three types of previous studies analyzed the effects of biomass plantations on the local or global climate. Studies using regional models resolve the effects of biomass plantations on local and regional ecosystems very finely but cannot represent global scales

(Clifton-Brown et al., 2004; Vanloocke et al., 2010; Le et al., 2011; Georgescu et al., 2011). Studies using Dynamic Global Vegetation Models (DGVMs) capture all land-based dynamics but lack feedbacks with the atmosphere and ocean (Beringer et al., 2011; Dass, 2013; Humpenöder et al., 2014; Heck et al., 2016; Boysen, 2016). Studies using global coupled Earth System Models (ESMs) for regional (Schaeffer et al. 2006) or global studies often idealize the land-use (Melillo et al., 2009; Hallgren et al., 2013), or represent biomass grasses as similar to other C4 grasses without accounting for their unique physiology (Hughes et al. 2010, see chapter 1). None of these studies analyzes the effects of herbaceous biomass plantations in a fully coupled model with a plausible land-use scenario. While most report average yields and associated potentials for climate mitigation, none assess the carbon dynamics and impacts to the extent analyzed here.

I study the effects of herbaceous biomass plantations in the fully coupled MPI-ESM using a hybrid scenario constructed from two representative concentration pathways (van Vuuren et al., 2011a). The hybrid scenario couples emissions from RCP8.5 (Riahi et al., 2011) to the land-use from RCP4.5 (Thomson et al., 2011). In RCP4.5, large areas of agricultural lands are abandoned (Hurtt et al., 2011). In my scenario, these areas are reclaimed for herbaceous biomass plantations. The hybrid scenario has three advantages: first, the high emissions from RCP8.5 allow maximum effects to be identified and isolated. Second, choice of the land-use of RCP4.5 prevents undesirable emissions from the displacement of natural ecosystems. In the land-use of RCP8.5, agricultural lands (crops and pastures) expand at the expense of natural areas. This expansion creates an emissions signal from deforestation which could counteract mitigation efforts and mask the signals from herbaceous biomass establishment and fossil-fuel substitution. The establishment of biomass plantations would further exacerbate this signal since they would displace even more natural ecosystems and hence increase emissions from land-use change even further. The original land-use of RCP4.5 does not determine the fate of the abandoned agricultural lands, they revert to whatever natural ecosystems successfully outcompete the others for that particular gridcell. Therefore, the establishment of herbaceous biomass plantations on these abandoned area is acceptable and would not generate additional emissions. Third, a previous study by Sonntag et al. 2016 uses the same hybrid scenario but with the original land-use from RCP4.5 as implemented in the MPI-ESM. They find that most areas revert to forests. Contrasting my results to those of Sonntag et al. 2016 allows a direct comparison between the effects of forest regrowth and the effects of herbaceous biomass plantations on the global climate.

Apart from the direct climatic effects, I explore the consequences of large-scale herbaceous biomass plantations for the land carbon budget. First, I analyze how changes in area and carbon density affect the land carbon stocks. Changes in area reflect the changes in land-use and dynamical vegetation changes while changes in carbon densities combine the effects of CO_2-fertilization, climate and disturbance on the vegetation. Second, I calculate the carbon budget of the areas reclaimed for herbaceous biomass

plantations. The carbon budget reflects the total change in carbon stocks on the abandoned areas between the afforestation scenario and the scenario with establishment of herbaceous biomass plantations. Third, I estimate the effectiveness of herbaceous biomass plantations at mitigating the climate compared to forests. The goal of this study is to comprehensively assess different aspects of the effects of herbaceous biomass plantations on the global climate and land carbon dynamics.

3.2 Simulation setup

I simulated large-scale deployment of herbaceous biomass plantations in the CMIP5 version of the global coupled model (MPI-ESM, see Chapter 2). All simulations combine emissions from the representative concentration pathway RCP8.5 and land-use from RCP4.5. The RCP4.5 land-use scenario projects large-scale abandonment of agricultural areas. In the original scenario, natural vegetation, especially forests, reclaim these areas. In my simulations herbaceous biomass plantations are established wherever abandoned agricultural areas would have reverted to forests in the original scenario. Only areas that would have reverted to forests are used because part of the goal of this study was to assess the mitigation potential of herbaceous biomass plantations as compared to that of afforestation in the original simulation from Sonntag et al. 2016. Simulations started in 2006 with the settings of the standard historical simulation and ended in 2100.

Table 3.1: Setup of the four simulations chosen for this study

	Low management input (harvest 55% of plant carbon)	**High management input (harvest 71% of plant carbon)**
No fossil-fuel substitution (FFS 0%)	HBPs55 0%FFS	HBPs71 0%FFS
Maximum fossil-fuel substitution (FFS 100%)	HBPs55 100% FFS	HBPs71 100% FFS

Management influences yields. In the case of biomass grasses, management influences the amount of harvestable material because biomass grasses optimize their carbon allocation to above- and below-ground plant-components depending on environmental factors (see chapter 2 for details). I explored a range of possible management options by harvesting different percentages, 55% and 71%, of total plant carbon. The percentages were chosen according to the root-to-shoot ratios measured by Meyer et al. 2010. I explored the effects of fossil-fuel substitution separately by simulating no substitution (0%) and maximum substitution (100%) for each management case. 0% fossil-fuel substitution represents a high global energy demand which would be met by any means

necessary. 100% fossil-fuel substitution represents an ideal case in which all harvested carbon substitutes and equal amount of coal and losses due to plantation management and transport are negligible (Cannell, 2003). Thus, I simulated a total of four scenarios, which together delimit the currently possible operating space. This operating space excludes any future developments in management techniques, genetic improvements or carbon capture and storage techniques (table 3.1).

3.3 Large-scale herbaceous biomass plantations influence global climate

Comparing my four simulations with the afforestation scenario shows how land-use change influences global climate. Herbaceous biomass plantations cover 5.6 million square kilometers at the end of the century, yet their cumulative yields account for significant changes in the global climate.

3.3.1 Cumulative global yields vary between 256 and 330 Pg

Globally herbaceous biomass plantations accumulate 256 Pg of harvested carbon over the 95 years of the simulation, in the 55% harvest scenario. In the 71% harvest scenario, herbaceous biomass plantations accumulate 330 Pg of harvested carbon. The level of fossil-fuel substitution has no effect on global accumulated yields which suggests that the climatic consequences of this form of terrestrial climate engineering do not negatively affect the productivity of herbaceous biomass plantations.

Table 3.2: Total yields for the 95 years of the simulation [Pg]

	Low management input (harvest 55% of plant carbon)	**High management input (harvest 71% of plant carbon)**
No fossil-fuel substitution (FFS 0%)	255.24	330.89
Maximum fossil-fuel substitution (FFS 100%)	256.29	333.67

3.3.2 Fossil-fuel substitution lowers atmospheric carbon dioxide concentrations and global temperatures

In all simulations global CO_2-concentrations (figure 3.1) more than double throughout the 21st century from 380 ppm in 2006 to more than 790 ppm in 2100 (table 3.3). CO_2-

concentrations surpass the levels of the baseline afforestation scenario in simulations with herbaceous biomass plantations but without fossil-fuel substitution by approximately 30 ppm. However, when herbaceous biomass plantations substitute fossil-fuels, CO_2-concentrations are lower than in the baseline afforestation scenario by 70-90 ppm. The temperature changes reflect changes in CO_2-concentrations. Temperatures in all simulations increase by 3-4°C throughout the 21st century. In the simulations without fossil-fuel substitution, they are slightly above those in the baseline afforestation scenario, whereas simulations with fossil-fuel substitution have lower temperatures.

Table 3.3: Carbon dioxide concentrations [ppm] and global temperatures [°C] at the end of the 21st century in the simulations with herbaceous biomass plantations compared to the beginning of the century (present day) and the afforestation baseline. HBPs: simulation with herbaceous biomass plantations; 55/71: 55% harvest or 71% harvest; 0/100% FFS: 0 or 100% fossil-fuel substitution.

Simulation	**Temperature [°C]**	**CO_2-concentrations [ppm]**
Present day (2006)	14.4	380.5
Afforestation	18.2	884.4
HBPs 55 0% FFS	18.5	915.7
HBPs 71 0% FFS	18.5	922.2
HBPs 55 100% FFS	17.6	814.7
HBPs 71 100% FFS	17.8	791.7

Herbaceous biomass plantations are C4 grasses and capable of living in a large variety of environments, hence the lack of variability in their global yields between the different climates analyzed in this study. C4 grasses react less sensitively to CO_2-fertilization than C3 plants because they decouple CO_2-uptake and photosynthesis. In spite of the growing advantages of C3 plants over C4 plants under higher CO_2-concentrations, herbaceous biomass plantations can significantly alter the global climate, especially when coupled with fossil-fuel substitution (figure 3.1). However, they are not capable of fully mitigating the effects of a high emission scenario such as RCP8.5 and temperatures and CO_2-concentrations still double compared to 2006. A reduction of 70-90 ppm agrees with Schaeffer et al. 2006, who find a reduction of 70-80 ppm compared to the standard SRES A1b scenario for woody biomass plantations on abandoned croplands in the northern extra-tropics.

The yields of 256-330 PgC fall within the 76-1424 PgC range reported by Boysen 2016 and the 4-570 PgC range found by Dass 2013 though both Boysen 2016 and Dass 2013 use a range of mostly idealized scenarios to calculate their potentials.

A temperature reduction of 0.4-0.6°C also agrees with the estimates of Dass 2013 (+0.1 to -0.35°C) and Boysen 2016 (-0.6 to -1.8°C). However, it contradicts the findings of Schaeffer et al. 2006 who find a decrease of only 0.1°C compared to a simulation with natural vegetation in the same areas, in spite of the similarity in the carbon

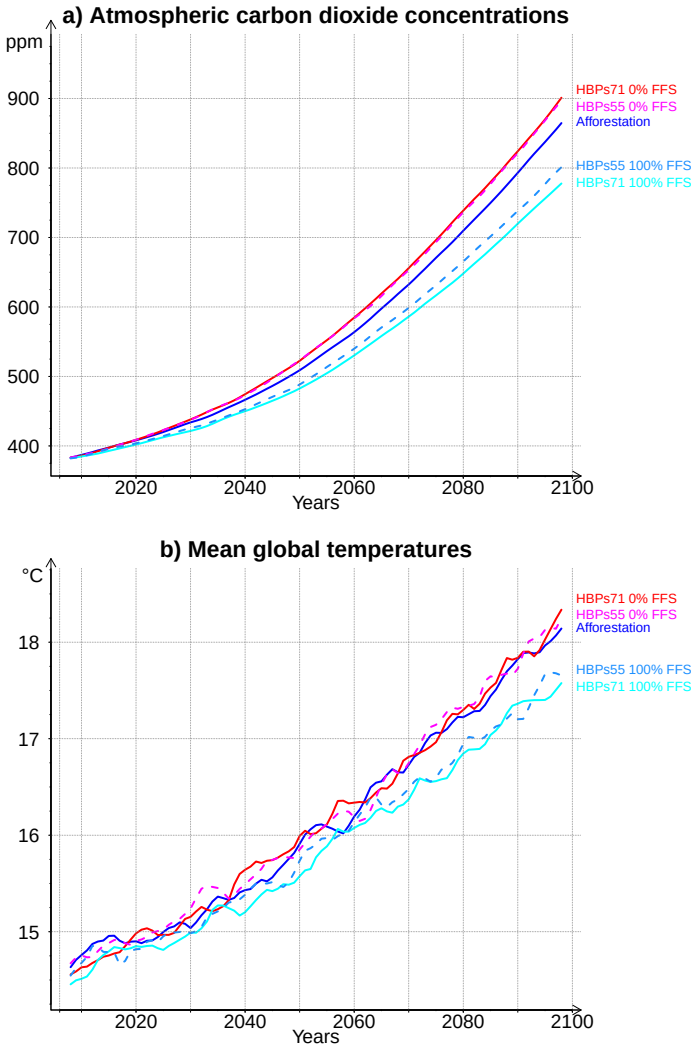

Figure 3.1: Global annual average CO_2-concentrations (in ppm) (a) and temperatures (in °C) (b) from 2006 to 2100 in the afforestation reference simulation and the four simulations with herbaceous biomass plantations (HBPs). Lines represent 5-year annual means. HBPs: herbaceous biomass plantations, 55/71: 55/71% harvest of total plant carbon, 0/100% FFS: 0/100% fossil-fuel substitution.

potential to our study. Possibly the choice of woody biomass plantations capable of snow-masking and associated albedo changes may have counteracted the carbon effects, although a difference in climate sensitivity between their model, IMAGE2.2, and MPI-ESM cannot be excluded. Hallgren et al. 2013 report a decrease of 0.01-0.06°C in 80-year equilibrium studies. In their study, the temperature reduction results from the biogeophysical effects associated with land-use change. These effects are partially counteracted by emissions due to displaced natural ecosystems. In my study, natural ecosystems are spared, preventing emissions on the same order of magnitude as the mitigation potential over the simulation period. Thus, the chosen land-use scenario, in part, determines the success of the chosen mitigation measure.
The global values show that herbaceous biomass plantations with fossil-fuel substitution are more effective at mitigating the climate than afforestation after approximately 15-20 years. They also show that without fossil-fuel substitution, afforestation is more effective. However, they cannot illustrate how much individual processes contribute to the overall effectiveness or determine the spatial distribution of carbon stocks.

3.3.3 Gross and net primary production respond to CO_2-concentrations

Primary production increases in all simulations, reacting to rising temperatures, CO_2-fertilization and land-cover change (figure 3.2). Gross primary production (GPP) reacts directly to climatic conditions and CO_2-concentrations. Net primary production (NPP) includes autotrophic respiration, which also responds to climate conditions. Land-cover change contributes to the increases in gross and net primary production. In all simulations large areas of crops and pastures are replaced by natural grasslands, forests or herbaceous biomass plantations, all of which are more productive than crops and pastures.
Gross and net primary production differ greatly between simulations (table 3.4), partly because of differing amounts of CO_2-fertilization and partly because of differing weather and climate conditions between the different simulations. In the simulations with herbaceous biomass plantations but without fossil-fuel substitution, gross primary production exceeds that in simulations with fossil-fuel substitution, a clear indication of the role of CO_2-fertilization. However, net primary production reacts to a combination of gross primary production and respiration. Both depend on climate variables such as temperature and precipitation, which can vary significantly between years.

Table 3.4: Gross and Net primary production for the different simulations in the year 2100. GPP: gross primary production; NPP: net primary production; HBPs: simulation with herbaceous biomass plantations; 55/71: 55% harvest or 71% harvest; 0/100% FFS: 0 or 100% fossil-fuel substitution.

Simulation	**GPP [PgC/a]**	**NPP [PgC/a]**
Present day (2006)	180	90
Afforestation	258.8	123.3
HBPs 55 0% FFS	271.0	123.5
HBPs 71 0% FFS	265.5	121.9
HBPs 55 100% FFS	267.7	124.1
HBPs 71 100% FFS	259.9	120.0

3.4 Changes in land carbon stocks

3.4.1 Mathematical analysis

Land carbon stocks change in response to changes in area occupied by different PFTs (area-driven) and by changes in densities of carbon on available areas (density-driven). Area-driven changes result from land-use change, dynamical vegetation and their interplay. Density-driven changes result from changes in plant productivity and respiration. The change in carbon stock is the difference between the carbon stocks at different times:

$$\Delta C = C_1 - C_0 \tag{3.1}$$

Where C_1 represents the carbon stocks at timestep 1, C_0 represents the carbon stocks at the beginning of the simulation and ΔC is the difference between the two.
The carbon stocks of any PFT at any given time are a function of the density multiplied by the area occupied by the PFT:

$$C = \rho A \tag{3.2}$$

Where ρ is the carbon density and A is the area occupied by the analyzed plant functional type.
By combining the two equations above, we can express the change in carbon stocks as a function of the densities and the areas:

$$\begin{aligned} \Delta C &= \rho_1 A_1 - \rho_0 A_0 \\ &= (\rho_0 + \Delta\rho)(A_0 + \Delta A) - \rho_0 A_0 \\ &= \rho_0 \Delta A + \Delta\rho A_0 + \Delta\rho\Delta A \end{aligned} \tag{3.3}$$

Where $\rho_0 \Delta A$ represents the area-driven changes in carbon stocks, $\Delta\rho A_0$ represents the density-driven changes in carbon stocks and $\Delta\rho\Delta A$ represents the synergy between the two. Any one of these terms can be positive or negative, so that total carbon stock changes may be smaller or larger than changes would be, if only one effect were present.

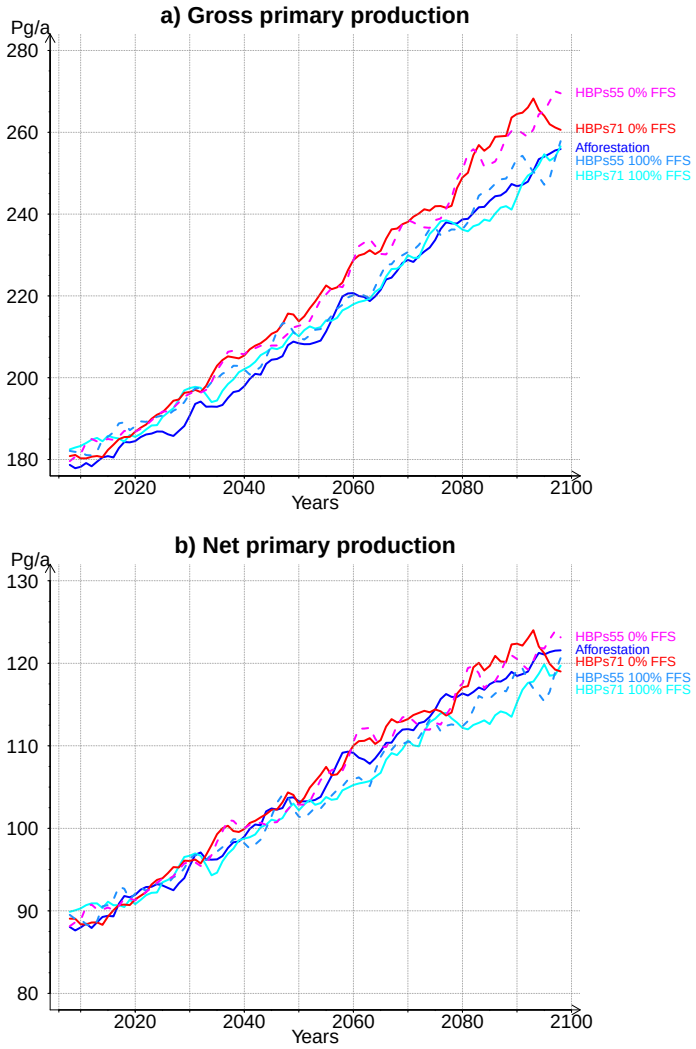

Figure 3.2: Gross (a) and net (b) primary production (in Pg) from 2006 to 2100 in the afforestation reference simulation and the four simulations with herbaceous biomass plantations (HBPs). Lines represent 5-year annual means. HBPs: herbaceous biomass plantations, 55/71: 55/71% harvest of total plant carbon, 0/100% FFS: 0/100% fossil-fuel substitution.

3.4.2 Forests dominate land carbon stocks

The areas of the different land-use types shrink and expand throughout the 21st century as a result of land-use change and climate-driven shifts of natural vegetation (figure 3.3). Forests expand in all simulations but most in the afforestation scenario, where they gain 8.4 million km^2 compared to 4.7 million km^2 in the simulations with herbaceous biomass plantations (table 3.5). In the afforestation scenario, two factors drive forest expansion: the abandonment of agricultural areas (crops and pastures) and the warming of the Arctic, which leads to more favorable growing conditions for forests in northern latitudes and a gradual replacement of grasses with forests, but forests can still expand onto grasslands in the boreal zone. In the scenarios with herbaceous biomass plantations, abandoned agricultural areas are reclaimed for herbaceous biomass plantations and are therefore not available for forests. The presence of herbaceous biomass plantations and the differences in climate influence the local dynamics of natural vegetation changes, so that total area of natural grasses is reduced in simulations with herbaceous biomass plantations compared to the afforestation baseline. Crops and pastures collectively shrink by approximately 6.5 million km^2 most of which (5.6 million km^2) is reclaimed for herbaceous biomass plantations.

Table 3.5: Area of the different land-use types in the year 2100 compared to present day conditions.

Simulation	**Area [10^6]km^2**			
	Forest	Grass	Pastures and Crops	Herbaceous biomass plantations
Present day	42	20	42	0
Afforestation	50.4	25.6	35.1	0
Modified land-use scheme	46.7	23.7	35.1	5.6

The other 0.9 million km^2 revert to grasslands. Nevertheless, the area of grasses are reduced compared to the afforestation scenario. Natural vegetation reacts dynamically to climatic conditions. In JSBACH, these interactions occur independently of the land-use scheme. However, just as in the land-use scheme, areas shift proportionally to the available areas. As forest areas are smaller in the herbaceous biomass plantations scenarios, any shifts to grasses will necessarily also be smaller, which leads to smaller grassland extents compared to the afforestation baseline.

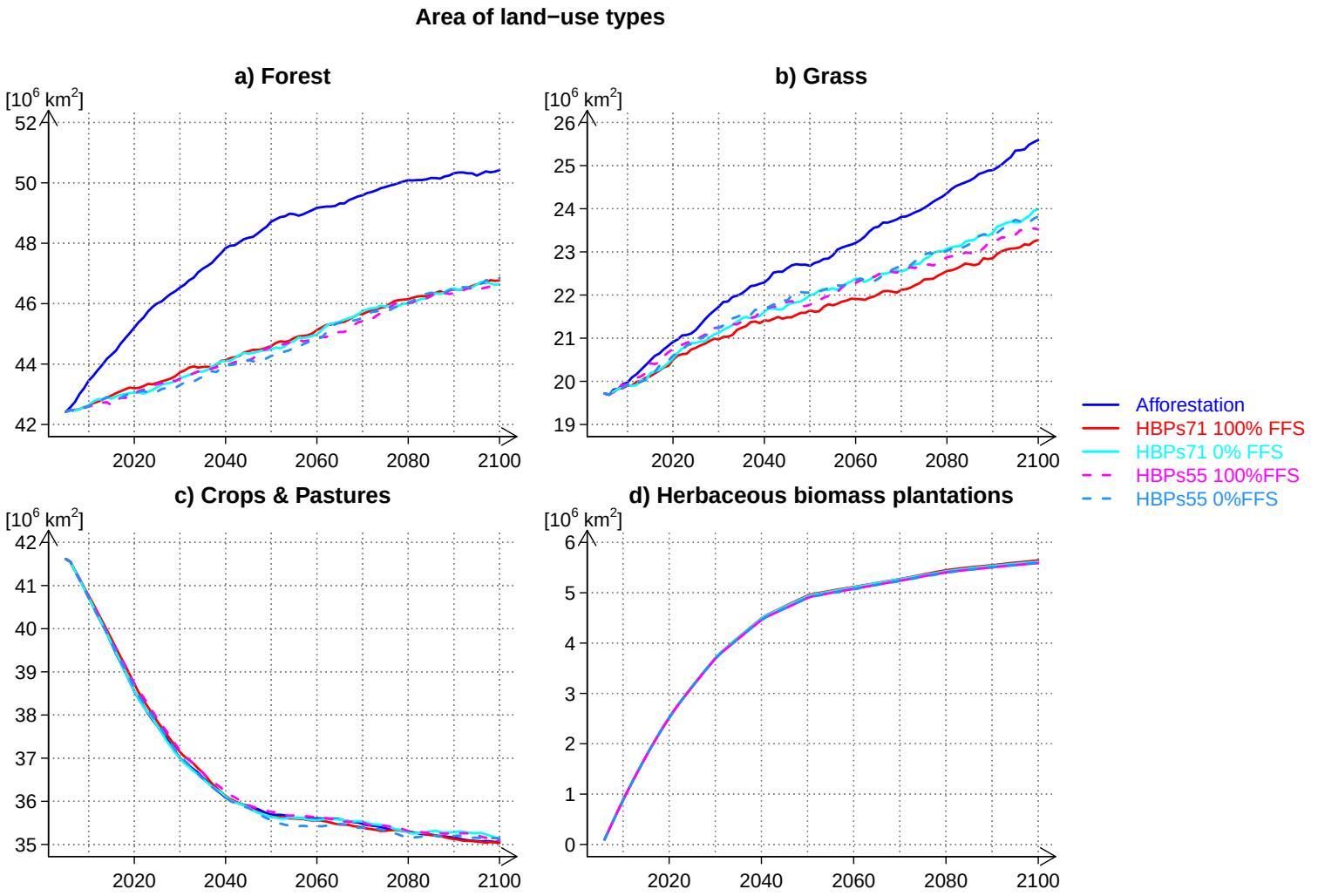

Figure 3.3: Area changes (in millions of square kilometers) of forests (a), grasses (b), crops and pastures (c) and herbaceous biomass plantations (d) from 2006 to 2100 in the afforestation reference simulation and the four simulations with herbaceous biomass plantations (HBPs). HBPs: herbaceous biomass plantations, 55/71: 55/71% harvest of total plant carbon, 0/100% FFS: 0/100% fossil-fuel substitution. The curves for crops and pastures as well as for herbaceous biomass plantations are all on top of each other showing that the land-use scenarios are consistent between simulations.

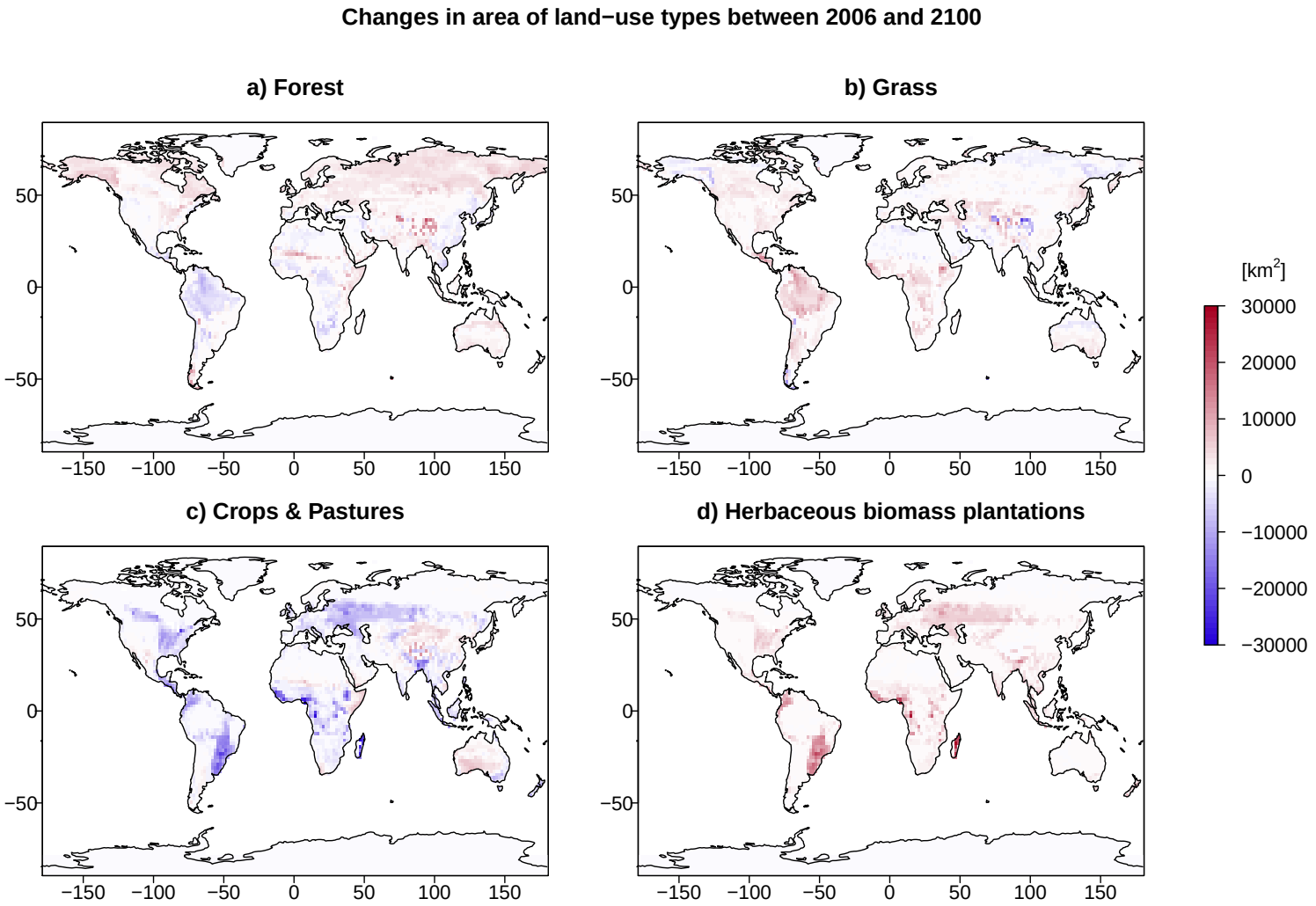

Figure 3.4: Changes in area (in square kilometers) of forests (a), grasses (b), crops and pastures (c) and herbaceous biomass plantations (d) from 2006 to 2100 in the simulation with 71% harvest and 100% fossil-fuel substitution.

Patterns of area changes (figure 3.4) differ between regions. Forests expand in the boreal zones and contract in the tropics. Grasses contract in the boreal zones and expand in the tropics, almost mirroring the patterns seen in forests. These changes are driven by changing climate conditions that alter the competitiveness of the two types compared to each other. Crops and pastures contract in Europe, most of Africa and the Americas. However, they expand in East Asia, Australia and the horn of Africa. These changes are solely driven by local land requirements as projected by the RCP4.5. Area and density changes drive changes in carbon stocks. Carbon density in plants is determined by plant type and CO_2-concentrations in the atmosphere. Higher concentrations of CO_2 increase photosynthetic efficiency and carbon fixation rates, especially in C3 plants. In the simulations with herbaceous biomass plantations, increases in forest carbon stocks are mainly density-driven (figure 3.5), both in the tropics and in the boreal regions. Area driven-changes decrease forest carbon stocks in the tropics because of area losses to grasses, but slightly increase carbon stocks in the boreal regions as forests expand northwards. The synergistic effects are small compared to the individual effects. In most areas plant carbon stocks in forests increase. However, in some areas of the Amazon basin, forest plant carbon stocks decrease because area-driven changes dominate in this region.

Plant carbon stocks of herbaceous biomass plantations increase throughout the century as a result of their expanding areas. Densities do not contribute to this increase since these C4 grasses reach their maximum plant carbon densities quickly and are not significantly affected by CO_2-fertilization. Total carbon changes in plants are much smaller than forests because these grasses do not accumulate woody biomass.

Soil carbon changes under forests are much more heterogeneous (figure 3.6). While soil carbon stocks increase in the northern hemisphere and some parts of the tropics, like central Africa, they decrease in parts of the Amazon basin, subtropical Africa and east Asia. The increase in the northern hemisphere is driven by both area and density changes, while the increases in the tropics are mainly density-driven and the decreases in the tropics are essentially area-driven. Again, the synergistic effects are minimal. Total soil carbon changes under forests in the tropics therefore depend on whether the area- or the density-driven changes dominate.

Soil carbon changes under herbaceous biomass plantations are dominated by the area-driven changes. The density-driven changes are minimal but the synergistic effects counteract the effects of herbaceous biomass plantations. Overall, soil carbon stocks under herbaceous biomass plantations increase throughout the century. However, this could result from herbaceous biomass plantations being established on soils already containing high amounts of carbon.

Total changes of carbon stocks in forests closely follow the soil carbon stock patterns which dominate over the plant carbon stocks (figure 3.7). For herbaceous biomass plantations, total carbon stocks increase throughout the century, mostly dominated by the area-driven and synergistic effects.

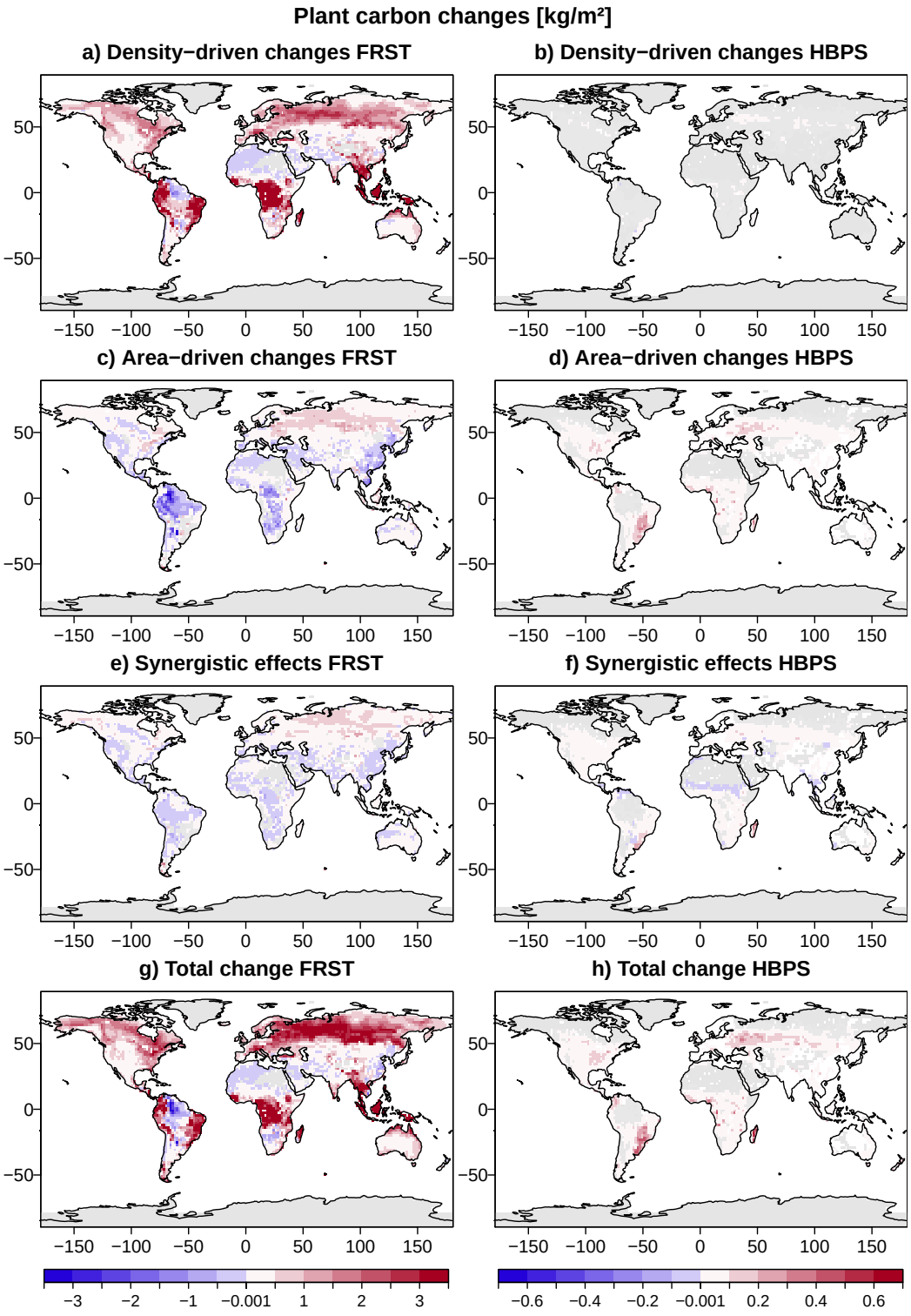

Figure 3.5: Density- (a,b) and area-driven (c,d) changes in plant carbon pools for forests (FRST) and herbaceous biomass plantations (HBPS) as well as synergistic effects (e,f) and total plant carbon change (g,h) all units in PgC. Red designates increases in carbon stocks, blue indicates decreases in carbon stocks, gray areas indicate no changes in carbon stocks. Forests and herbaceous biomass plantations are plotted to different scales because carbon stocks in plants in these two land-use types differ by two orders of magnitude. Data shown for the simulation with 71% harvest and 100% fossil-fuel substitution.

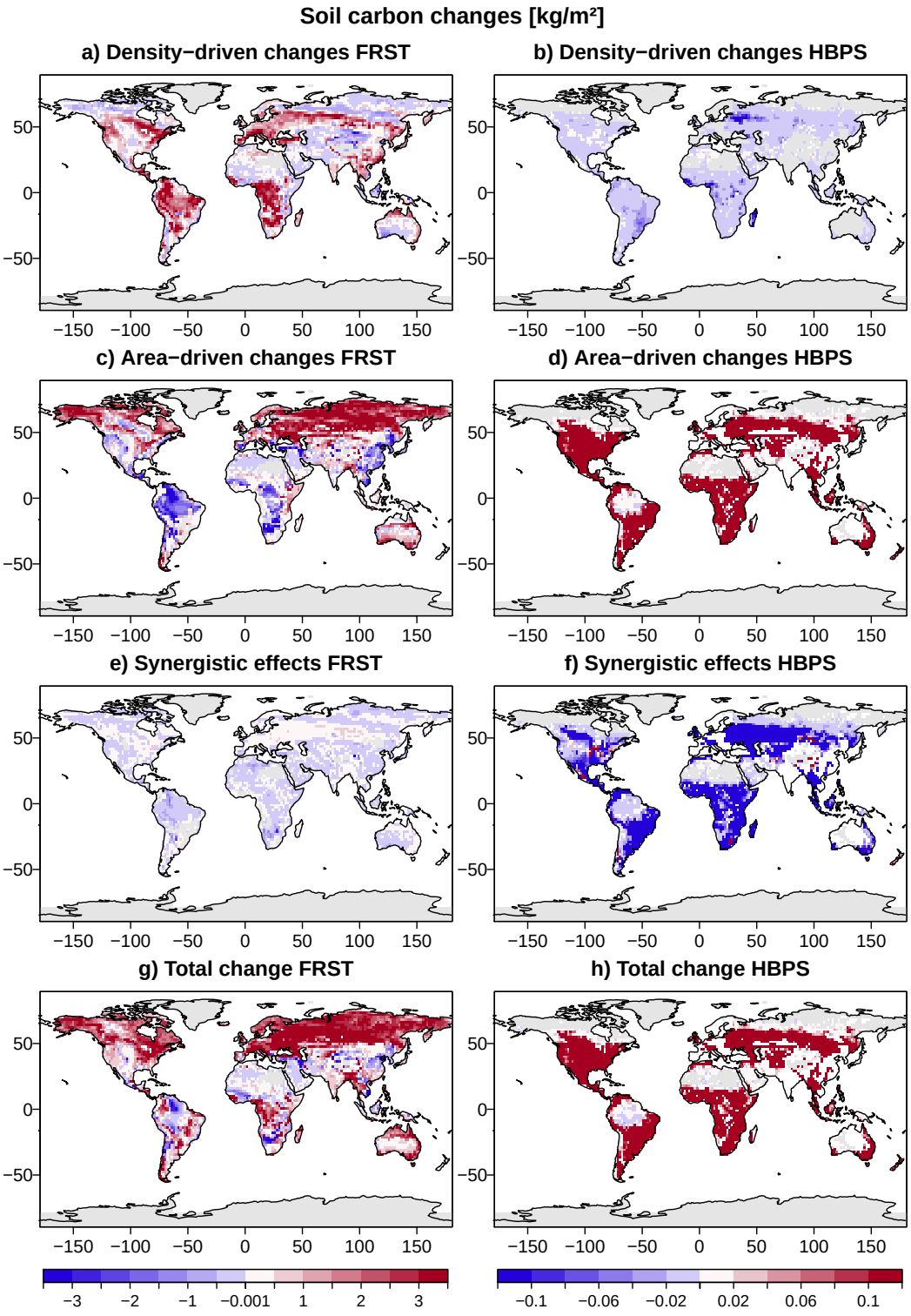

Figure 3.6: Density- (a,b) and area-driven (c,d) changes in soil carbon pools for forests (FRST) and herbaceous biomass plantations (HBPS) as well as synergistic effects (e,f) and total plant carbon change (g,h) all units in PgC. Red designates increases in carbon stocks, blue indicates decreases in carbon stocks, gray areas indicate no changes in carbon stocks. Data shown for the simulation with 71% harvest and 100% fossil-fuel substitution.

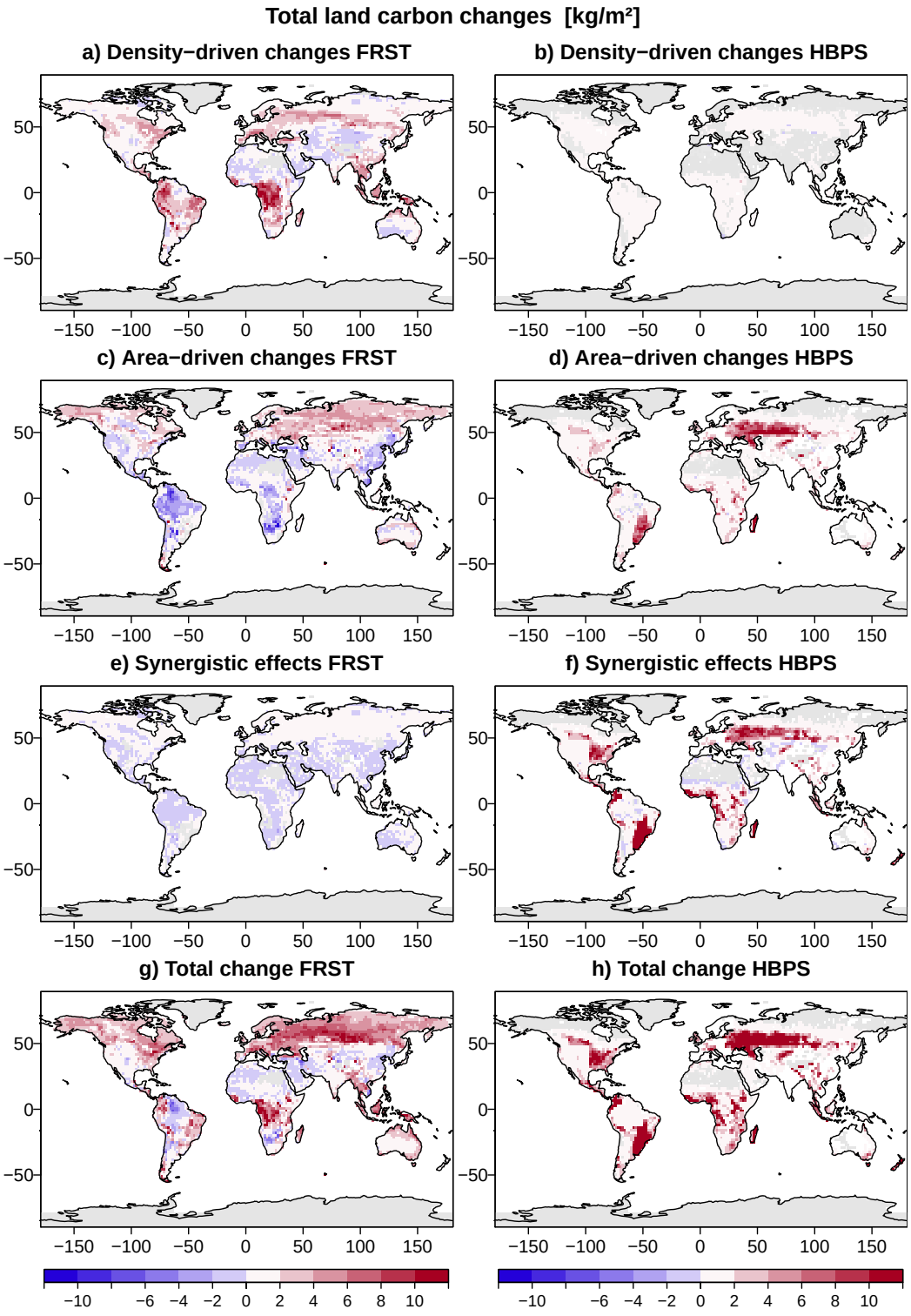

Figure 3.7: Density- (a,b) and area-driven (c,d) changes in total carbon pools for forests (FRST) and herbaceous biomass plantations (HBPS) as well as synergistic effects (e,f) and total plant carbon change (g,h) all units in PgC. Red designates increases in carbon stocks, blue indicates decreases in carbon stocks, gray areas indicate no changes in carbon stocks. Carbon pools for herbaceous biomass plantations include the harvested carbon. Data shown for the simulation with 71% harvest and 100% fossil-fuel substitution.

3.4.3 Forest carbon densities increase while herbaceous biomass plantations areas expand

Increases in carbon density are mainly driven by climate, primarily caused by CO_2-fertilization. However, outside the tropics, increasing temperatures in early spring and late autumn prolong growing seasons, adding to carbon accumulation and density increases. Densities decrease when plants die because of unfavorable conditions. Plants can die because of a variety of reasons. Drought, frost or disturbances, such as fire or storms, can kill plants or plants may be outcompeted by a plant type which is better adapted to the new climate.

Areas change for three reasons: land-use change, competition between plant types and expansion or contraction of unsuitable areas. Land-use change responds to demographic, social and economic pressures. Competition between plant types responds to climatic changes. Unsuitable areas such as glaciers or deserts expand and contract in response to climatic conditions, such as when glaciers melt due to rising temperatures, or in response to human activities, such as when deserts expand in response to deforestation or overgrazing. In the RCP4.5 scenario, land-use change is driven by social pressures to intensify agriculture and reduce meat consumption. As a result, agricultural areas shrink freeing space which my study reclaims for herbaceous biomass plantations.

Land carbon stocks result from the interplay between area and density. Area increases decrease carbon densities because densities are averaged over the available area. This can decrease densities, especially for carbon stocks that accumulate slowly over long periods of time, such as wood or soil carbon stocks. Conversely, area decreases don't necessarily increase densities because plant carbon escapes to the atmosphere while soil carbon remains on site and is attributed to the new plant type. Plant carbon is lost from the land either directly as a result of biomass burning, or indirectly by removal for human use. In both cases, JSBACH assumes that most plant carbon is returned to the atmosphere rapidly. Moreover, plant productivity governs both densities and areas simultaneously. Increased productivity increases carbon fixation and therefore densities but it also increases the competitive fitness of a plant type, leading to an area expansion at the expense of other plant types. Decreased productivity reduces both densities and areas by the same effect. Thus, densities and areas vary in synchrony, creating synergistic effects.

My study disentangles the area- and density-driven changes as well as the synergistic effects. Most of the changes in carbon stocks of forests and herbaceous biomass plantations can be explained either by the density-driven or by the area-driven changes, while the synergistic effects play a relatively minor role. Unsurprisingly, changes in forest carbon stocks are much larger than changes in herbaceous biomass plantations. This results from the overall larger carbon stocks present in forests.

In JSBACH, agricultural products are not harvested but added to the soil carbon annually to simulate harvest. The model thus tends to overestimate soil carbon on

agricultural areas (Nyawira et al., 2016). This may influence the distribution of soil carbon even on natural areas, since the soil carbon is attributed to the new areas when agricultural fields are abandoned. These legacy-effects may lead to an over-estimation of soil carbon under herbaceous biomass plantations at the beginning of the simulation when large areas of former agricultural lands are reclaimed for herbaceous biomass plantations. Additionally, since for herbaceous biomass plantations the harvest is removed from the fields, the model may show an unrealistic depletion of soil carbon due to the establishment of herbaceous biomass plantations. Some literature results suggest that herbaceous biomass plantations increase soil carbon and improve soil properties on heavily degraded lands because of their capacity to recycle nutrients (Beale and Long, 1997). Thus, caution must be applied when interpreting soil carbon changes.

3.5 Carbon budget of areas with herbaceous biomass plantations

The previous section analyzed the global changes in carbon stocks. This section analyzes how carbon stocks change on the abandoned agricultural areas which are transformed into herbaceous biomass plantations in my simulations and compares them to the carbon stocks on the same areas in the afforestation scenario. The goal is to estimate the change in sink capacity (CISC), the total change in carbon between the afforestation and herbaceous biomass plantation simulations, on the area under scrutiny.

3.5.1 Mathematical analysis

The change in sink capacity is defined as the change in carbon stocks of forests minus the change in carbon stocks of herbaceous biomass plantations:

$$CISC := \Delta C_{FRST} - \Delta C_{HBPs} = (\rho_{2100FRST} - \rho_{2100HBPs}) * A_{HBPs} \tag{3.4}$$

Where ΔC_{FRST} is the difference in carbon stocks of forests between 2006 and 2100 and ΔC_{HBPs} is the difference in carbon stocks of herbaceous biomass plantations between 2006 and 2100, $\rho_{2100FRST}$ and $\rho_{2100HBPs}$ are the carbon densities of forests and herbaceous biomass plantations in 2100 and A_{HBPs} is the are of herbaceous biomass plantations in 2100. The density of forests can further be broken down into the density of forest in 2006 (ρ_{0FRST}) plus the change in density ($\Delta\rho$). The change in sink capacity then becomes:

$$CISC = \Delta A_{HBPs} * \rho_{0FRST} + \Delta A_{HBPs} * \Delta\rho_{FRST} - \Delta A_{HBPs} * \rho_{2100HBPs} \tag{3.5}$$

Three terms emerge from this equation. The first term describes the potential carbon stocks of a mature forests on the areas covered by herbaceous biomass plantations

under present-day climate conditions. They therefore represent the prevented forest sink in a constant climate under the assumption that all areas are abandoned at the beginning of the simulation. Interestingly, the term simultaneously describes the amount of carbon emissions avoided by establishing herbaceous biomass plantations on abandoned agricultural areas rather than forests. These avoided emissions (AVEM) do not contain increases in carbon densities due to forest growth or carbon dioxide fertilization.

$$AVEM = \Delta A_{HBPs} * \rho_{0FRST} \tag{3.6}$$

When biomass plantations claim abandoned agricultural areas, they prevent forest establishment on these areas. If forests had reclaimed these areas, they would have acted as a carbon sink equivalent to the avoided emissions and an additional carbon sink due to CO_2-fertilization throughout the century. The second term of equation 3.5 describes this loss of additional sink capacity (LASC).

$$LASC = \Delta A_{HBPs} * \Delta \rho_{FRST} \tag{3.7}$$

The areas on which herbaceous biomass plantations grow are not barren. In order to assess the change in sink capacity, the carbon stored in herbaceous biomass plantations in 2100 has to be accounted for:

$$\text{land HBPs sink} = \rho_{2100HBPs} * \Delta A_{HBPs} \tag{3.8}$$

Thus, equation 3.5 shows the carbon budget of the areas covered by herbaceous biomass plantations:

$$CISC = \underbrace{\Delta A_{HBPs} * \rho_{0FRST}}_{\text{AVEM}} + \underbrace{\Delta A_{HBPs} * \Delta \rho_{FRST}}_{\text{LASC}} - \underbrace{\Delta A_{HBPs} * \rho_{2100HBPs}}_{\text{land HBPs sink}} \tag{3.9}$$

Here, the harvested carbon used for fossil-fuel substitution is not included in the carbon density of herbaceous biomass plantations, because only the land carbon sink is assessed. All relations are calculated for the carbon stored in plants, the carbon stored in soils and for total ecosystem carbon. Total ecosystem carbon gives a measure of the extreme change in sink capacity for a replacement of forests by herbaceous biomass plantations, assuming that all carbon stored in soils were lost over the period and replaced with carbon input from herbaceous biomass plantations.

3.5.2 114 Pg of carbon less on areas with herbaceous biomass plantations compared to afforestation

Areas covered by herbaceous biomass plantations store 114 Pg less carbon than if they were covered by forests (table 3.6) under the assumption that after 95 years, all carbon previously stored in soils has decayed and was emitted to the atmosphere.

Over the same time period, forests could have developed a potential sink of 248 Pg carbon (212+36 PgC), a sink almost equivalent to the 255 PgC minimum harvest estimate for herbaceous biomass plantations under the 55% harvest scheme (table 3.2). However, if the harvest sink of 255-330 PgC (table 3.2) is added to the on-site sink of herbaceous biomass plantations (114 PgC), the total sink becomes 390-468 PgC and the total carbon balance becomes negative, with additional 142-220 PgC sequestered by herbaceous biomass plantations compared to forests.

Table 3.6: Global carbon budget of areas with herbaceous biomass plantations compared to afforestation. AVEM: avoided emissions; LASC: loss of additional sink capacity; HBPs Sink: carbon sink of herbaceous biomass plantations; CISC: change in sink capacity due to the replacement of forests with herbaceous biomass plantations. All numbers for the simulation with 71% harvest and 100% fossil fuel substitution. Differences between simulations are small. The harvested carbon is not included in the HBPs Sink.

Carbon type	**AVEM [Pg]**	**LASC [Pg]**	**HBPs Sink [Pg]**	**CISC [Pg]**
Plant	42	22	4	61
Soil	170	14	131	53
Total	212	36	135	114

Regionally, the patterns of avoided emissions, loss of additional sink capacity and change in sink capacity match the distribution of herbaceous biomass plantations (figure 3.8). The highest values are found in south-eastern South America, south-eastern North America, central Eurasia and western Africa, where herbaceous biomass plantations cover the largest extents. Without the harvested carbon, the carbon balance is positive almost everywhere, except for a few sites in the Himalayas where the carbon balance is negative. Results coincide between simulations.

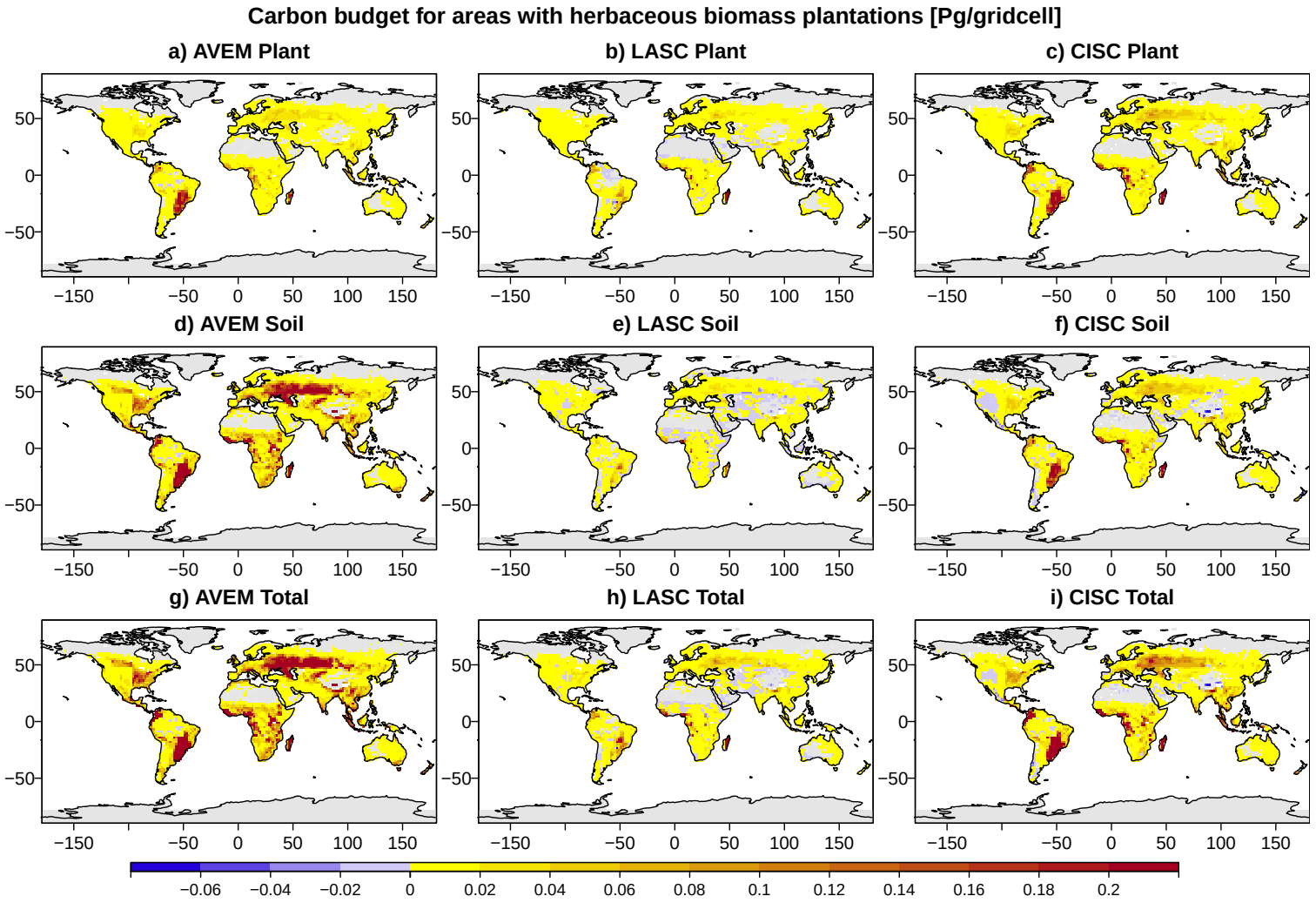

Figure 3.8: Avoided emissions (AVEM, a,d,g), loss of additional sink capacity (LASC, b,e,h) and change in sink capacity (c,f,i) of plant (a,b,c), soil (d,e,f) and total ecosystem carbon (g,h,i).

3.5.3 The potential forest sink almost equates the estimated harvest

JSBACH computes each plant functional type in every gridcell so that the productivity of each plant type can be assessed even when the extent of that plant type is negligible. Importantly, this setup allows estimating the potential productivity and carbon storage capacity of any plant type on any area within the same climate. Here, I estimate the carbon storage capacity of forests on the areas covered by herbaceous biomass plantations and calculate the carbon budget of these areas.
The avoided emissions represent two different, yet similar, carbon pools. On the one hand, the avoided emissions are the amount of carbon forest ecosystems would have lost if herbaceous biomass plantations had been established, in 2006, at the expense of forests rather than on agricultural areas. On the other hand, the avoided emissions also represent a prevented sink, the amount of carbon forests could have stored, had they been established on these agricultural fields in 2006. However, the avoided emissions are only valid under constant climate.
The loss of additional sink capacity represents the amount of additional carbon forests could store on the same area, due to CO_2-fertilization in the changing climate of a simulation. Similarly to the avoided emissions, this could apply to a forest hypothetically displaced by herbaceous biomass plantations or to a hypothetical forest growing on the areas reclaimed for herbaceous biomass plantations. The avoided emissions and the loss of additional sink capacity together represent the maximum amount of carbon forests could store on the area used for herbaceous biomass plantations.
The HBPs-sink represents the actual amount of carbon stored on the areas under scrutiny due to the presence of herbaceous biomass plantations in 2100. This sink only accounts for the amount of carbon in the fields and does not include the carbon stored in the form of unburnt fossil-fuels. Thus, the change in sink capacity only represents the changes in land carbon sink, not the total mitigation potential of herbaceous biomass plantations.
In all simulations the potential forest sink (avoided emission and loss of additional sink capacity) of 248 PgC (table 3.6) almost equates the estimated harvest of 255-330 PgC (table 3.2). This similarity limits the mitigation potential of herbaceous biomass plantations compared to forests and illustrates the trade-off between carbon storage on land and fossil-fuel substitution. Every square meter of land used for herbaceous biomass plantations cannot be used to store carbon in forests.
Importantly, many factors that the model represents only in a very limited way could influence actually realizable yields of herbaceous biomass plantations. Localized recurring droughts, storms or flooding events could limit plant productivity and shift the balance in favor of forests. On the other hand, literature values suggest that some areas may produce even higher yields, which would shift the carbon balance in favor of herbaceous biomass plantations (see Chapter 2).
These findings illustrate the spatial and temporal dimensions involved. In order to

maximize the mitigation potential of herbaceous biomass plantations, policy makers need to identify the areas where the effectiveness of herbaceous biomass plantations is highest compared to forests. Yet, even on the least effective areas, herbaceous biomass plantations eventually will be more effective than forests at mitigating the climate because the effects of fossil-fuel substitution accumulate over time whereas the land carbon sink saturates. Nevertheless, choosing areas where herbaceous biomass plantations quickly become more effective than forests increases their mitigation potential. However, avoided emissions, loss of additional sink capacity, the HBPs-sink and the change in sink capacity are all dependent on the chosen land-use scenario.

3.6 Effectiveness of herbaceous biomass plantations

The scenario setup allows a direct comparison of herbaceous biomass plantations with afforestation. This allows answering several central questions:

- Which of the two land-use types mitigates the climate most effectively?
- Can fossil-fuel substitution make herbaceous biomass plantations more effective than afforestation and what level of substitution is needed to achieve this increased effectiveness?
- On what timescales do the relevant processes operate?

3.6.1 Mathematical analysis

Effectiveness is the carbon density (per unit vegetated area, that is the area covered by that land-use type) of one land-use type compared to another. The effectiveness of herbaceous biomass plantations compared to afforestation is the carbon density of forests minus the carbon density of herbaceous biomass plantations:

$$Eff = \rho_{FRST} - \rho_{HBPS} \tag{3.10}$$

Where ρ is the carbon density per unit vegetated area, FRST stands for forest and HBPS for herbaceous biomass plantations. The effectiveness emerges from the change in sink capacity (eq. 3.5) and expresses the difference in capacity of a given area to draw carbon from the atmosphere depending on whether it is covered by forests or herbaceous biomass plantations. The change in sink capacity can also be expressed as:

$$CISC = Eff * \Delta A_{HBPs} \tag{3.11}$$

In the case of herbaceous biomass plantations with fossil-fuel substitution, the amount of carbon harvested and used for fossil-fuel substitution over the lifetime of the plantation has to be added to its carbon density, because the harvested carbon is part of

plantation's ability to draw carbon from the atmosphere. Since the substitution-effect accumulates over time, herbaceous biomass plantations become more effective the longer they are in use. Herbaceous biomass plantations mitigate the climate more effectively than forests if the effectiveness is negative. The effectiveness is calculated for every year of the simulation. Herbaceous biomass plantations are considered more effective than afforestation for a gridcell in a given year, if the running mean effectiveness of five consecutive years is negative. I use a running mean to reduce the effects of short-term variations in productivity, especially in forests.
The level of substitution required for herbaceous biomass plantations to become more effective than afforestation is calculated by linearly interpolating between the effectiveness of 0% fossil-fuels substitution and the effectiveness of 100% fossil-fuel substitution. The relation is interpolated for each year so that the effectiveness of any given level of fossil-fuel substitution can be assessed for any given year. For my study I chose two levels of fossil-fuel substitution, 30% and 70%, which reflect typical values of currently technologically achievable carbon savings for bioenergy compared to fossil-fuels (Gallagher, 2008).

3.6.2 The effectiveness of herbaceous biomass plantations compared to forests increases over time

In the year 2100 herbaceous biomass plantations with 100% fossil-fuel substitution mitigate the climate more effectively than afforestation in all gridcells (figure 3.9a). Compared to herbaceous biomass plantations without fossil-fuel substitution, afforestation is more effective (figure 3.9b). In most gridcells, herbaceous biomass plantations with fossil-fuel substitution are more effective than afforestation even at lower levels of substitution (figure 3.9d). At 70% fossil-fuel substitution, herbaceous biomass plantations are effective over much of the globe, while at 30% fossil-fuel substitution, only some areas, such as North America, the Amazon basin and small areas of Asia and Africa, favor herbaceous biomass plantations over afforestation.
Fossil-fuel substitution increases the effectiveness of herbaceous biomass plantations because the harvested carbon accumulates and increases the total carbon storage capacity of this plant type. Since the effectiveness compares the potential of afforestation and herbaceous biomass plantations to draw CO_2 out of the atmosphere, the harvested carbon must be included in all effectiveness calculations. In JSBACH, wood harvest is currently not used for fossil-fuel substitution, however, if it was, this would greatly change the effectiveness of herbaceous biomass plantations compared to forests.
In many gridcells herbaceous biomass plantations become more effective than afforestation within only a few years after establishment (figures 3.9c and 3.10a & b). However, the time needed for herbaceous biomass plantations to become more effective decreases with increasing levels of fossil-fuel substitution. At 30% fossil-fuel substitution, areas where herbaceous biomass plantations become effective early are restricted to areas

where forests do not grow particularly well, such as the Western US. In most areas, this level of substitution only becomes more effective than afforestation in the last decades of the 21st century.
At 100% fossil-fuel substitution, the area of herbaceous biomass plantations needed to mitigate climate at the same level as forests in the afforestation simulation amounts to 2.9 million km^2. This is slightly more than half the area available. All additional land used for herbaceous biomass plantations mitigates the climate beyond the capacities of forests.

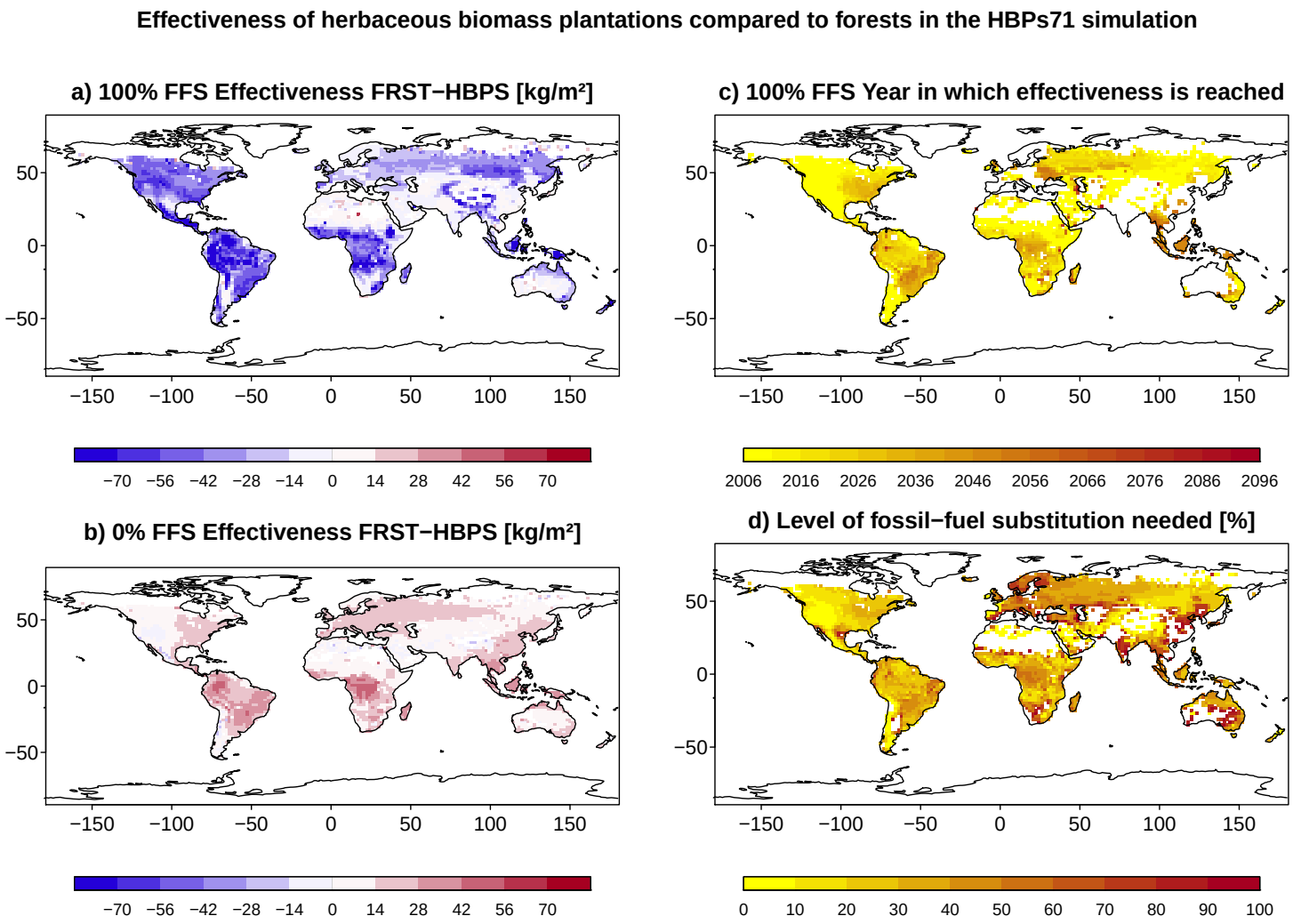

Figure 3.9: Effectiveness of herbaceous biomass plantations compared to forests: a) for 100% fossil-fuel substitution, b) for 0% fossil-fuel substitution. c) Year in which 5-year mean effectiveness becomes negative in each gridcell for 100% fossil-fuel substitution. d) Level of fossil-fuel substitution needed for herbaceous biomass plantations to exceed the effectiveness of forests in the year 2100. All graphs refer to the simulations with 71% harvest (HBPs71). FFS: fossil-fuel substitution, FRST-HBPS: measure of effectiveness, carbon density of forests minus carbon density of herbaceous biomass plantations (including fossil-fuel substitution for the lifetime of the plantations).

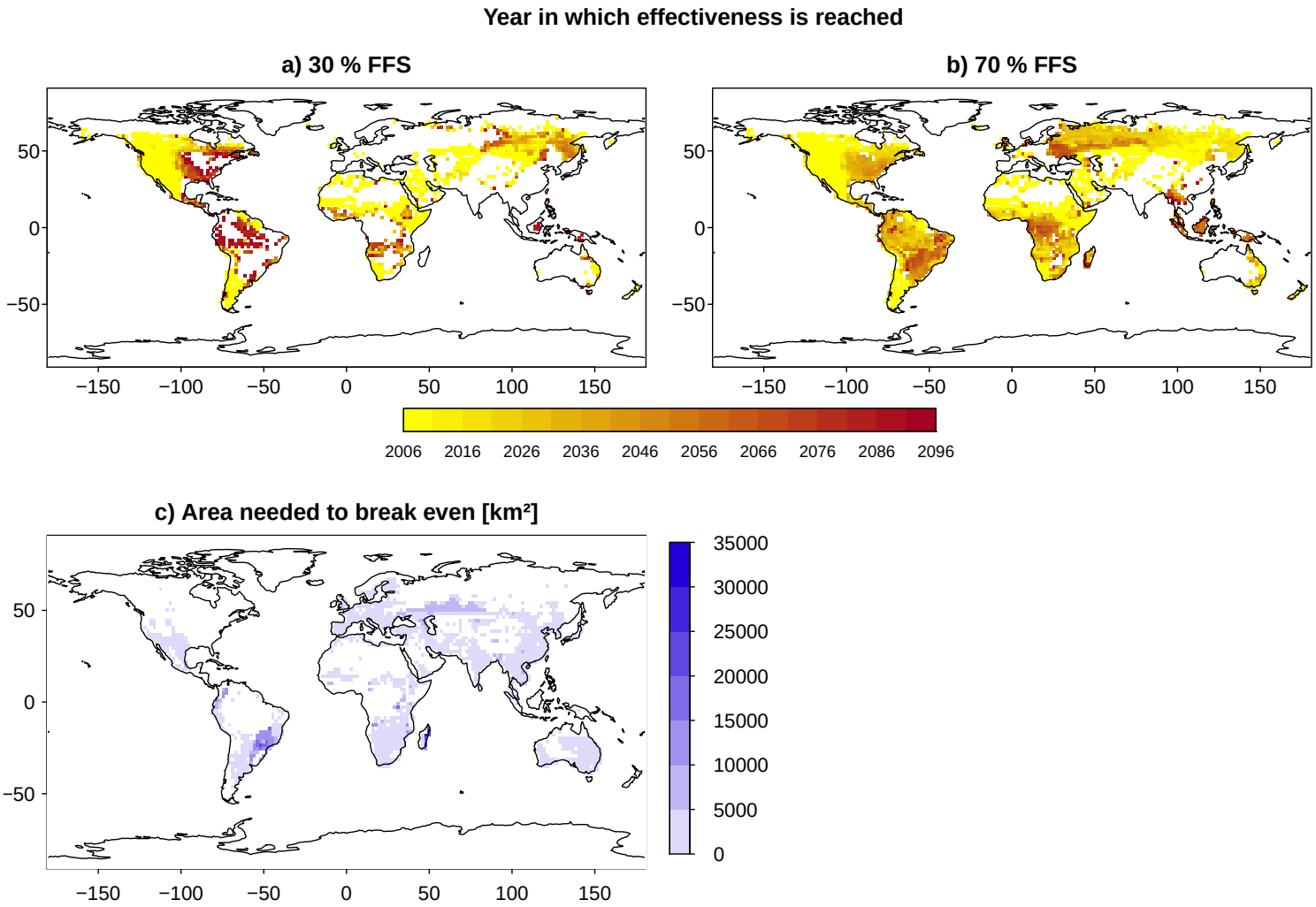

Figure 3.10: Year in which effectiveness is reached (5-year mean), for a) 30% fossil-fuel substitution (FFS) and b) 70% fossil-fuel substitution. c) Area needed for carbon stocks of herbaceous biomass plantations (including harvested carbon) to reach the level of carbon stocks in the afforestation scenario; in 2100 in the herbaceous biomass plantation simulation with 71% harvest (break-even point).

3.6.3 Effectiveness depends on choices of location, technology and timescales

This is the first study that directly quantifies the mitigation potentials of herbaceous biomass plantations and compares it with that of afforestation. The effectiveness weighs one square meter of forest against one square meter of herbaceous biomass plantations in each gridcell, independently of the chosen land-use scenario. This study highlights the different dimensions affecting the mitigation potential of herbaceous biomass plantations: the extent of the plantations, the level of fossil-fuel substitution, and the timeframe considered. Ideally, herbaceous biomass plantations would be established over large areas using optimal technology (close to 100% fossil-fuel substitution) with management times spanning many decades. However, my study shows that herbaceous biomass plantations can also be more effective than forests at lower levels of substitution and on shorter timescales, especially in areas where forest productivity is limited such as the western USA.
These findings clearly identify areas where herbaceous biomass plantations are most effective when compared to forests and show that a little over half the abandoned area in RCP4.5 would suffice to surpass the mitigation potential of forests.

3.7 General remarks

One factor that limits this study is the size of the gridcells. The gridcells are much larger than the typical fields planted by farmers. MPI-ESM averages all variables over the entire gridcell. However, local conditions can vary due to topography, underlying bedrock, soil conditions and microclimates. Therefore, average yields may not be achievable in all areas of a gridcell. The modified RCP4.5 land-use scenario establishes herbaceous biomass plantations on abandoned agricultural areas. Farmers tend to abandon the least fertile lands first, which could depress yields significantly. I address this issue by keeping the yields at their lower estimated potential (see chapter 2).
Herbaceous biomass plantations depend on water availability. In some areas, irrigation and fertilization can significantly improve yields (Ercoli et al., 1999; Miguez et al., 2008). However, JSBACH cannot simulate irrigation. Plants, therefore, rely solely on rainfall. Thus, effectiveness in some areas may be underestimated due to lack of irrigation in the model. However, irrigation uses energy which in turn reduces the achievable level of fossil-fuel substitution. How these opposing effects would interact in different regions cannot be estimated in this study.
Land carbon dynamics influence the climate significantly and should be considered when choosing between land-use options. However, land-use change alters many other factors besides land carbon dynamics which also need to be considered. Previous studies indicate that large-scale establishment of biomass plantations may decrease

food-security and biodiversity and alter water cycles more than crops would (Boysen, 2016; Heck et al., 2016). Establishing herbaceous plant types instead of forests on any lands also alters the physical properties of the land surface. JSBACH cannot analyze food-security or biodiversity in detail but it can simulate the physical changes associated with land-use changes and analyze its effects on the atmosphere. These effects will be discussed in Chapter 5.

3.8 Conclusion

Herbaceous biomass plantations affect the global carbon cycle significantly. On the one hand, they sequester carbon through photosynthesis and mitigate climate change through fossil-fuel substitution. On the other hand, they prevent forest regrowth and the additional sinks associated with it. Their net effect greatly depends on the chosen land-use scenario. This study highlights three main effects:

- The greatest potential of herbaceous biomass plantations lies in fossil-fuel substitution. Simulations without fossil-fuel substitution have higher CO_2-concentrations than in the afforestation baseline, while simulations with fossil-fuel substitution have lower CO_2-concentrations than in the afforestation baseline.

- When established on abandoned agricultural areas, they become effective quickly and within current technological limits, in spite of the limited areas available for their establishment.

- Even though herbaceous biomass plantations prevent forest regrowth, a potential carbon sink on the order of magnitude of total yields of herbaceous biomass plantations, they still reduce temperatures and atmospheric CO_2-concentrations through fossil-fuel substitution compared to forest regrowth. Effectiveness of herbaceous biomass plantations depends on the chosen deployment method. This study explores a plausible land-use scenario which preserves both food production and natural ecosystems. In this scenario, herbaceous biomass plantations are effective in spite of the relatively small areas available. Importantly, maximizing climate mitigation requires minimizing the impacts on land carbon stocks.
  This study shows that herbaceous biomass plantations mitigate global CO_2-emissions and reduce temperatures more effectively than afforestation as long as they are established on abandoned agricultural lands and direct or indirect emissions from forest displacement are avoided. Although their potential is limited by area availability and technological feasibility, they could contribute significantly to emissions reductions through their ability to substitute fossil-fuels.

Chapter 4

Biogeophysical effects of herbaceous biomass plantations on land surface properties and local climate

4.1 Introduction

Plants influence the atmosphere by exchanging matter and energy directly and indirectly with the air surrounding them (Bonan, 2008). While biochemical interactions, such as photosynthesis and respiration, have been intensively studied, biogeophysical interactions have received much less attention. This chapter analyzes the biogeophysical effects of large-scale biomass plantations on the climate.
Several previous studies analyzed the biogeophysical effects of land-use change in idealized scenarios or of historical land-use change on the climate (Claussen et al., 2001; Brovkin et al., 2006; Betts et al., 2007; Pongratz et al., 2009a; Bathiany et al., 2010; Pongratz et al., 2010; Brovkin et al., 2013). Some of these studies suggest, that, historically, biogeophysical effects may have counteracted biogeochemical effects on local scales (Betts et al., 2007). Similarly some studies on regional scales have found significant biogeophysical impacts for herbaceous biomass plantations replacing crops (Georgescu et al., 2011). The biogeophysical effects of herbaceous biomass plantations may affect the future climate on global or local scales and hence need to by analyzed. Herbaceous biomass plantations can be used to substitute fossil energy sources. As such, they are a potent tool for climate engineering (see chapter 3). However, their surface properties differ significantly from those of other plants which could affect their ability to mitigate climate change. Also, because biogeophysical effect often affect local climate more than global climate, they could conceivably mitigate the climate on global scales while decreasing the quality of life in their immediate surroundings (Pongratz et al., 2010). This could lead to conflicts between global policy agreements and local communities affected by the changes. Therefore, how biogeophysical properties

of herbaceous biomass plantations affect the local climate may well determine if they are deployed at levels sufficient to mitigate climate change.

Plants interact with the atmosphere by exchanging chemicals and by altering the physical properties of the land surface (Bonan, 2008). This change in physical properties can be optical or mechanical. Optical changes involve the color and reflectivity of the surface. They determine how much sunlight the surface absorbs and reflects. Furthermore, plants can absorb sunlight and radiate it back as heat. Mechanical changes involve surface area and texture. They impact air movement in and around canopies and wind speeds and direction. These factors influence the local and global climate.

Water fluxes, mainly evaporation and transpiration, count as biogeophysical interactions because the evaporation of water requires energy which in turn cools the surface (Bonan, 2008). Thus, evapotranspiration serves to transport energy from the surface to the atmosphere. Plants influence transpiration for two reasons: first, their extensive root systems source water from deeper soil layers increasing the amount of water available for transpiration, and second, their extensive canopies increase the surface area over which transpiration occurs. These fluxes affect the amount of soil-, ground- and river-water available for human use (Schilling et al., 2008). Since humans need water for themselves, for their crops and their domesticated animals, the effects of land-use change on water cycles and local water availability should be considered.

In nature, biogeophysical and biogeochemical effect of land-use change occur simultaneously. Attributing any response to one of these effects requires precise analysis. Representing as many relevant processes as possible in a global Earth System Model only partially resolves this issue. While the simulation quantifies all effects it represents, the model also captures many feedbacks between the different processes. The question of how to disentangle these effects remains. One possible solution is to eliminate one of the two effects under scrutiny (Brovkin et al., 2013).

Chapter 3 described the hybrid scenario developed to compare afforestation and large-scale herbaceous biomass deployment. This scenario couples emissions from RCP8.5 to the land-use from RCP4.5. The RCP4.5 land-use projects large-scale agricultural abandonment. In the afforestation baseline simulated by Sonntag et al. 2016, the majority of these areas revert to forests, while in my modified land-use scenario, these same areas are reclaimed for biomass plantations. All simulations described in chapter 3 represent both biogeochemical and biogeophysical effects of the two land-use types.

In order to eliminate the biogeochemical effects on the climate, I developed an additional simulation based on the modified land-use scenario of RCP4.5: the abandoned agricultural areas are still reclaimed for herbaceous biomass plantations, but the scenario uses the greenhouse gas concentrations of the afforestation baseline. This new simulation has the same biogeochemical climate as the afforestation baseline, but differs from the baseline because of the biogeophysical effects of herbaceous biomass plantations. Thus any differences between this simulation and the baseline must be caused by the physical alterations engendered by replacing forests by herbaceous biomass plantations. I use this simulation to analyze how the biogeophysical effects of large-scale

herbaceous biomass plantations influence the local and global climate when compared to afforestation.

4.2 Material and methods

4.2.1 Setup of original simulations

The simulations analyzed so far consist of a hybrid scenario between the RCP8.5 emissions and the RCP4.5 land-use (for details see description of land-use transitions in chapter 2). In the RCP4.5 land-use scenario, agricultural areas are abandoned throughout the century. These areas revert to natural lands in the afforestation baseline. I modified this land-use scenario so that areas reverting to forests in the original scenario are reclaimed for herbaceous biomass plantations. These scenarios are further described in chapters 2 and 3. The Afforestation baseline was simulated by Sebastian Sonntag and is described in detail in Sonntag et al. 2016. All simulations were conducted with the Max-Planck-Institute Earth System Model which encompasses the atmospheric global circulation model ECHAM, the ocean model MPI-OM, which includes the ocean biogeochemistry model HAMOCC, and the land component JSBACH. The model version and setup was identical to that used for the Coupled Model Intercomparison Project 5.

4.2.2 Isolating biogeophysical effects by mathematical means from preexisting simulations is complicated by the system's internal non-linearity

In all available simulations biogeophysical and biogeochemical effects are entangled. In order to isolate the effects of land-use on the temperature, I introduced a scaling factor for each gridcell which links the actual temperature in each gridcell to the radiative forcing of carbon dioxide. This should, in theory, eliminate all biogeochemical effects and leave the biogeophysical effects as remaining differences between one simulation and another.
The radiative forcing of CO_2 is expressed as a logarithmic function of the CO_2-concentration (Lenton and Vaughan, 2009):

$$F(t) = 5.35 * \ln \frac{\rho_{CO_2}(t)}{\rho_{CO_2}(t_0)} \tag{4.1}$$

Where $\rho_{CO_2}(t)$ is the CO_2-concentration at timestep t and $\rho_{CO_2}(t_0)$ is the CO_2-concentration at the beginning of the simulation (reference timestep). The change in local temperature in each gridcell is a linear function of the radiative forcing.

$$\Delta T_{i,j}\,(2100) = \gamma_{i,j} * F\,(2100) \tag{4.2}$$

Where $\Delta T_{i,j}$ (2100) is the change in temperature in the gridcell with coordinates i and j between 2006 and 2100 and $\gamma_{i,j}$ is the scaling factor. Since the temperature for each gridcell is known and the radiative forcing can be calculated, this equation yields the scaling factor.
By calculating and comparing the scaling factor for different simulations with the same land-use, but differing CO_2-concentrations, I determined whether the scaling factor is constant given a certain land-use regardless of the CO_2-concentration.
I found that the scaling factor differs between different simulations with similar land-use which indicates a strong non-linearity of the system. This method cannot be used to isolate the biogeophysical effects of herbaceous biomass plantations.

4.2.3 Additional simulation to isolate biogeophysical effects

In a second attempt to isolate the biogeophysical effects of herbaceous biomass plantations, I prescribed the greenhouse-gas concentrations of the afforestation baseline simulation to the modified land-use including herbaceous biomass plantations. Thus, the biogeochemical effects of herbaceous biomass plantations are eliminated in the new simulation, leaving only the biogeophysical effects. Because the two land-use scenarios diverge from the same initial state (historical land-use), only the last twenty years of the simulations were compared. Students t-test was used to test for significance in individual gridcells.

4.3 Results and Discussion

4.3.1 Temperatures and surface radiation

Mean global temperatures of the additional simulation resemble those of the afforestation baseline (see figure 4.1). In chapter 3, comparisons between the afforestation baseline and the fully coupled models showed that herbaceous biomass plantations significantly alter the climate compared to forests. The absence of such differences in the additional simulation shows that biogeochemical effects dominate the global climate and biogeophysical effects play a minor role on global scales. Yet, average global temperatures can mask local changes too small to be captured in global trends.

Air temperatures at 2 m height and surface temperatures show no significant differences between the additional simulations and afforestation for most areas (see figure 4.2). On land, only three areas with significant differences can be identified: in western Alaska, temperatures are slightly lower for the additional simulation compared with afforestation, in Siberia and western Russia temperatures are slightly warmer than in Afforestation (Students t-test 5% significance level). However, only the area in western Russia coincides with abundant herbaceous biomass plantations. The

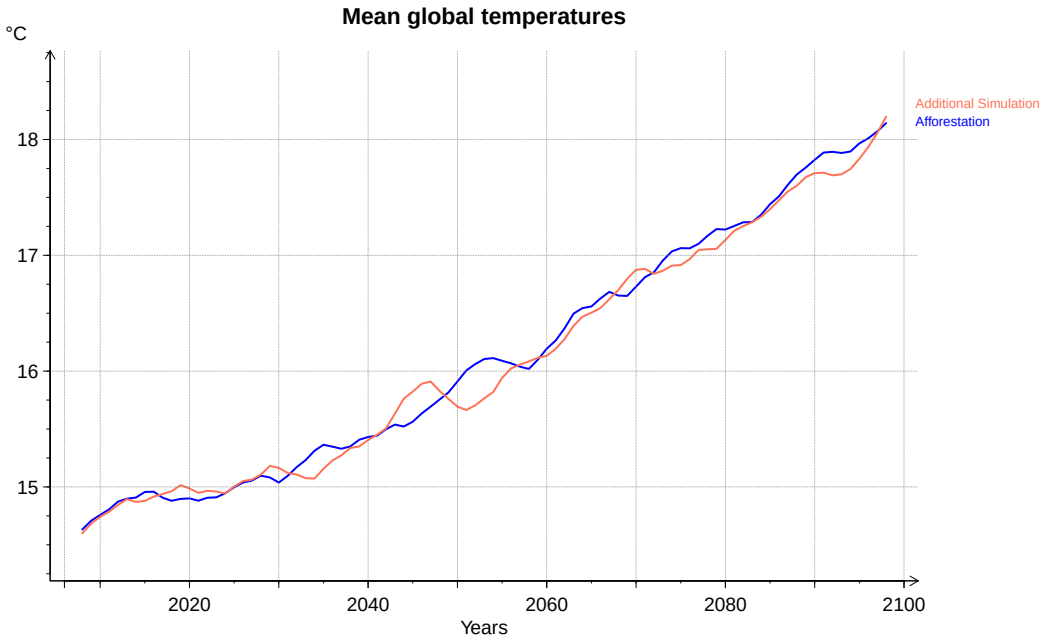

Figure 4.1: Annual average global temperatures (5-year running means) in the Afforestation and the additional simulation throughout the century.

remaining areas showing significance are likely false positives of the test, clustered together because of spatial correlation of neighboring gridcells. Nevertheless, non-local biogeophysical effects of herbaceous biomass plantations cannot be excluded.

Seasonal minimum and maximum 2 m air temperatures show no significant seasonal effects which could be correlated to herbaceous biomass plantations (see figures 4.3 and 4.4).

Of all variables analyzed, albedo correlates best with land-use change (figure 4.5). Albedo in a gridcell increases as the percentage of the gridcell covered with herbaceous biomass plantations increases. This is not surprising as different plant types reflect differing amounts of sunlight. Herbaceous biomass plantations reflect more sunlight than forests and therefore, surface albedo within a gridcell correlates with their extent (correlation coefficient R=0.88). Different continents are affected similarly by this effect. This is unexpected, as forest canopies reflect differing amounts of light depending on the dominant species. However, these differences between forests may be negligible next to the more substantial differences between forests and herbaceous biomass plantations.

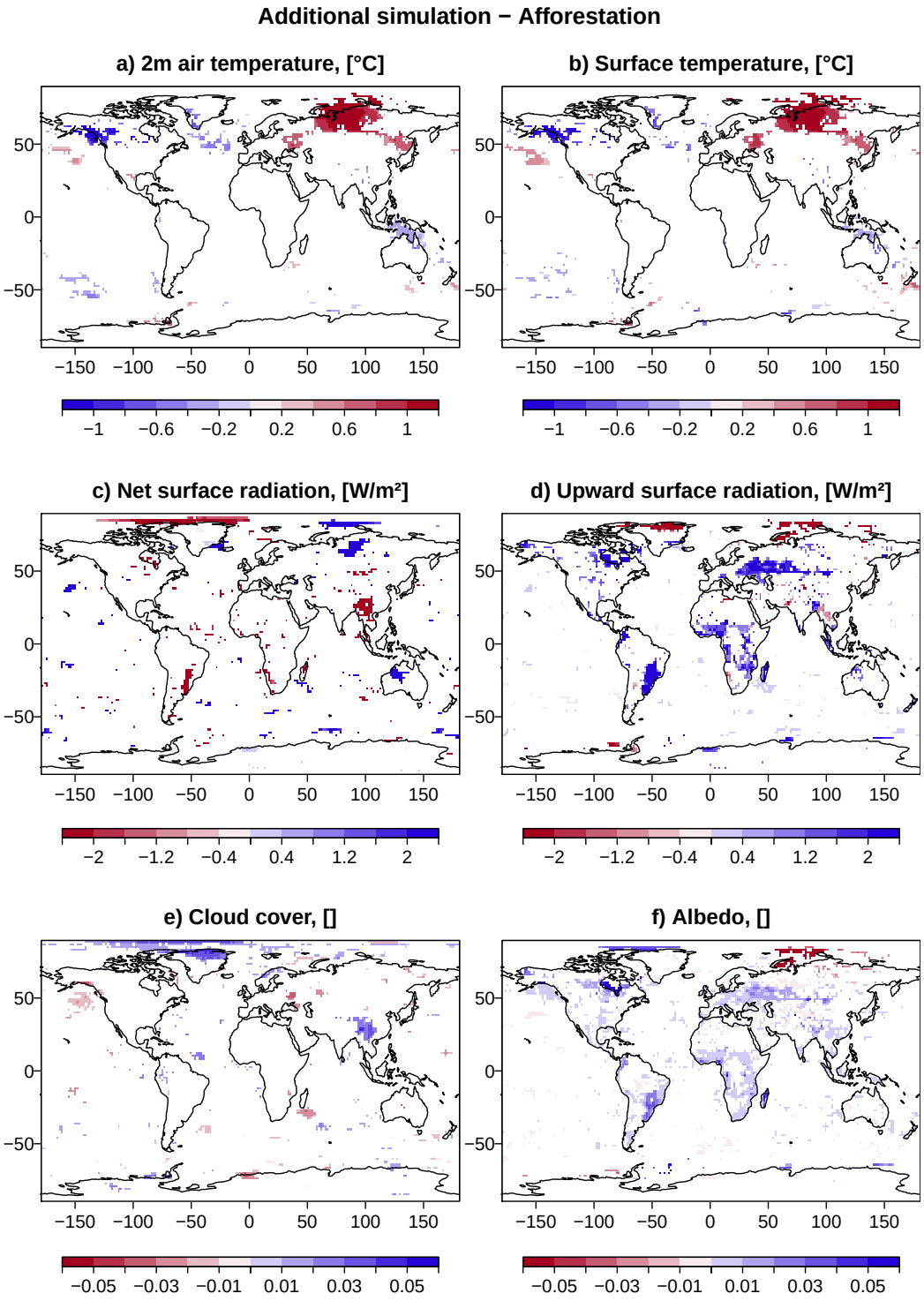

Figure 4.2: Difference between the additional simulation and the afforestation baseline in 2 m air temperatures and surface temperatures (top), net and upward surface radiation (middle) and cloud cover and surface albedo (bottom). Only significant differences shown (Student's t-test 5% confidence level)

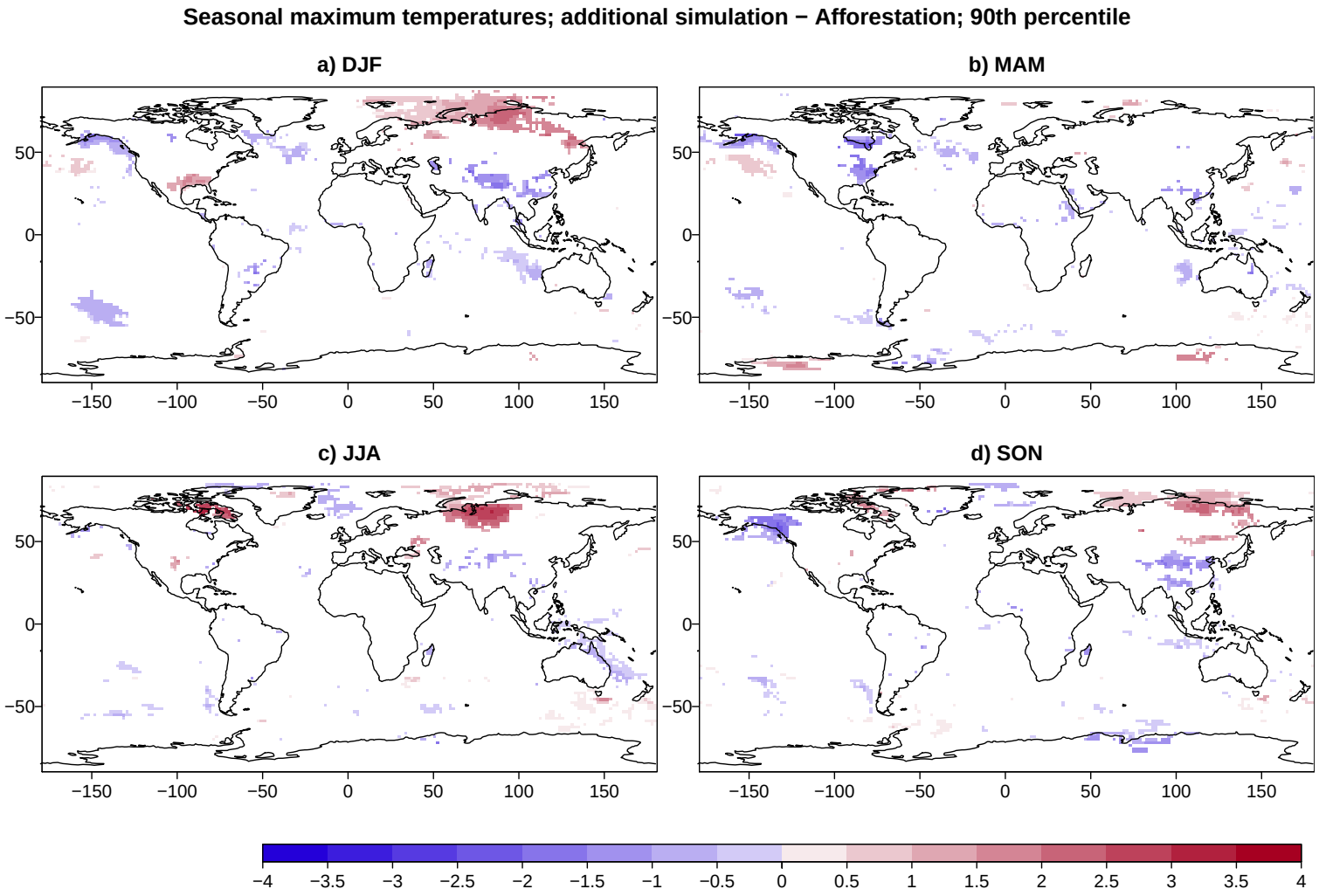

Figure 4.3: 90^{th} percentile of maximum temperatures for each season. DJF: December, January, February; MAM: March, April, May; JJA: June, July, August; SON: September, October, November

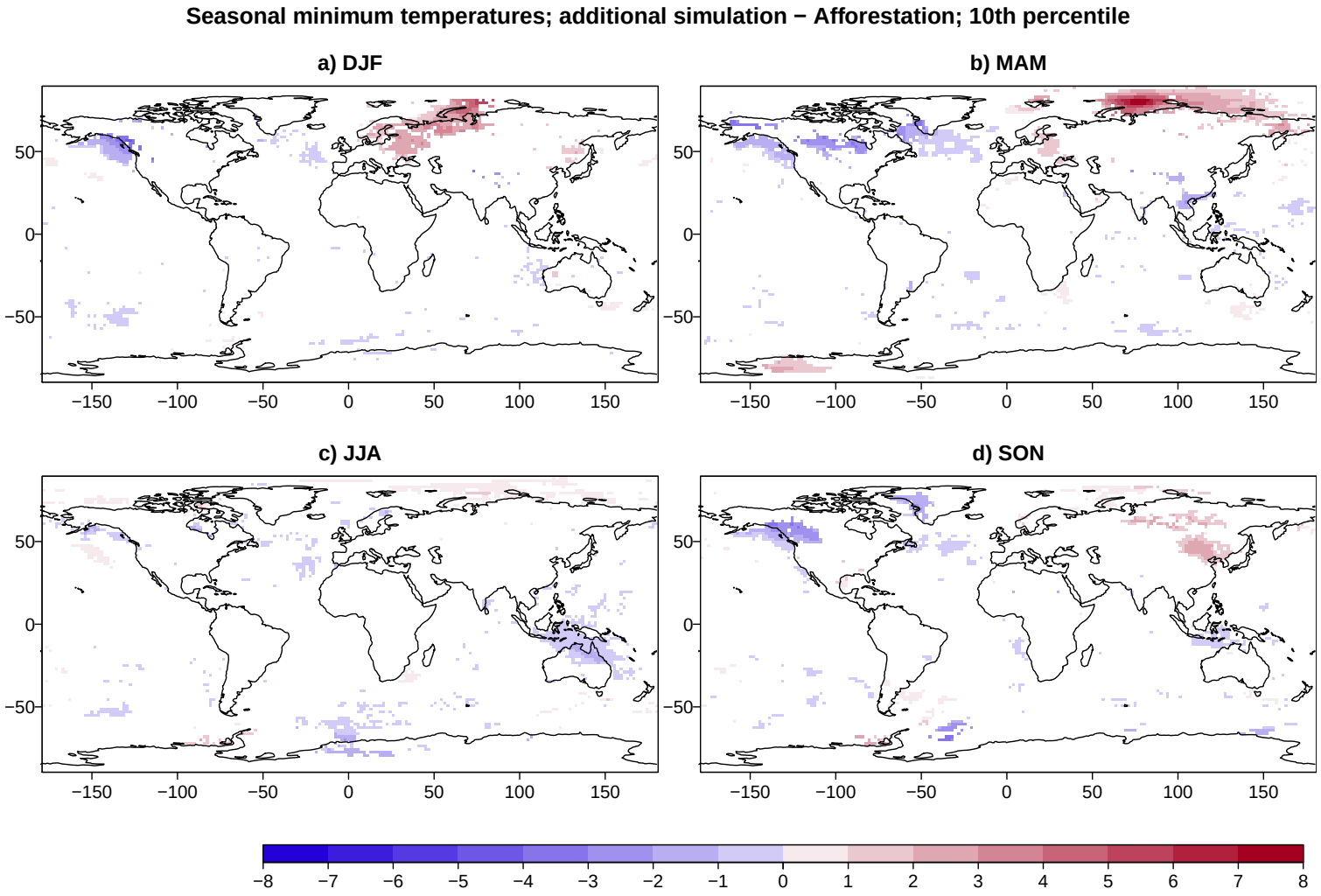

Figure 4.4: 10^{th} percentile of minimum temperatures for each season. DJF: December, January, February; MAM: March, April, May; JJA: June, July, August; SON: September, October, November

In areas with herbaceous biomass plantations, upward surface radiation exceeds that of the afforestation scenario, which results from higher albedo of herbaceous biomass plantations compared to forests. However, the effects on net surface radiation are weak. Net surface radiation is reduced by these changes in South America, East Asia and parts of Africa. In other areas, such as western Russia, the higher albedo does not affect net radiation significantly. Three mechanisms could be responsible for the latter observation: either the long, dark, boreal winters reduce the effects of higher albedo, or the albedo changes are too small to significantly alter net surface radiation, lastly other effects might counter the albedo effects. Changes in cloud cover due to altered transpiration which might counteract alterations in upward surface radiation were excluded.

4.3.2 Water cycle

Precipitation does not change significantly between simulations (Students t-test 5% significance level) even though herbaceous biomass plantations reduce transpiration rates significantly (see figure 4.6), in South America and Africa. Herbaceous biomass plantations transpire less than forests, even though forests have a lower leaf area index in the model. This is surprising since transpiration correlates with leaf area index (Chase et al., 1996). In some areas, reduced transpiration increases soil water levels such as in South America. Interestingly, soil water levels also increase in East Asia, where changes in transpiration are not significant. Possibly, decreases in transpiration were too slight to be detected, yet significantly increased soil water nonetheless. Yet the overall small numbers of gridcells showing significant changes could also result from false positives. Runoff is not significantly affected.

Transpiration decreases with increasing cover fraction of herbaceous biomass plantations (figure 4.7, correlation coefficient R=-0.45). Herbaceous biomass plantations transpire less than forests for several reasons. First, they are C4-plants which use water significantly more efficiently by closing or partially closing their stomata under hot dry conditions. This reduces transpiration compared to C3-plants, usually present in forests, which must keep their stomata open in order to photosynthesize. Second, their higher albedo reflects more radiation and cools their surface, reducing overall transpiration. The extent of these effects depends on climate. Third, trees often extend their root systems much further than grasses, allowing them to tap into water resources not available to grasses.

4.3.3 Comparison to other studies

Few studies consider the biogeophysical effect of land-use change, even though some studies found that they could alter local and global climate substantially (Betts, 2001; Claussen et al., 2001; Brovkin et al., 2006; Betts et al., 2007; Pongratz et al., 2009a;

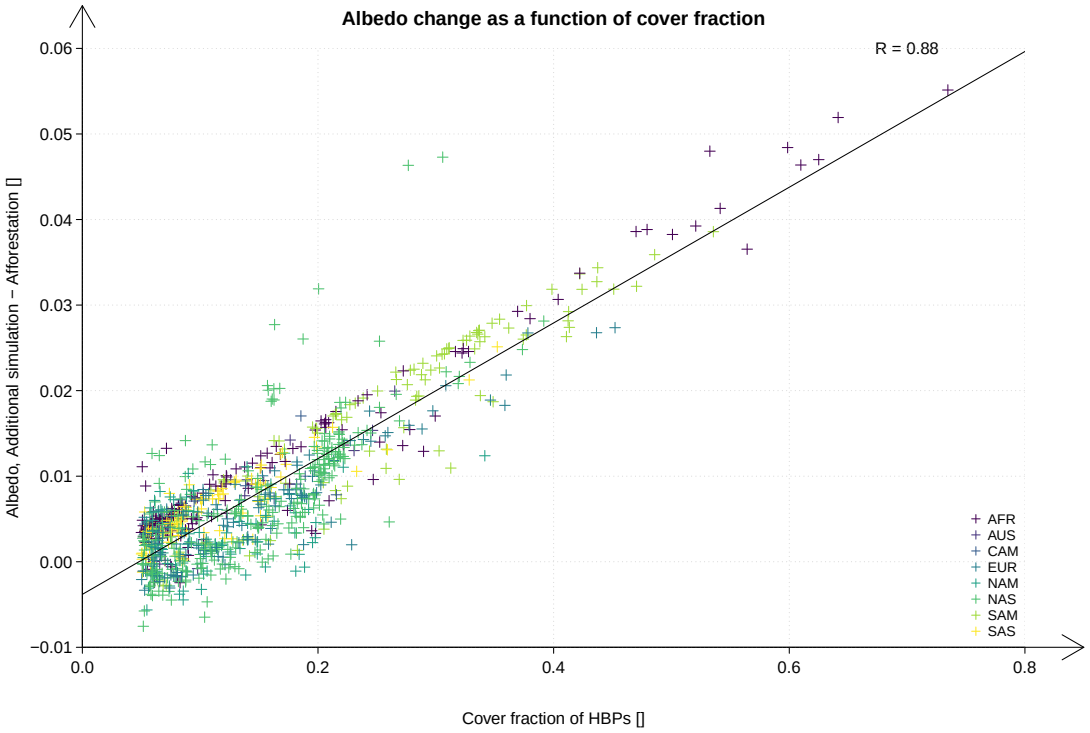

Figure 4.5: Land surface albedo differences between the additional simulation and the afforestation baseline as a function of the cover fraction of herbaceous biomass plantations (HBPs). Only gridcells in which the cover fraction of herbaceous biomass plantations exceeded 0.05 were included. The black line shows the linear regression. AFR: Africa, AUS: Australia, CAM: Central America, EUR: Europe, NAM: North America, NAS: Northern Asia, SAM: South America, SAS: South Asia

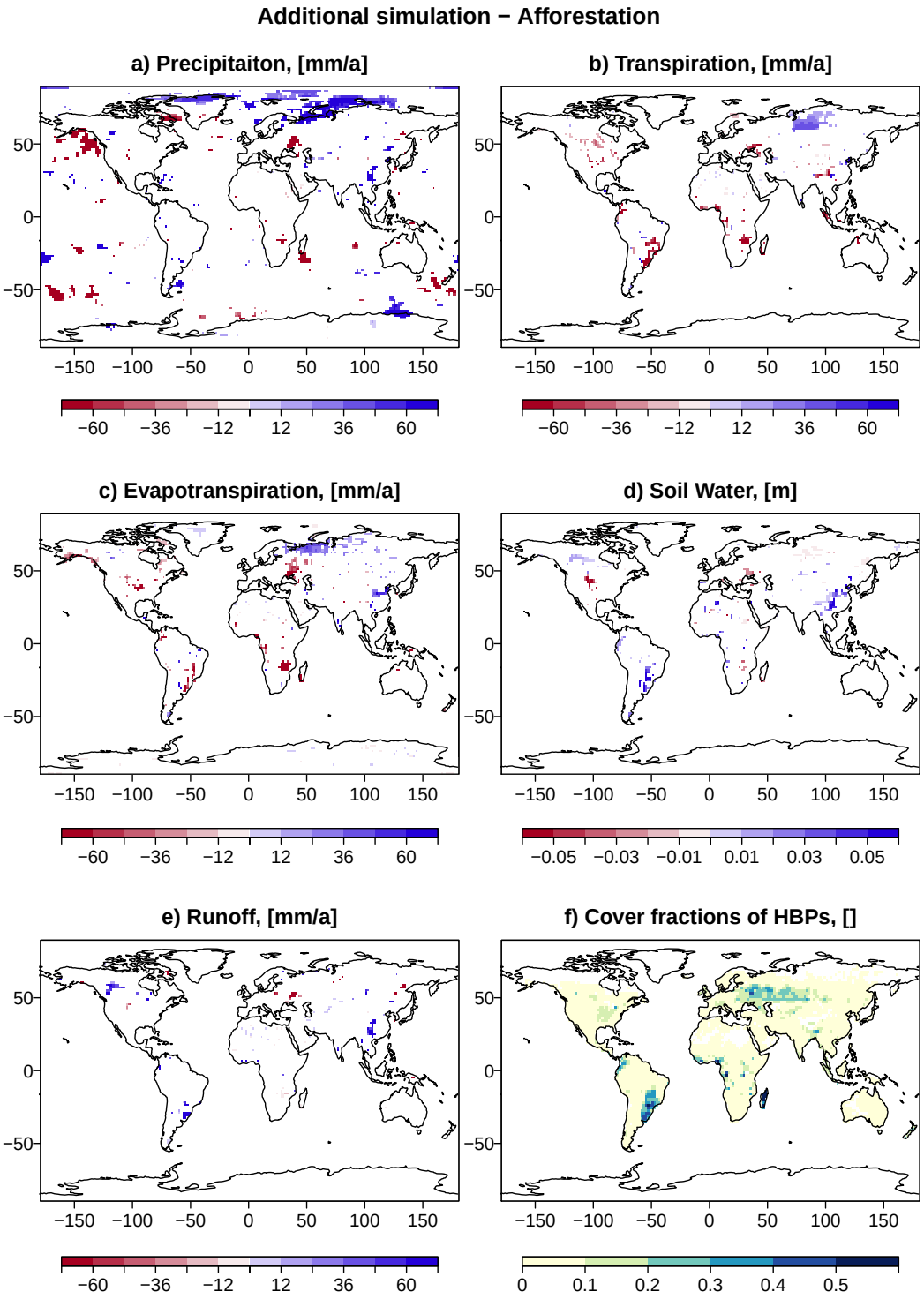

Figure 4.6: Difference between the additional simulation and the afforestation baseline in precipitation, transpiration, evapotranspiration, soil water and runoff. Only significant differences shown (Student's t-test 5% confidence level)

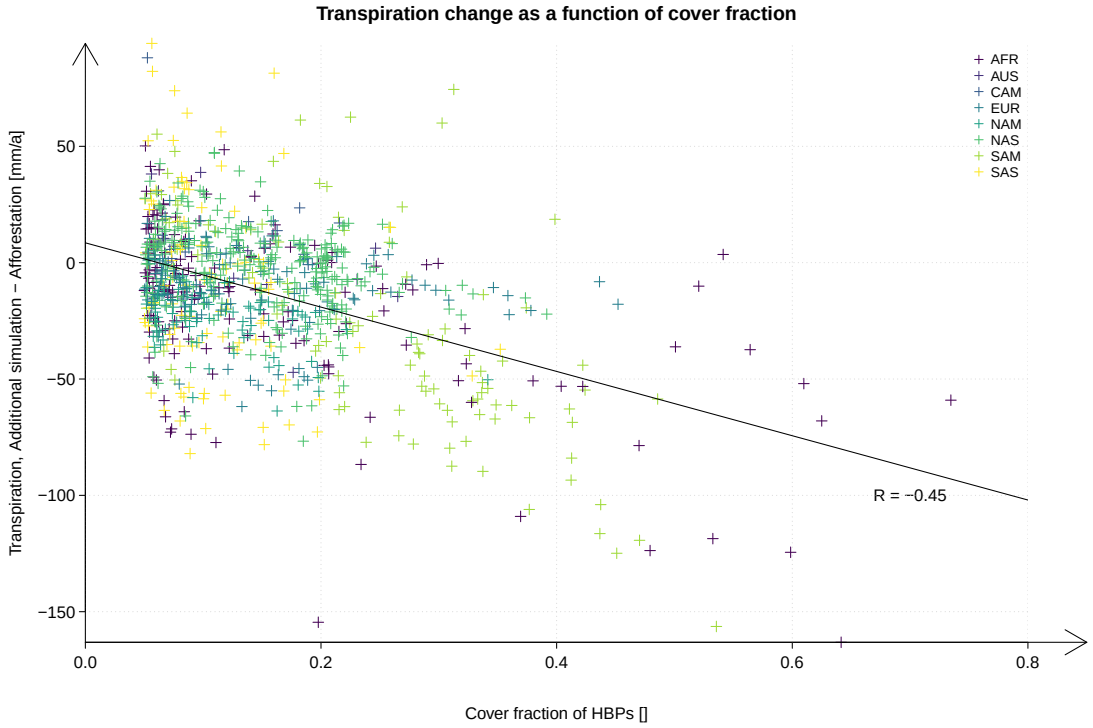

Figure 4.7: Transpiration differences between the additional simulation and the afforestation baseline as a function of the cover fraction of herbaceous biomass plantations (HBPs). Only gridcells in which the cover fraction of herbaceous biomass plantations exceeded 0.05 were included. The black line shows the linear regression. AFR: Africa, AUS: Australia, CAM: Central America, EUR: Europe, NAM: North America, NAS: Northern Asia, SAM: South America, SAS: South Asia

Bathiany et al., 2010; Pongratz et al., 2010; Brovkin et al., 2013). Several idealized studies suggest that deforestation in the tropics warms the climate while deforestation in temperate and boreal regions cools the climate (Claussen et al., 2001; Brovkin et al., 2006; Bathiany et al., 2010). Brovkin et al. 2006, Betts et al. 2007 and Pongratz et al. 2009a found that historical land-use cooled the northern hemisphere by increasing albedo as forests were converted to agricultural areas. Brovkin et al. 2013 show that the biogeophysical effects of the land-uses of RCP2.6 and RCP8.5 do not influence global climate but can have a local effect in areas where total land-use change exceeds 10%. In light of these findings, the small changes on both local and global scales found in my study are surprising.

Schaeffer et al. 2006 analyzed the effects of large-scale woody biomass plantations on albedo and transpiration in the northern hemisphere as compared to afforestation. They found changes in albedo of up to 10% in individual gridcells. My findings are of a similar magnitude but with two major differences: first, my scenario uses herbaceous biomass plantations rather than woody biomass plantations and second, my scenario encompasses all regions, not just the northern extra-tropics. Woody biomass plantations are harvested every 4-7 years leading to widely fluctuating leaf area indices and albedo and transpiration changes between years. Herbaceous biomass plantations are harvested annually and grow back quickly, thus their canopies, albedo and transpiration are more homogenous between years.

Several studies consider the biogeophysical effects of herbaceous biomass plantations on local conditions. Le et al. 2011 model the effects of *Miscanthus*, *Panicum* and *Zea mais* on the hydrology of the Midwestern United States of America. They find that *Miscanthus* and *Panicum* have significantly higher transpiration than *Zea mais*. Importantly, they show that overall hydrology in the Midwestern US is affected by the choice of species. However, they only compare different C4-grasses. My study shows that compared to forests, that are mainly composed of C3-species, herbaceous biomass plantations transpire less, even though C3-plants profit more from higher atmospheric CO_2-concentrations as they are more affected by CO_2-fertilization. In situations of local water limitation, planting C4-grasses or crops may therefore be preferable to planting forests.

Georgescu et al. 2011 also analyzed the effects of converting annual crops into perennial herbaceous biomass plantations. They find increases in both albedo and transpiration. Their simulations, like Le et al. 2011, illustrate the importance of the reference. They analyze the effects of converting crops to herbaceous biomass plantations and compare the new plant type with the initial plant type. I compare the effects of two alternative choices, afforestation and herbaceous biomass plantations. Thus, compared to crops, both forests and herbaceous biomass plantations would increase overall transpiration, but, compared to afforestation, herbaceous biomass plantations decrease transpiration. On the other hand, herbaceous biomass plantations increase albedo compared to crops and compared to afforestation.

4.3.4 Limitations of this study

This study is limited by a number of factors. While the MPI-ESM attempts to capture as many relevant aspects of the Earth System as possible, some aspects are difficult to model in a global Earth System Model. The coarse resolution may obscure some local effects of land-use change. In addition, cloud formations and dynamics are difficult to model which could lead to underestimation of differences in transpiration-precipitation feedbacks due to land-use change. My study focuses on one global land-use scheme without considering how other distributions of herbaceous biomass plantations might affect the climate. Lastly, my study limits the extent of herbaceous biomass plantations to the abandoned agricultural areas of RCP4.5. How larger areas would affect the climate remains unclear.

The resolution of JSBACH is relatively coarse compared with the fine-scale topography of the Earths surface. Land-use often is determined by topography. Rivers or mountains are often used as boundaries between jurisdictions. Streams and ridges determine the shapes and sizes of fields. Microtopography and microclimates also affect which species grow in a given area and which land-use will be most profitable. While JSBACH attempts to capture as many of these elements as possible, it fails to capture these small-scale variations, as it averages over the gridcells.

As microtopography and microclimates can enhance as well as reduce certain effects, they average out on the large scales as long as land-use is assigned randomly. Yet, land-use is rarely assigned randomly as it is usually profit-oriented. Decision makers can assign land-use based on revenue, maximum production or minimum energy input. My land-use scenario assumes that biomass plantations are established on former agricultural areas that are abandoned. Thus, it generally assumes that herbaceous biomass plantations would be established on depleted, less productive or even contaminated soils. Because JSBACH averages local conditions over any gridcell it cannot capture the effects of establishing herbaceous biomass plantations only on those soils. While herbaceous biomass plantations can grow efficiently on soils unsuitable for more demanding crops, how their productivity and all related properties would change over time if they were established on less productive soils remains unclear.

The coarse resolution of global models also limits the details of cloud simulation. Consequently, any processes linked to clouds, such as cloud formation and precipitation, are represented only on the broad scales of the gridcells. This is important when considering land-use for several reasons. First, the microtopographic and microclimatic issue discussed above can lead to large variations in precipitation regimes within one gridcell. Second, precipitation influences the amount of water available for plant growth and transpiration. Third, the amount of transpiration influences the amount of water vapor available for cloud formation. This feedback can only be represented on the large scales of the gridcells in the my simulations. For smaller scales, local models should provide more detailed insights.

My study focuses on one specific land-use scenario. This scenario allocates herbaceous

biomass plantations based on agricultural abandonment. While this considers potential capacities for plantations, it doesn't factor in potential future demands. If areas of future demand are far from areas of production, transportation costs might outweigh potential benefits which could drive land-use patterns in different directions. This could potentially lead to very different establishment patterns for herbaceous biomass plantations witch in turn could have other consequences for the climate.
The areas used for herbaceous biomass plantations in my study are limited to the abandoned crops and pastures from RCP4.5. Should future anthropogenic climate change prove more severe than expected, societies might decide to expand biofuel and bioenergy production far beyond these areas. My study cannot predict how such an expansion would affect either the climate or local conditions.

4.4 Conclusions

Biogeochemical effects dominate both on global and local scales. Biogeophysical effects play only a minor part, reducing the potentials for conflicts between global carbon dioxide reductions and local decision makers whose lives might be impacted by the deployment of herbaceous biomass plantations. Nevertheless, biogeophysical effects or herbaceous biomass plantations affect two fundamental parts of land-atmosphere interactions:

- Higher albedo of herbaceous biomass plantations increases surface reflectivity compared to afforestation.
- Lower transpiration of herbaceous biomass plantations compared to forests may increase soil moisture, compared to the afforestation scenario.
- Overall biogeophysical effects of herbaceous biomass plantations on the global and local climate are negligible.

These effects could play a larger part on sub-grid scales. Importantly, temperature changes due to higher albedo may be offset by temperature changes due to lower transpiration since these effects counteract each other. How such effects might interact on sub-grid scales remains to be determined.

Chapter 5

Consequences of alternative socioeconomic pathways on carbon distribution

5.1 Introduction

Land-use change influences climate and global carbon distribution. Humans influence where carbon is stored and how it flows between and through the different components of the Earth System. This study analyzes how alternative, potential, socioeconomic pathways would influence future global carbon distribution. This chapter aims to set herbaceous biomass plantations as an alternative to other possible future energy systems.

Herbaceous biomass plantations are a land-based method of climate engineering because their harvest can be used to substitute fossil-fuels and generate energy in a sustainable way. Afforestation can also be considered a land-based climate engineering method if trees are viewed primarily as a carbon storage unit. Each method affects carbon stocks in a unique way which in turn affects all other components of the Earth System. Knowing where and how carbon is stored could help policy makers coordinate decisions on carbon removal programs.

Land ecosystems provide many different environmental services, one of which is carbon dioxide removal. They also provide food, fiber and timber, filter pollutants from the air and the water, produce medically useful substances and some also serve as recreational areas. Management techniques can seek to optimize one particular service or to integrate different services. Many of these services depend on the amount of carbon in the system, for example, forestry yields more wood if more carbon is stored in tree-trunks and crops yield more food if they store more carbon as sugars, starches or oils. Thus carbon can be used as a measure for the ability of an ecosystem to provide its most basic services. The more carbon the system contains, the more service it can

potentially provide.
Alternative socioeconomic pathways analyzed here, include the representative concentration pathways RCP4.5 and RCP8.5, the afforestation baseline calculated by Sonntag et al. 2016 and the herbaceous biomass plantation simulations described in the previous chapters. I compare the carbon stocks of the different scenarios to analyze how the carbon emissions are distributed to the different pools of the Earth System. I emphasize the land-based carbon pools since they are most affected by the land-use choices underlying the different scenarios.

5.2 Material and methods

All simulations were calculated using the fully coupled MPI-ESM which encompasses the atmospheric global circulation model ECHAM, the ocean model MPI-OM, which includes the ocean biogeochemistry model HAMOCC, and the land component JSBACH. The RCP4.5 and RCP8.5 scenarios were simulated as part of the Coupled Model Intercomparison Project 5 (CMIP5) and are described in detail in Giorgetta et al. 2013. The afforestation baseline was simulated by Sonntag et al. 2016 and is described in detail in Sonntag et al. 2016. It consists of a hybrid scenario which couples emissions from RCP8.5 to the land-use of RCP4.5. This scenario is referred to as afforestation baseline because in the land-use of RCP4.5 large areas of formerly agricultural lands are abandoned and the vast majority revert to forests as natural ecosystems invade fields left fallow.
I modified the hybrid scenario developed by Sonntag et al. 2016 reclaiming the abandoned agricultural areas for herbaceous biomass plantations. Herbaceous biomass plantations are used for energy production. I simulated four scenarios: two with 100% fossil-fuel substitution, two with 0% fossil fuel substitution, two with high yields (71% of total plant carbon) and two with low yields (55% of total plant carbon). Each yield scenario was paired with each fossil-fuel substitution choice.

5.3 Results and Discussion

5.3.1 Atmospheric carbon dioxide concentrations and global temperatures

Global carbon dioxide (CO_2) concentrations increase in all simulations (figure 5.1). RCP4.5 (green line) shows the smallest increase whereas RCP8.5 shows the largest increase (black line). In the afforestation scenario, forests expand onto abandoned agricultural areas and become additional carbon sinks. This lowers CO_2-concentrations

compared to RCP8.5 by 85 ppm (table 5.1). When herbaceous biomass plantations replace these forests (red and magenta lines), they sequester slightly less CO_2 than forests, lowering atmospheric carbon dioxide concentrations by only 47-53 ppm compared to the vegetation in the RCP8.5 land-use. When herbaceous biomass plantations additionally substitute fossil-fuels they prevent emissions from fossil energy sources and thereby reduce CO_2-concentrations far below the level of the afforestation scenario. Atmospheric CO_2-concentrations are 154-177 ppm lower in the simulations with 100% fossil-fuel substitution than in RCP8.5 and 70-93 ppm lower than the afforestation simulation. However, all simulations forced with the RCP8.5 emissions have higher CO_2-concentrations than RCP4.5. Neither afforestation nor herbaceous biomass plantations can fully mitigate these high emissions.
Global average temperatures follow the CO_2-patterns (figure 5.1 and table 5.1). Afforestation lowers global temperatures by 0.4°C compared to RCP8.5. Herbaceous biomass plantations without fossil-fuel substitution have hardly any influence on temperatures. In simulations with herbaceous biomass plantations but without fossil-fuel substitution, temperatures increase to slightly above those in the afforestation scenario but not beyond the RCP8.5 level. Fossil-fuel substitution, however, reduces global temperatures by 0.8-1° compared to RCP8.5 and by 0.4-0.6° compared to afforestation.
Afforestation mitigates the climate more effectively than biomass plantations, as long as biomass plantations do not substitute fossil-fuels. Herbaceous biomass plantations could contribute to reducing global CO_2-concentrations and temperatures, as long as they are deployed on abandoned agricultural areas and are used for fossil-fuel substitution. However, if herbaceous biomass plantations are intended as an additional energy source, they can still contribute to reducing CO_2-concentrations compared to the RCP8.5 land-use.

Table 5.1: Carbon dioxide concentrations [ppm] and global temperatures [°C] at the end of the 21st century in the simulations with herbaceous biomass plantations compared to the beginning of the century (present day) and the afforestation baseline. HBPs: simulation with herbaceous biomass plantations; 55/71: 55% harvest or 71% harvest; 0/100% FFS: 0 or 100% fossil-fuel substitution.

Simulation	**Temperature [°C]**	**CO_2-concentrations [ppm]**
Present day	14.4	380.5
RCP4.5	16.2	538.4
RCP8.5	18.6	969.0
Afforestation	18.2	884.4
HBPs 55 0% FFS	18.5	915.7
HBPs 71 0% FFS	18.5	922.2
HBPs 55 100% FFS	17.6	814.7
HBPs 71 100% FFS	17.8	791.7

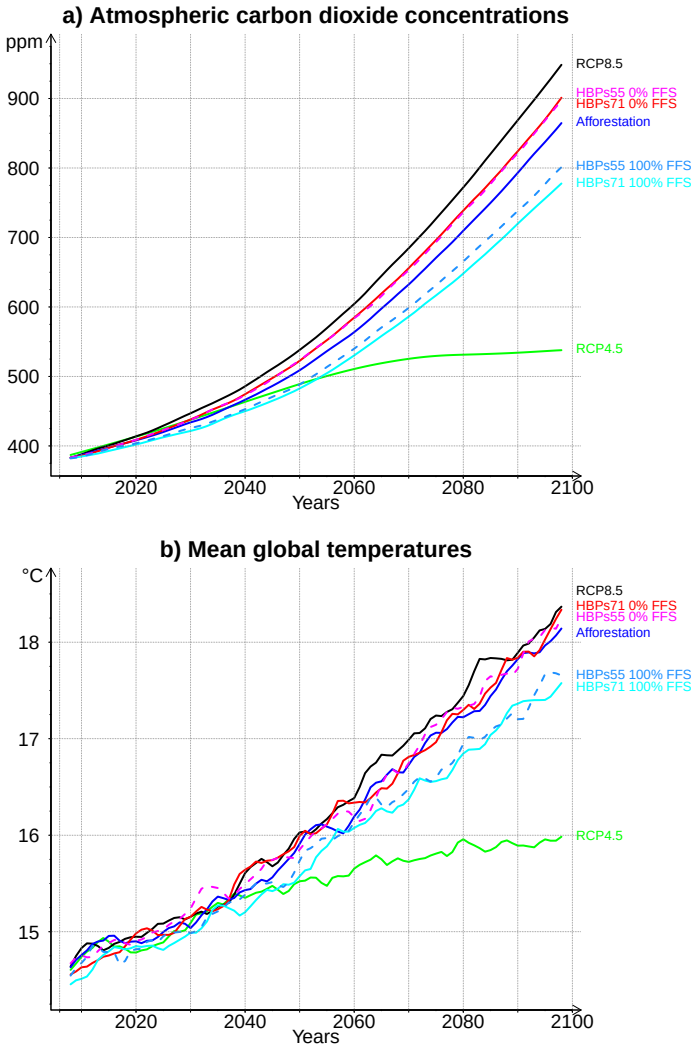

Figure 5.1: Atmospheric carbon dioxide concentrations (a) and mean annual global temperatures (b) of all scenarios analyzed in this section (5-year annual means). RCP: representative concentration pathway; Afforestation: hybrid baseline afforestation scenario; HBPs: herbaceous biomass plantations; 55/71%: percentage of total biomass harvested ; FFS: fossil fuel substitution; 0/100%: percentage of fossil-fuel substitution.

5.3.2 Carbon storage

The ocean stores the greatest amount of carbon in the Earth system (figure 5.2). Land is the second largest carbon pool and the atmosphere the smallest. However throughout the century the share of carbon that remains in the atmosphere increases in all simulations. The share of the land carbon pool also increases slightly. Importantly, the fossil-fuel storage in the simulation with 100% fossil-fuel substitution seems negligible next to the larger pools. Nevertheless it has the potential to substantially reduce the amount of carbon in the atmosphere.
Land carbon stocks are divided into plant and soil pools (figure 5.3). Soil pools are much larger than plant pools. Forest carbon pools exceed all other carbon pools and on global scales natural ecosystems dominate the land carbon pools, excluding geological carbon storage. Forest pools increase most in the afforestation scenario, which is not surprising for this land-use scenario. Interestingly, forest carbon pools increase more in the afforestation scenario than in the RCP4.5 scenario, even though they have the same land-use. This difference is caused by the higher CO_2-fertilization in the afforestation scenario.
Forest carbon pools are lowest in RCP8.5. CO_2-concentrations in this scenario increase more than in any other, yet the land stores the least amount of carbon. In spite of the high CO_2-fertilization, forest carbon stocks increase less as they are partly displaced by the expansion of agricultural areas. This illustrates the importance of land-use choices for overall land carbon storage.
In all scenarios except RCP8.5, carbon pools in crops and pasture areas decrease, mainly due to the reduction in area dictated by the RCP4.5 land-use scenario. In spite of rapidly increasing carbon stocks in herbaceous biomass plantations especially in the soil, they cannot sequester as much carbon as forests. This explains why CO_2-concentrations are higher in the simulations without fossil-fuel substitution than in the afforestation scenario.
Herbaceous biomass plantations, though highly productive, have lower plant and soil carbon stocks and therefore cannot fully compensate the reduced increase in forest carbon stocks. Therefore, land ecosystems lose part of their ability to sequester carbon, even though the chosen scenarios do not contain any deforestation for the establishment of herbaceous biomass plantations.
Natural ecosystems store more carbon in the simulations without fossil-fuel substitution (figure 5.3, red and magenta bars). This results from higher CO_2-fertilization compared to other simulations. Nevertheless, their total carbon storage is lower because they lack the fossil-fuel storage of the simulations with 100% fossil-fuel substitution. This illustrates an inherent trade-off between land-based climate engineering techniques such as fossil-fuel substitution and land-based carbon storage in ecosystems: higher CO_2-concentrations fertilize plants and trigger additional draw-down of carbon from the atmosphere, but higher fossil-fuel substitution rates reduce CO_2-concentrations more than simple draw-down of CO_2 by ecosystems, yet

simultaneously reduce the draw-down capacity of land-based ecosystems. Carbon stocks in crops and pastures decrease as their area decreases. This questions the scenario assumption that more food can be cultivated on less area. However, JSBACH does not include different management options such as irrigation or fertilization, which might additionally increase food production.
If herbaceous biomass plantations are cultivated on abandoned crop and pasture areas which would otherwise have reverted to forests, they prevent forest regrowth and reduce the land's carbon sequestration potential. However, the abandoned areas in the RCP4.5-scenario are large enough to significantly reduce carbon dioxide concentrations, if they are used to substitute fossil-fuels. This trade-off could be minimized by planting herbaceous biomass plantations in areas where forests cannot grow or are less productive. Ultimately, the choice of whether and where to plant biomass plantations depends on the prioritization of goals.

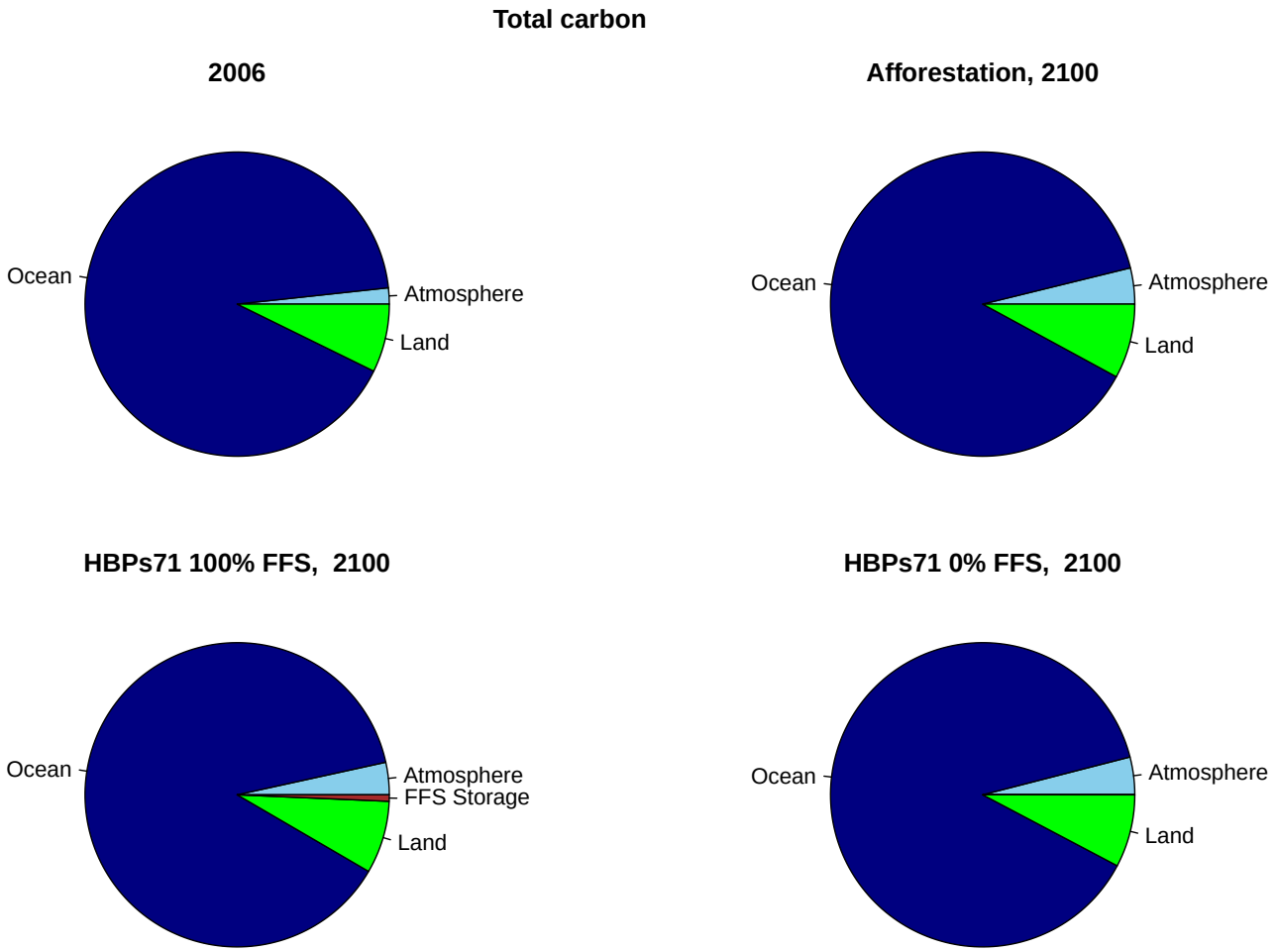

Figure 5.2: Total carbon [Pg] contained in the ocean, the atmosphere, and the land in 2006 and 2100 for the afforestation scenario and two scenarios with herbaceous biomass plantations, the first with 0% fossil-fuel substitution and the second with 100% fossil-fuel substitution. The one with 100% fossil-fuel substitution also shows the amount of fossil-fuels that remain in the ground thanks to substitution by biomass (FFS Storage).

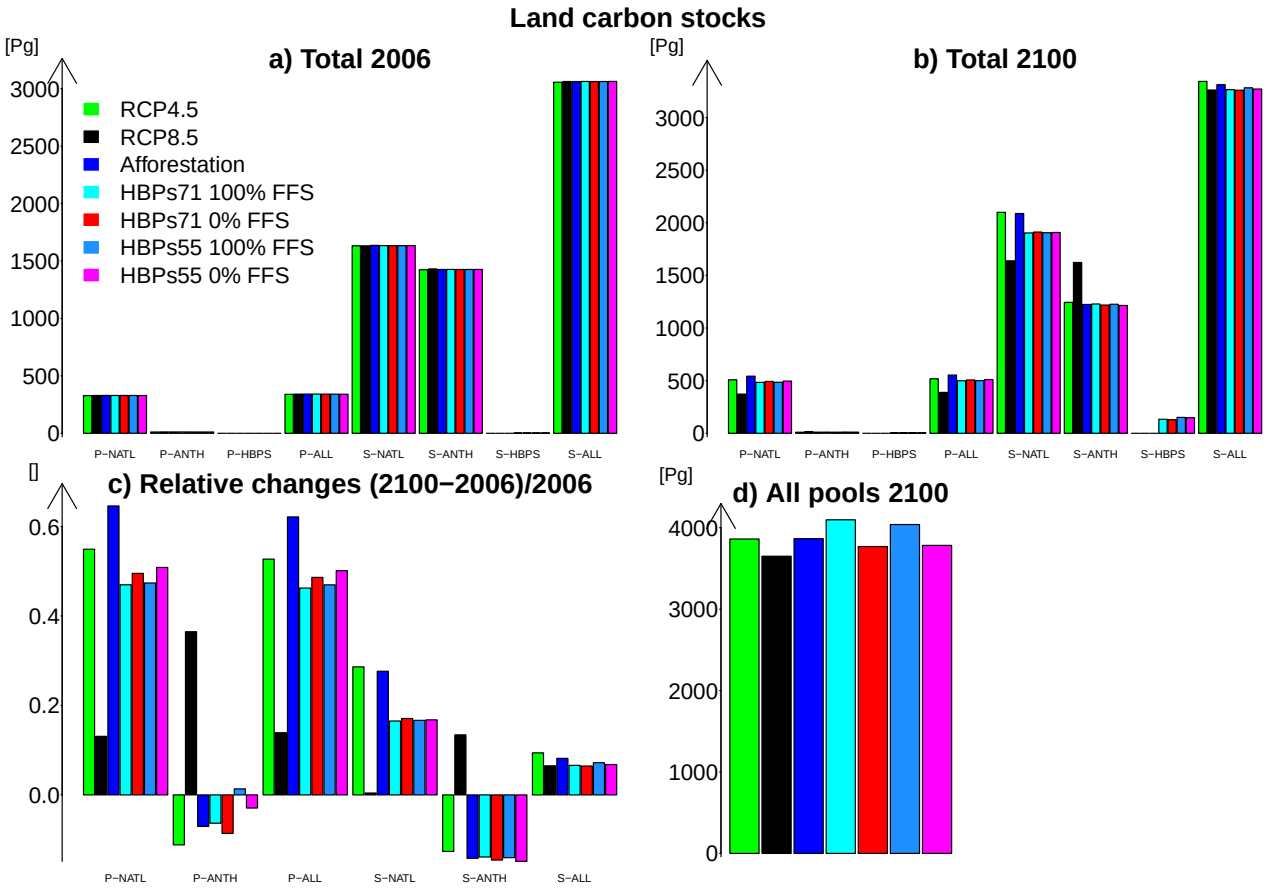

Figure 5.3: Land carbon pools in 2006 (a) and 2100 (b) for all simulations considered, as well as relative changes (c) and the sum of all land-based carbon pools in 2100, including the total harvest from 2006-2100 (d). RCP: Representative concentration pathway, HBPs: herbaceous biomass plantations, FFS: fossil-fuel substitution, 55/71: 55/71% of plant carbon is harvested, 0/100%: level of fossil-fuel substitution, P-NATL: plant carbon in natural lands, P-ANTH: plant carbon in crops and pastures, P-HBPS: plant carbon in herbaceous biomass plantations, P-ALL: plant carbon in all vegetation types, S-NATL: soil carbon under natural vegetation, S-ANTH: soil carbon under crops and pastures, S-HBPS: soil carbon under herbaceous biomass plantations, S-ALL: sum of all soil carbon

This study is limited in one fundamental way: JSBACH cannot account for the many different management options which could improve carbon stocks in forests, grasslands, fields or plantations. JSBACH does not include fertilizers and pesticides. JSBACH also fails to account for possible future improvements resulting from more productive strains or technologies still in development. Numerous studies have shown that some regions lag behind their full food production capacities because of lack of technologies such as efficient irrigation techniques or energy supplies needed to pump water (Matson et al., 1997; Niles et al., 2002; Harvey et al., 2014). Similarly, silvicultural techniques can influence carbon stocks in forests and their soils (Niles et al., 2002; López-Díaz et al., 2017). Thus JSBACH cannot estimate how much additional carbon land ecosystems could store, if optimal management techniques were established globally.

5.4 Conclusions

This chapter shows that land-use choices fundamentally influence the distribution of carbon in land ecosystems and the entire Earth System. Additionally, it illustrates how different methods of carbon dioxide removal from the atmosphere can influence each other. This study illustrates two main effects:

- Substituting fossil-fuels with herbaceous biomass plantations increases the overall draw-down capacity of land-based ecosystems.
- Substituting fossil-fuels with herbaceous biomass plantations simultaneously decreases the capacity of forests to store carbon due to the reduction of CO_2-fertilization.

Chapter 6

Summary and Conclusions

This study combines several important aspects. First, all scenarios were simulated in a global coupled model, unlike most previous studies on biomass plantations which used either local or regional models or dynamic vegetation models. Second, the RCP4.5 land-use ensures food security and ample wood supply while providing areas for the establishment of herbaceous biomass plantations. Third, the high emissions of RCP8.5 help explore the maximum potentials of herbaceous biomass plantations as a tool for climate engineering. Lastly, I examine many different aspects in order to develop a comprehensive and holistic view of herbaceous biomass plantations and their potential effects on the Earth System.

This study analyzes the effects of herbaceous biomass plantations on the climate in a plausible rather than idealized scenario. The baseline scenario couples the emissions of RCP8.5 with the land-use of RCP4.5. In this scenario large areas of agricultural lands are abandoned throughout the 21st century. They revert to natural lands, mainly forests (afforestation baseline). This afforestation baseline was simulated by Sonntag et al. 2016. My scenario establishes herbaceous biomass plantations on the abandoned croplands and pastures that revert to forests in the baseline scenario, avoiding emissions resulting from the displacement of natural ecosystems.

I developed four scenarios, with two different harvest rates, 55% and 71% of plant carbon, and two differing fossil-fuel substitution options, 0% and 100% of harvested carbon used for fossil-fuel substitution. Each harvest rate was paired with each fossil-fuel substitution option. I simulated all four scenarios from 2005 to 2100 in the fully coupled Max-Planck-Institute Earth System Model (MPI-ESM).

I compare my scenarios with the baseline afforestation scenario as well as the two original RCPs. I examine the effectiveness of herbaceous biomass plantations compared to afforestation in different regions and examine how their presence affects carbon redistribution in the Earth System. In addition to the biogeochemical effects, I analyze the biogeophysical effects of herbaceous biomass plantations on the properties of the Earths surface and on the climate.

My study highlights these main effects of herbaceous biomass plantations on the Earth

System:

- Their greatest potential lies in fossil-fuel substitution. Simulations without fossil-fuel substitution have higher CO_2-concentrations than in the afforestation baseline, while simulations with fossil-fuel substitution have lower CO_2-concentrations than in the afforestation baseline.
- When established on abandoned agricultural areas, they become effective quickly and within current technological limits, in spite of the limited areas available for their establishment.
- Even though herbaceous biomass plantations prevent forest regrowth, a potential carbon sink on the order of magnitude of total yields, they still reduce temperatures and atmospheric CO_2-concentrations through fossil-fuel substitution compared to forest regrowth.
- Higher albedo of herbaceous biomass plantations increases surface reflectivity compared to afforestation.
- Herbaceous biomass plantations, when planted on abandoned agricultural areas on the scales of my study, have little potential to negatively affect local conditions
- Substituting fossil-fuels with herbaceous biomass plantations simultaneously decreases the capacity of forests to store carbon due to the reduction of CO_2-fertilization.

This study analyzed the potentials for side-effects on the climate or for human well-being. Specifically, I analyzed how biogeophysical effects of herbaceous biomass plantations might affect the local climate and if these effects might counteract or enhance the biogeochemical effects. I show that herbaceous biomass plantations increase albedo and decrease transpiration resulting in a net neutral effect compared to forests. Also, reduced transpiration may increase local soil water availability. Importantly, I show that conflict potentials between the need for global actions and the risk of local land-use change negatively affecting human well-being are low, for the alternative scenarios analyzed here.
This study contributes to a global discussion surrounding methods of mitigating climate change. Both afforestation and herbaceous biomass plantations used for fossil-fuel substitution are viewed as methods of climate engineering. My study highlights the advantages and disadvantages of each method. Both can draw down significant amounts of CO_2. Yet, neither method can fully compensate the high CO_2-emissions of RCP8.5. Therefore, any policy measures using land-use to mitigate high CO_2-emissions should also consider complementary methods. Importantly, the two methods compete for both land and CO_2, as the draw-down potential of C3-forests depends on atmospheric CO_2-concentrations.

In conclusion, herbaceous biomass plantations can mitigate climate change more effectively than afforestation in nearly all climates. They become effective quickly and within technological limits. Their effectiveness is limited by the amount of suitable land available. However, as decision makers struggle to balance food, fiber, timber and energy production, they may contribute a small amount to some solutions.

Chapter 7

Outlook

This study analyzes different aspects of herbaceous biomass and their effects on land carbon pools and the local and global climate. However, many aspects remain unclear. Herbaceous biomass plantations affect land properties in many different ways and through many different mechanisms. Some parameters that are not considered here are surface roughness or carbon turnover rates. Different distributions of herbaceous biomass plantations could potentially lead to very different results.
All changes in land-surface properties could potentially affect the atmosphere as well. For example, surface wind speeds and directions could be affected by surface roughness. Considering the small effects of other biogeophysical properties of herbaceous biomass plantations, analyzed so far, on the climate, it is questionable whether any other effects would be significant. Nevertheless, a thorough analysis would be necessary to reveal any unexpected side-effects.
The effects of herbaceous biomass plantations on the oceans also warrants further study. Ocean pH and productivity depend on atmospheric CO_2-concentrations, but also on other factors such as sea surface temperatures. None of these effects are analyzed in my study. Sea-ice extent would also be an interesting factor to study because of its role in ocean-albedo feedbacks.
Apart from the effects of my chosen scenario on the components of the Earth system, other options are conceivable. Further exploration of agricultural and technological possibilities could carbon draw-down potential of biomass plantations compared to forests. Bioenergy could be used not only for fossil-fuel substitution but also with carbon capture and storage which would effectively double carbon savings. Numerous cultivation techniques such as irrigation, fertilization but also breeding or genetic engineering could shift the boundaries of biomass productivity far beyond their current limits. Exploring these possibilities could help determine the upper limits of climate engineering with bioenergy.

Appendices

A.1 Detailed implementation of altered land-use transition scheme in JSBACH

A.1.1 Original land-use scheme

The original land-use scheme in JSBACH distinguishes between the four cover types: crops, pastures, grasses and forests (Reick et al., 2013). Transitions are initially read from transitions maps describing the yearly changes between crops, pastures and natural lands (grasses and forests). These transitions are then broken down to daily values describing the gross changes between the four cover types. The new cover fractions for each type are computed by the matrix T:

$$\begin{pmatrix} c'_C \\ c'_P \\ c'_G \\ c'_F \end{pmatrix} = T \begin{pmatrix} c_C \\ c_P \\ c_G \\ c_F \end{pmatrix} \tag{A.1}$$

Where c_i is the cover fraction of the cover type i of the previous day, c_i is the new cover fraction of the cover type i, the indices designate the four cover types used in the original scenario: C stands for crops, P for pastures, G for grasses and F for forests. The transition matrix T describes the transitions between the four cover types:

$$T = \begin{pmatrix} T_{C\to C} & T_{P\to C} & T_{G\to C} & T_{F\to C} \\ T_{C\to P} & T_{P\to P} & T_{G\to P} & T_{F\to P} \\ T_{C\to G} & T_{P\to G} & T_{G\to G} & T_{F\to G} \\ T_{C\to F} & T_{P\to F} & T_{G\to F} & T_{F\to F} \end{pmatrix} \tag{A.2}$$

Where $T_{i\to j}$ is the fraction of area that is transferred from cover type i to cover type j. Importantly all cover fractions must sum up to 1:

$$\sum_i c_i = \sum_i c'_i = 1 \tag{A.3}$$

Additionally, because the transitions maps do not distinguish between grasses and forests but consider both to be natural lands, all transitions between grasses and forests are always zero:

$$T_{G\to F} = T_{F\to G} = 0 \tag{A.4}$$

A.1.2 Modified land-use scheme

In order to incorporate herbaceous biomass plantations into the original land-use scheme, an expanded transition matrix was inserted into the model which separated herbaceous biomass plantations from the other cover types. This matrix uses the original matrix T as input for its calculations. In the original matrix, herbaceous biomass plantations are considered to be forest. The new transition matrix $\tilde{T}$ is described by the equation:

$$\tilde{T} = \begin{pmatrix} \tilde{T}_{C\to C} & \tilde{T}_{P\to C} & \tilde{T}_{G\to C} & \tilde{T}_{F\to C} & \tilde{T}_{H\to C} \\ \tilde{T}_{C\to P} & \tilde{T}_{P\to P} & \tilde{T}_{G\to P} & \tilde{T}_{F\to P} & \tilde{T}_{H\to P} \\ \tilde{T}_{C\to G} & \tilde{T}_{P\to G} & \tilde{T}_{G\to G} & \tilde{T}_{F\to G} & \tilde{T}_{H\to G} \\ \tilde{T}_{C\to F} & \tilde{T}_{P\to F} & \tilde{T}_{G\to F} & \tilde{T}_{F\to F} & \tilde{T}_{H\to F} \\ \tilde{T}_{C\to H} & \tilde{T}_{P\to H} & \tilde{T}_{G\to H} & \tilde{T}_{F\to H} & \tilde{T}_{H\to H} \end{pmatrix} \tag{A.5}$$

Where H denotes the new cover type, herbaceous biomass plantations. All transitions between crops, pastures and grasses remain identical, since there are no modifications in the transitions between these cover types. Additionally, there should be no transitions between forests or grasses and herbaceous biomass plantations, since herbaceous biomass plantations are only planted on abandoned crops or pastures. Thus, $\tilde{T}_{F\to H} = \tilde{T}_{H\to F} = \tilde{T}_{G\to H} = \tilde{T}_{H\to G} = 0$. Lastly, equation (A.4) shows that there are no transitions between grasses and forests either. So the modified matrix can be described by:

$$\tilde{T} = \begin{pmatrix} T_{C\to C} & T_{P\to C} & T_{G\to C} & \tilde{T}_{F\to C} & \tilde{T}_{H\to C} \\ T_{C\to P} & T_{P\to P} & T_{G\to P} & \tilde{T}_{F\to P} & \tilde{T}_{H\to P} \\ T_{C\to G} & T_{P\to G} & T_{G\to G} & 0 & 0 \\ \tilde{T}_{C\to F} & \tilde{T}_{P\to F} & 0 & \tilde{T}_{F\to F} & 0 \\ \tilde{T}_{C\to H} & \tilde{T}_{P\to H} & 0 & 0 & \tilde{T}_{H\to H} \end{pmatrix} \tag{A.6}$$

Where $T_{i\to j}$ are transition elements conserved by the modified matrix and $\tilde{T}_{i\to j}$ are the transition elements of the modified matrix. Ten transition elements are still unknown in the new matrix. In the following, new equations are developed to determine these transition elements. Importantly, all transitions elements must fall in the range from zero to one because the model assumes that within a single timestep farmers would not convert more than the currently available area of one plant type, for example abandon cropland to forests and then immediately reclaim it along with more forest, such transitions would count as a single transition, and to avoid cover fractions that are negative (negative area is illogical) or larger than one (area larger than the gridcell is undesirable and would impede proper model functioning). The modified matrix allows calculating the new cover fractions:

$$\begin{pmatrix} c'_C \\ c'_P \\ c'_G \\ \tilde{c}'_F \\ \tilde{c}'_H \end{pmatrix} = \tilde{T} \begin{pmatrix} c_C \\ c_P \\ c_G \\ \tilde{c}_F \\ \tilde{c}_H \end{pmatrix} \tag{A.7}$$

This equation ensures that the cover fractions of crops, pastures and grasses are conserved by the modified matrix and are identical to the cover fractions calculated by the original scheme:

$$\tilde{c}_i = c_i \text{ for } i \in \{C, P, G\} \tag{A.8}$$

The sums of all cover fractions must be one:

$$\sum_i \tilde{c}_i = \sum_i \tilde{c}'_i = 1 \text{ for } i \in \{C, P, G, F, H\} \tag{A.9}$$

The cover fractions of forests and herbaceous biomass plantations are modified and need to be recalculated along with all transition elements describing transitions to and from these cover types. Since the cover fractions of crops pastures and grasses must be identical to those in the original scenario, the cover fractions of forests and herbaceous biomass plantations, in the new scenario, together must be identical to the cover fractions of forests from the original scenario:

$$\tilde{c}_F = c_F\,(t = 2005) \underset{A.8,\,A.9}{\overset{A.4}{\Longrightarrow}} c_F = \tilde{c}_F + \tilde{c}_H \text{ and } c'_F = \tilde{c}_F + \tilde{c}_H \tag{A.10}$$

Where $c_F\,(t = 2005)$ indicates the cover fraction of forests in 2005.

A.1.2.1 Matrix derived equations

The structure of the modified transition matrix determines that column sums must be equal to one (A.9) because the transition elements in each column describe all possible transitions from one cover type to either itself or the other cover types and since the entire area covered by that cover type must be accounted for, the sums of the transition elements must be one:

$$T_{C\to C} + T_{C\to P} + T_{C\to G} + \tilde{T}_{C\to F} + \tilde{T}_{C\to H} = 1 \tag{A.11}$$

$$T_{P\to C} + T_{P\to P} + T_{P\to G} + \tilde{T}_{P\to F} + \tilde{T}_{P\to H} = 1 \tag{A.12}$$

$$\tilde{T}_{F\to C} + \tilde{T}_{F\to P} + \tilde{T}_{F\to F} = 1 \tag{A.13}$$

$$\tilde{T}_{H\to C} + \tilde{T}_{H\to P} + \tilde{T}_{H\to H} = 1 \tag{A.14}$$

This relationship holds true for grasses as well, however, all transition elements in this column are known, therefore the equation is not considered here. The relationship is also valid for the original transition matrix:

$$T_{C\to C} + T_{C\to P} + T_{C\to G} + T_{C\to F} = 1 \tag{A.15}$$

$$T_{P\to C} + T_{P\to P} + T_{P\to G} + T_{P\to F} = 1 \tag{A.16}$$

Thus equations (A.11) and (A.15) can be combined to:

$$\tilde{T}_{C\to F} + \tilde{T}_{C\to H} = T_{C\to F} \tag{A.17}$$

Similarly equations (A.12) and (A.16) are combined to:

$$\tilde{T}_{P\to F} + \tilde{T}_{P\to H} = T_{P\to F} \tag{A.18}$$

A.1.2.2 Equations resulting from the specific land-use scenario

On the global scale, RCP4.5 projects a contraction of agricultural lands. However, agricultural lands may expand in individual gridcells. The scenario produces three possible cases that need to be dealt with separately: contraction of agricultural lands, expansion of agricultural lands in the presence of herbaceous biomass plantations and expansion of agricultural lands in the absence of herbaceous biomass plantations in the gridcell.

A.1.2.2.1 First case: contraction of agricultural lands

Precondition for the first case: $c'_F \geq c_F$

The first case is the most common case in the RCP4.5 scenario. It reflects abandonment of agricultural areas. In the original scenario, these areas revert to forests. In the new scenario they are allocated to herbaceous biomass plantations. The precondition reflects an increase in forests in the original scenario.

A.1.2.2.1.1 Equations specific for the first case

When agricultural lands contract, the abandoned areas are converted to herbaceous biomass plantations. Forests conserve their cover fractions from the previous timestep. There are no conversions from herbaceous biomass plantations to crops or pastures:

$$\tilde{T}_{H\to C} = 0 \tag{A.19}$$

$$\tilde{T}_{H\to P} = 0 \tag{A.20}$$

Inserting equations (A.19) and (A.20) into the transition matrix (A.6) yields the following four equations for the new cover fractions (according to equation (A.7) the cover fractions of crops and pastures keep their original value).

$$T_{C\to C} * c_C + T_{P\to C} * c_P + T_{G\to C} * c_G + \tilde{T}_{F\to C} * \tilde{c}_F = c'_C \tag{A.21}$$

$$T_{C\to P} * c_C + T_{P\to P} * c_P + T_{G\to P} * c_G + \tilde{T}_{F\to P} * \tilde{c}_F = c'_P \tag{A.22}$$

$$T_{C\to F} * c_C + T_{P\to F} + \tilde{T}_{F\to F} * \tilde{c}_F = \tilde{c}'_F \tag{A.23}$$

$$T_{C\to H} * c_C + T_{P\to H} + \tilde{T}_{H\to H} * \tilde{c}_H = \tilde{c}'_H \tag{A.24}$$

The transition matrix would yield a similar equation for grasses but since all elements in that equation are known, it is omitted here. The same relationships as above apply for the original dynamic:

$$T_{C\to C} * c_C + T_{P\to C} * c_P + T_{G\to C} * c_G + T_{F\to C} * c_F = c'_C \tag{A.25}$$

$$T_{C\to P} * c_C + T_{P\to P} * c_P + T_{G\to P} * c_G + T_{F\to P} * c_F = c'_P \tag{A.26}$$

Thus, equations (A.21) and (A.25) can be combined and simplified to:

$$\tilde{T}_{F\to C} * \tilde{c}_F = T_{F\to C} * c_F \tag{A.27}$$

Similarly, equations (A.22) and (A.26) can be combined and simplified to:

$$\tilde{T}_{F\to P} * \tilde{c}_F = T_{F\to P} * c_F \tag{A.28}$$

Since herbaceous biomass plantations are established on areas that revert to forests, the new cover fractions of forests are smaller or equal to the original cover fractions, thus $\tilde{c}_F \leq c_F$. Yet the crop and pasture areas must not divert from the original scheme. Gross transitions can lead to reclaiming of forests for agriculture even when total agricultural area shrinks. Therefore, transitions from forests to agricultural lands are not necessarily zero. In such cases, transitions from forests to crops or pastures must be larger than in the original scheme because the new cover fraction of forests is smaller, thus $\tilde{T}_{F\to C} \geq T_{F\to C}$ and $\tilde{T}_{F\to P} \geq T_{F\to P}$. If the forest cover fraction is very small, or the transitions to anthropogenic areas particularly large, the equations may result in transition elements larger than one, i.e. $\tilde{T}_{F\to C} \geq 1$ or $\tilde{T}_{F\to P} \geq 1$. However, transition elements larger than one. To avoid this, a scaling factor, S, is introduced into equations (A.27) and (A.28):

$$S := (T_{F\to C} + T_{F\to P}) \frac{c_F}{\tilde{c}_F} \tag{A.29}$$

The transition elements from forests to anthropogenic areas are then calculated as:

$$\tilde{T}_{F\to i} := \frac{1}{max\,(1, S)} * T_{F\to i} \frac{c_F}{\tilde{c}_F} \text{ for } i \in \{C, P\} \tag{A.30}$$

Additionally, the scenario demands that cover fractions of forests remain constant from one timestep to the next:

$$\tilde{c}'_F = \tilde{c}_F \tag{A.31}$$

Lastly, a relationship is needed to describe how much abandoned cropland and how much abandoned pasture area is converted to herbaceous biomass plantations rather than forests. For this, I introduce the proportionality factor lambda, λ, and assume that herbaceous biomass plantations are established proportionally to the total amount of abandoned agricultural areas:

$$\tilde{T}_{C\to H} * \tilde{c}_C = \lambda T_{C\to F} * c_C \tag{A.32}$$

$$\tilde{T}_{P\to H} * \tilde{c}_P = \lambda T_{P\to F} * c_P \tag{A.33}$$

A.1.2.2.1.2 Solutions for the first case

All values for cover fractions and transition elements must belong to the codomain $[0, 1]$. The cover fractions describe the fraction of a gridcell covered by the respective cover types and must be positive because negative area is illogical, but cannot exceed 1 because the maximum area any cover type can occupy is the entire gridcell. The transition elements describe the fractions of an area occupied by one cover type that is converted into another. The minimum area converted is none, represented by a transition element equal to zero, the maximum area converted is the entire area, represented by a transition element equal to 1. Each relationship must therefore be tested to ensure that it does not violate this precondition. The equations above provide the modified cover fractions of forests and herbaceous biomass plantations. Equation (A.31) shows that the cover fractions of forests are constant (precondition of the modified scenario). This ensures that the cover fractions of forests are positive but do not exceed one.

$$\tilde{c}'_F = \tilde{c}_F \Rightarrow 0 \leq \tilde{c}'_F \leq 1 \tag{A.34}$$

Equation (A.10) and (A.34) can be combined to calculate the new cover fractions of herbaceous biomass plantations.

$$\text{(A.10): } c'_F = \tilde{c}'_F + \tilde{c}'_H \overset{\text{(A.34)}}{=} \tilde{c}_F + \tilde{c}'_H \tag{A.35}$$

$$\tilde{c}'_H = c'_F - \tilde{c}_F \Rightarrow 0 \leq \tilde{c}'_H \leq 1 \tag{A.36}$$

Building on the equations established above, the ten unknown transition elements of the modified transition matrix can now be determined: $\tilde{T}_{H\to C}$ and $\tilde{T}_{H\to P}$ result directly from equations (A.19) and (A.20), $\Rightarrow \tilde{T}_{H\to C} = \tilde{T}_{H\to P} = 0$. Since these transition elements are zero, they are automatically within the intended codomain $[0, 1]$. $\tilde{T}_{F\to C}$ and $\tilde{T}_{F\to P}$ result from equation (A.30): $\tilde{T}_{F\to i} \coloneqq \frac{1}{max\,(1,S)} * T_{F\to i} \frac{c_F}{\tilde{c}_F}$ for $i \in \{C, P\}$. The scaling factor ensures that the values of these transition elements always lie between zero and one. $\Rightarrow 0 \leq \tilde{T}'_{F\to i} \leq 1$, $i \in \{C, P\}$. In order to determine the transition elements from forests to anthropogenic areas I define:

$$\Delta_{F\to A} \coloneqq (T_{F\to C} + T_{F\to P})\, c_F \tag{A.37}$$

as the conversion fraction (Δ) of forests to anthropogenic areas from the original scenario,

$$\Delta_{A\to F} \coloneqq T_{C\to F} * c_C + T_{P\to F} * c_P \tag{A.38}$$

as the conversion fraction of anthropogenic areas to forests from the original scenario, and

$$\tilde{\Delta}_{A\to H} \coloneqq \tilde{T}_{C\to H} * c_C + \tilde{T}_{P\to H} * c_P \tag{A.39}$$

as the conversion fraction of anthropogenic areas to herbaceous biomass plantations in the new modified scenario.

Equations (A.10) and (A.35) can be rewritten to represent the difference in forest cover

fraction before and after conversion of anthropogenic areas in the original scheme as equal to the difference in the sums of cover fractions of forests and herbaceous biomass plantations before and after conversion of anthropogenic areas.

$$\begin{aligned} c'_F - c_F &\overset{\substack{A.35\\A.10}}{=} \tilde{c}_F + \tilde{c}'_H - (\tilde{c}_F + \tilde{c}_H) = \tilde{c}'_H - \tilde{c}_H \\ &\overset{A.24}{=} \tilde{T}_{C\to H} * c_C + \tilde{T}_{P\to H} * c_P + \tilde{T}_{H\to H} * \tilde{c}_H - \tilde{c}_H \\ &= \tilde{T}_{C\to H} * c_C + \tilde{T}_{P\to H} * c_P + \left(\tilde{T}_{H\to H} - 1\right) \tilde{c}_H \\ &\overset{A.14}{=} \tilde{T}_{C\to H} * c_C + \tilde{T}_{P\to H} * c_P - \left(\underbrace{\tilde{T}_{H\to C} + \tilde{T}_{H\to P}}_{\text{0 because of (A.19), (A.20)}} \right) \tilde{c}_H \end{aligned} \tag{A.40}$$

$$c'_F - c_F = \tilde{T}_{C\to H} * c_C + \tilde{T}_{P\to H} * c_P = \tilde{\Delta}_{A\to H} \tag{A.41}$$

On the other hand, the same cover change in forests corresponds to the difference in conversion fractions between forests and anthropogenic areas in the original scheme:

$$c'_F - c_F = \Delta_{A\to F} - \Delta_{F\to A} \tag{A.42}$$

This relationship is only possible because all transitions between grasses and forests are zero. Since the modified scenario prescribes that all net increase in forests be ascribed to herbaceous biomass plantations, the difference in cover fractions is equal to the conversion fraction of anthropogenic areas to herbaceous biomass plantations:

$$\tilde{\Delta}_{A\to H} = \Delta_{A\to F} - \Delta_{F\to A} \tag{A.43}$$

The same relationship described for the transition elements of anthropogenic areas to herbaceous biomass plantations holds true for the corresponding conversion fractions:

$$\tilde{\Delta}_{A\to H} = \lambda \Delta_{A\to F} \tag{A.44}$$

Inserting equation (A.44) into equation (A.43) yields λ:

$$\lambda = 1 - \frac{\Delta_{A\to F}}{\Delta_{F\to A}} \tag{A.45}$$

This first case covers all gridcells and timesteps in which forests expand in the original scenario, $c'_F \geq c_F$. This implies that the conversion fraction from anthropogenic areas to forests is larger than the conversion fraction from forests to anthropogenic areas. Neither of these conversion fractions can be negative, therefore λ falls within the codomaine of zero to one, $[0, 1]$.
The equation for λ is inserted in equations (A.32) and (A.33) to determine the transitions from anthropogenic areas to herbaceous biomass plantations:

$$\left.\begin{aligned} \tilde{T}_{C\to H} &= 1 - \frac{\Delta_{A\to F}}{\Delta_{F\to A}} * T_{C\to F} \\ \tilde{T}_{P\to H} &= 1 - \frac{\Delta_{A\to F}}{\Delta_{F\to A}} * T_{P\to F} \end{aligned}\right\} \Rightarrow 0 \leq \tilde{T}_{i\to H} \leq 1,\ i \in \{C, P\} \tag{A.46}$$

Since λ varies between zero and one, transitions from anthropogenic areas to herbaceous biomass plantations in the modified scenario cannot be larger than transitions from anthropogenic areas to forests in the original scenario, thus $0 \leq \tilde{T}_{C\to H} \leq T_{C\to F}$ and $0 \leq \tilde{T}_{P\to H} \leq T_{P\to F}$.
Equations (A.17) and (A.18) describe the relationship between transitions from anthropogenic areas to forests and to herbaceous biomass plantations in the new scenario and from anthropogenic areas to forests in the old scenario. Therefore, the modified transitions from anthropogenic areas to forests can be described as:

$$\left.\begin{aligned} \tilde{T}_{C\to F} &\overset{A.17}{=} T_{C\to F} - \tilde{T}_{C\to H} \overset{A.32}{=} (1-\lambda)\, T_{C\to F} \\ \tilde{T}_{P\to F} &\overset{A.18}{=} T_{P\to F} - \tilde{T}_{P\to H} \overset{A.33}{=} (1-\lambda)\, T_{P\to F} \end{aligned}\right\} \Rightarrow 0 \leq \tilde{T}_{i\to H} \leq 1,\ i \in \{C, P\} \quad \text{(A.47)}$$

Since λ varies between zero and one, transitions from anthropogenic areas to forests in the modified scenario cannot be larger than transitions from anthropogenic areas to forests in the original scenario, thus $0 \leq \tilde{T}_{C\to F} \leq T_{C\to F}$ and $0 \leq \tilde{T}_{P\to F} \leq T_{P\to F}$.
The area that remains forests is the residual when transitions from forests to anthropogenic areas are subtracted from the sum of all transitions from forests (equation (A.13)), because transitions between natural areas and from natural areas to herbaceous biomass plantations are zero.

$$\tilde{T}_{F\to F} = 1 - \left(\tilde{T}_{F\to C} + \tilde{T}_{F\to P}\right) \quad \text{(A.48)}$$

Equations (A.27) and (A.28) describe the transitions from forests to anthropogenic areas. Since these equations ensure that transitions from forests to anthropogenic areas stay within the range from zero to one, and their sum does not exceed one either, $\tilde{T}_{F\to C} + \tilde{T}_{F\to P} \leq 1$, the residual term falls within the target range of zero to one, $0 \leq \tilde{T}_{F\to F} \leq 1$.
All transitions from herbaceous biomass plantations to other land-use types are zero, hence the residual term describing the amount of area that remains herbaceous biomass plantations is equal to one (equations (A.14), (A.19) and (A.20)):

$$\tilde{T}_{H\to H} = 1 \quad \text{(A.49)}$$

Thus, all modified values are within their permissible codomain of $[0, 1]$.

A.1.2.2.2 Second case: expansion of agricultural lands in gridcells where herbaceous biomass plantations are larger or equal to the reclaimed area

Preconditions of the second case: $c'_F \leq c_F$ but $\tilde{c}_H \geq c_F - c'_F$.
Agricultural expansion leads to shrinking of forests in the original scenario. The precondition that herbaceous biomass plantations extent must be larger than the area by which forests shrink, ensures that the increased demand in agricultural lands can be met entirely by reclaiming herbaceous biomass plantations for agriculture. Separating the second and third cases prevents the cover fraction of herbaceous

biomass plantations from becoming negative.

A.1.2.2.2.1 Equations specific for the second case

Equations (A.17), (A.18), (A.13) and (A.14) are all valid for this case. All other equations must be reestablished. Since agricultural areas are expanding, there should be no transitions between agricultural areas and herbaceous biomass plantations:

$$\tilde{T}_{C\to H} = 0 \tag{A.50}$$

$$\tilde{T}_{P\to H} = 0 \tag{A.51}$$

In this case, the modified transition matrix of equation (A.6), yields the following four new equations:

$$T_{C\to C} * c_C + T_{P\to C} * c_P + T_{G\to C} * c_G + \tilde{T}_{F\to C} * \tilde{c}_F + \tilde{T}_{H\to C} * \tilde{c}_H = c'_C \tag{A.52}$$

$$T_{C\to P} * c_C + T_{P\to P} * c_P + T_{G\to P} * c_G + \tilde{T}_{F\to P} * \tilde{c}_F + \tilde{T}_{H\to P} * \tilde{c}_H = c'_P \tag{A.53}$$

$$\tilde{T}_{C\to F} * c_C + \tilde{T}_{P\to F} * c_P + \tilde{T}_{F\to F} * \tilde{c}_F = \tilde{c}'_F \tag{A.54}$$

$$\tilde{T}_{H\to H} * \tilde{c}_H = \tilde{c}'_H \tag{A.55}$$

Equation (A.54) is equivalent to equation (A.10). Equations (A.25) and (A.26) result from the original dynamic and are therefore also valid here. Therefore, equations (A.52) and (A.53) can be simplified as follows:

$$\tilde{T}_{F\to C} * \tilde{c}_F + \tilde{T}_{H\to C} * \tilde{c}_H = T_{F\to C} * c_F \tag{A.56}$$

$$\tilde{T}_{F\to P} * \tilde{c}_F + \tilde{T}_{H\to P} * \tilde{c}_H = T_{F\to P} * c_F \tag{A.57}$$

Similarly to the first case, the second case demands an additional condition to determine the proportions of herbaceous biomass plantations converted to pastures and crops. I use the proportionality factor lambda, λ, to describe this relationship:

$$\tilde{T}_{H\to C} * \tilde{c}_H = \lambda T_{F\to C} * c_F \tag{A.58}$$

$$\tilde{T}_{H\to P} * \tilde{c}_H = \lambda T_{F\to P} * c_F \tag{A.59}$$

Finally, the scenario demands that forest area remains constant, because there are enough herbaceous biomass plantations to meet agricultural needs:

$$\tilde{c}'_F = \tilde{c}_F \tag{A.60}$$

This last equation is identical to equation (A.34), from the first case.

A.1.2.2.2.2 Solutions for the second case

Transitions from agricultural areas to herbaceous biomass plantations are zero (see equations (A.50) and (A.51)). Therefore, transitions from agricultural areas to forests should be identical to those in the original scenario (see equations (A.17) and (A.18)):

$$\left.\begin{aligned}\tilde{T}_{C\to F} &= T_{C\to F}\\ \tilde{T}_{P\to F} &= T_{P\to F}\end{aligned}\right\} \Rightarrow 0 \leq \tilde{T}_{i\to F} \leq 1,\ i \in C, P \tag{A.61}$$

Analogously to the first case, the cover fractions of forests remain constant (equation (A.60)), therefore equation (A.36) is also valid. Inserting this equation in equation (A.55) yields the residual transition element which describes the amount of herbaceous biomass plantations that are not converted:

$$\tilde{T}_{H\to H} = \frac{c'_F - \tilde{c}_F}{\tilde{c}_H} \overset{A.1}{=} \frac{c'_F - (c_F - \tilde{c}_H)}{\tilde{c}_H} = 1 - \frac{c_F - c'_F}{\tilde{c}_H} \tag{A.62}$$

Since the preconditions of the second case exclude instances where the area of herbaceous biomass plantations is insufficient to satisfy the demand for agricultural area, this transition element is within the codomain zero to one, $0 \leq \tilde{T}_{H\to H} \leq 1$.
The proportionality factor λ, can now be determined using the change in forest cover fraction:

$$\begin{aligned} c_F - c'_F &\overset{\substack{A.35\\A.10}}{=} \tilde{c}_F + \tilde{c}_H - (\tilde{c}_F + \tilde{c}'_H)\\ &= \tilde{c}_H - \tilde{c}'_H\\ &\overset{A.55}{=} \left(1 - \tilde{T}_{H\to H}\right)\tilde{c}_H\\ &\overset{A.14}{=} \left(\tilde{T}_{H\to C} + \tilde{T}_{H\to P}\right)\tilde{c}_H\\ &= \tilde{\Delta}_{H\to A} \end{aligned} \tag{A.63}$$

Equation (A.42) is also valid here, so that it can be combined with equation (A.63):

$$\tilde{\Delta}_{H\to A} = \Delta_{F\to A} - \Delta_{A\to F} \tag{A.64}$$

The proportionality factor λ is used in equations (A.58) and (A.59). The same relationship is valid for the conversion fractions, therefore:

$$\tilde{\Delta}_{H\to A} = \lambda \Delta_{F\to A} \tag{A.65}$$

Thus the proportionality factor λ is determined:

$$\lambda = 1 - \frac{\Delta_{A\to F}}{\Delta_{F\to A}} \tag{A.66}$$

In the second case, forests shrink in the original scenario and $c'_F < c_F$, therefore $\Delta_{A\to F} < \Delta_{F\to A}$. Neither the cover fractions nor the conversion fractions can be negative, therefore λ is within the targeted codomain, $0 \leq \lambda \leq 1$. Combining equations

(A.58) and (A.59) with equation (A.66) yields the transitions from herbaceous biomass plantations to anthropogenic areas:

$$\left.\begin{aligned}\tilde{T}_{H\to C} &= \lambda T_{F\to C} * \frac{c_F}{\tilde{c}_H}\\ \tilde{T}_{H\to P} &= \lambda T_{F\to P} * \frac{c_F}{\tilde{c}_H}\end{aligned}\right\} 0 \leq \tilde{T}_{H\to i} \leq 1,\ i \in C, P \tag{A.67}$$

According to equation (A.9) the sums of all transitions from herbaceous biomass plantations to all types must equal one. Equations (A.58) and (A.59), show that $\tilde{T}_{H\to C} \geq 0$ and $\tilde{T}_{H\to P} \geq 0$. This implies that the sum of the two transition elements from herbaceous biomass plantations to anthropogenic areas must be smaller or equal to 1, $\tilde{T}_{H\to C} + \tilde{T}_{H\to P} \leq 1$, if $\tilde{T}_{H\to C} \leq 1$ and $\tilde{T}_{H\to P} \leq 1$. Thus, the two transition elements are in the targeted codomain.

Transitions from forests to agricultural areas are calculated from equations (A.56) and (A.57), with the help of equations (A.58) and (A.59) and λ from equation (A.66):

$$\begin{aligned}\left(\tilde{T}_{F\to C} + \tilde{T}_{F\to P}\right)\tilde{c}_F &= \left(T_{F\to C} + T_{F\to P}\right)c_F - \lambda\left(T_{F\to C} + T_{F\to P}\right)c_F\\ &= (1-\lambda)\,\Delta_{F\to A}\\ &\overset{A.66}{=} \Delta_{A\to F} \Rightarrow \tilde{T}_{F\to C} + \tilde{T}_{F\to P}\\ &= \frac{\Delta_{A\to F}}{\tilde{c}_F}\end{aligned} \tag{A.68}$$

$$\tilde{T}_{F\to i} = (1-\lambda)\,T_{F\to i}\frac{c_F}{\tilde{c}_F},\ i \in C, P \tag{A.69}$$

In this equation $\Delta_{A\to F}$ can be larger than $\tilde{c}_F$, in which case the sum of transitions from forests to agricultural areas would be larger than 1, $\tilde{T}_{F\to C} + \tilde{T}_{F\to P} > 1$. This would lead to a negative forest area and a negative residual transition element in equation (A.13). To avoid this, the transitions from forests to anthropogenic areas are scaled:

$$\tilde{T}_{F\to i} := (1-\lambda)\,T_{F\to i}\frac{c_F}{max\left(\Delta_{A\to F},\,\tilde{c}_F\right)},\ i \in C, P \tag{A.70}$$

This scaling ensures that $\tilde{T}_{F\to C} + \tilde{T}_{F\to P} \leq 1$ so that the residual transition $\tilde{T}_{F\to F}$ falls within the permissible codomain, $0 \leq \tilde{T}_{F\to F} \leq 1$. The residual transition $\tilde{T}_{F\to F}$ can now be determined from equation (A.13) with the help of equation (A.70):

$$\begin{aligned}\tilde{T}_{F\to F} &= 1 - \left(\tilde{T}_{F\to C} + \tilde{T}_{F\to P}\right)\\ &= 1 - \left[(1-\lambda)\,T_{F\to C}\frac{c_F}{max\left(\Delta_{A\to F},\,\tilde{c}_F\right)} + (1-\lambda)\,T_{F\to P}\frac{c_F}{max\left(\Delta_{A\to F},\,\tilde{c}_F\right)}\right]\end{aligned} \tag{A.71}$$

$$\tilde{T}_{F\to F} = 1 - \left(T_{F\to C} + T_{F\to P}\right)\frac{(1-\lambda)\,c_F}{max\left(\Delta_{A\to F},\,\tilde{c}_F\right)} \tag{A.72}$$

In the second case, the cover fraction of herbaceous biomass plantations is equal to the difference between the cover fraction of forests in the original scenario and the new scenario. Because the cover fractions of forests and herbaceous biomass plantations from the modified scenario sum up to the cover fractions of forests from the original scenario, $c'_F \overset{A.10}{=} \tilde{c}'_F + \tilde{c}'_H \overset{A.60}{=} \tilde{c}_F + \tilde{c}'_H$, and $\tilde{c}'_H = c'_F - \tilde{c}_F$.

A.1.2.2.3 Third case: expansion of agricultural lands when herbaceous biomass plantations are too small to satisfy demand

Preconditions of the second case: $c'_F \leq c_F$ but $\tilde{c}_H \leq c_F - c'_F$.
In the third case, herbaceous biomass plantations cannot satisfy the demand for agricultural lands. When they are used up, forests are reclaimed for agricultural use. As a result, forest area shrinks, $\tilde{c}'_F < \tilde{c}_F$.

A.1.2.2.3.1 Equations specific for the third case

The third case demands that all remaining areas of herbaceous biomass plantations be used for agriculture. After the transition occurs, the cover fraction of herbaceous biomass plantations must be zero:

$$\tilde{c}'_H = 0 \tag{A.73}$$

All herbaceous biomass plantations revert to crops or pastures, the transition element describing the fraction of their area that remains constant becomes 0:

$$\tilde{T}_{H\to H} = 0 \tag{A.74}$$

Analogously to the second case, no transitions occur from anthropogenic areas to herbaceous biomass plantations:

$$\tilde{T}_{C\to H} = 0 \tag{A.75}$$

$$\tilde{T}_{P\to H} = 0 \tag{A.76}$$

These equations correspond to (A.50) and (A.51) from the second case. Equations resulting from the transition matrix are valid for the third case:

$$\tilde{T}_{C\to F} * c_C + \tilde{T}_{P\to F} * c_P + \tilde{T}_{F\to F} * \tilde{c}_F = \tilde{c}'_F \tag{A.77}$$

Equation (A.77) is equivalent to equation (A.54) from the second case and (A.10). The relationships between transitions from forests and herbaceous biomass plantations to agricultural areas described in the second case (equations (A.56) and (A.57)) are still valid:

$$\tilde{T}_{F\to C} * \tilde{c}_F + \tilde{T}_{H\to C} * \tilde{c}_H = T_{F\to C} * c_F \tag{A.78}$$

$$\tilde{T}_{F\to P} * \tilde{c}_F + \tilde{T}_{H\to P} * \tilde{c}_H = T_{F\to P} * c_F \tag{A.79}$$

Lastly, the proportionality factor, lambda, is used identically to the second case:

$$\tilde{T}_{H\to C} * \tilde{c}_H = \lambda T_{F\to C} * c_F \tag{A.80}$$

$$\tilde{T}_{H\to P} * \tilde{c}_H = \lambda T_{F\to P} * c_F \tag{A.81}$$

A.1.2.2.3.2 Solutions for the third case

Since herbaceous biomass plantations are too small to satisfy the demand for crops and pastures, all transitions to herbaceous biomass plantations become 0 (equations (A.75), (A.76), (A.74)):

$$\tilde{T}_{C\to H} = \tilde{T}_{P\to H} = \tilde{T}_{H\to H} = 0 \tag{A.82}$$

Consequently, the cover fraction of herbaceous biomass plantations also becomes 0 (equation (A.73)):

$$\tilde{c}'_H = 0 \tag{A.83}$$

Transitions from crops or pastures to forests are equivalent to those in the original scheme (combine equations (A.17), (A.75) and (A.18), (A.75)):

$$\tilde{T}_{C\to F} = T_{C\to F} \tag{A.84}$$

$$\tilde{T}_{P\to F} = T_{P\to F} \tag{A.85}$$

λ can be calculated from equations (A.80) and (A.81):

$$\left(\tilde{T}_{H\to C} + \tilde{T}_{H\to P}\right) = \lambda \Delta_{F\to A} \tag{A.86}$$

Additionally, inserting equation (A.74) into (A.14) results in:

$$\tilde{T}_{H\to C} + \tilde{T}_{H\to P} = 1 \tag{A.87}$$

By combining equations (A.86) and (A.87), λ can be calculated as:

$$\lambda = \frac{\tilde{c}_H}{\Delta_{F\to A}} \tag{A.88}$$

The new cover fraction of forests is equivalent to the old cover fraction plus the change in area which can be expressed as the difference in conversion fractions to and from forests (see equation (A.42)):

$$c'_F = c_F + \Delta_{A\to F} - \Delta_{F\to A} \tag{A.89}$$

The precondition of the third case expresses that herbaceous biomass plantations are smaller than forest area loss from the original scheme:

$$\tilde{c}_H < c_F - c'_F = \Delta_{A\to F} - \Delta_{F\to A} \tag{A.90}$$

By combining this equation with equation (A.88), I find that λ remains within the confines of the target codomain:

$$\lambda < 1 - \frac{\Delta_{A\to F}}{\Delta_{F\to A}} \underbrace{\leq}_{\text{because } c_F > c'_F \text{ and } \Delta_{F\to A} > \Delta_{A\to F}} 1 \Rightarrow 0 < \lambda < 1 \tag{A.91}$$

Transitions from herbaceous biomass plantations to crops and pastures can be expressed with the help of equations (A.80), (A.81), and (A.88):

$$\tilde{T}_{H\to i} = \frac{\lambda}{\tilde{c}_H} T_{F\to i} * c_F = T_{F\to i} \frac{c_F}{\Delta_{F\to A}} = T_{F\to i} \frac{c_F}{(T_{F\to C} + T_{F\to P})\, c_F}, \text{ with } i \in C, P \quad \text{(A.92)}$$

Thus,

$$\tilde{T}_{H\to i} = \frac{T_{F\to i}}{\underbrace{T_{F\to C} + T_{F\to P}}_{\leq 1}} \leq 1 \quad \text{(A.93)}$$

Transitions from forests to crops and pastures are calculated from equations (A.78) and (A.79):

$$\tilde{T}_{F\to i} = \frac{1}{\tilde{c}_F} \left(T_{F\to i} * c_F - \tilde{T}_{H\to i} * \tilde{c}_H \right) = (1-\lambda)\, T_{F\to i} \frac{c_F}{\tilde{c}_F}, \text{ where } i \in C, P \quad \text{(A.94)}$$

$$\tilde{T}_{F\to C} + \tilde{T}_{F\to P} = (1-\lambda)\, \frac{\Delta_{F\to A}}{\tilde{c}_F} \quad \text{(A.95)}$$

Numerically, $\tilde{T}_{F\to C} + \tilde{T}_{F\to P}$ can exceed 1 if $\Delta_{F\to A} > \tilde{c}_F$. Therefore, $\tilde{T}_{F\to C}$ and $\tilde{T}_{F\to P}$ must be scaled to prevent negative areas. $\tilde{T}_{F\to i}$ is redefined as:

$$\tilde{T}_{F\to i} := (1-\lambda)\, T_{F\to i} \frac{c_F}{max\,(\Delta_{F\to A},\, \tilde{c}_F)}, \text{ where } i \in C, P \quad \text{(A.96)}$$

This ensures that $\tilde{T}_{F\to C}$ and $\tilde{T}_{F\to P}$ remain within the target codomain. Inserting equation (A.96) in equation (A.13) yields the amount of area that remains forests:

$$\tilde{T}_{F\to F} = 1 - \left(\tilde{T}_{F\to C} + \tilde{T}_{F\to P} \right) \quad \text{(A.97)}$$

A.2 Parameters for herbaceous biomass plantations as a new PFT in JSBACH

Table A.1: Input parameters for herbaceous biomass plantations. All flags are boolean (0 if off and 1 if on).

Parameter	**Value**	**Unit**	**Reference/Provenence**
Lct number	22/23		serial number
Landcover class	8		new class introduced for herbaceous biomass plantations
Phenology type	6		new type introduced for herbaceous biomass plantations
Nitrogen scaling flag	1		this flag controls nitrogen distribution within the canopy
C4 flag	1		since *Miscanthus* and *Panicum* are C4-plants, this flag must be on (=1)
Maximum PEP carboxylation rate	44.9	10^{-6} mol(CO_2)/m^2/s	Dohleman et al. 2009
PEPcase CO2 specificity	140	mmol(CO_2)/m^2/s	same as C4 grasses and C4 pasture
Vegetation height	3	m	Heaton et al. 2008
Vegetation roughness length	0.3	m	Bonan 2002: " roughness length for vegetation is one-tenth of canopy height..." p272
Fraction NPP to wood pool	0		*Miscanthus* and *Panicum* do not contain wood
Fraction NPP to reserve pool	0.2		same as C4 crops
Fraction NPP to exudates	0		
Fraction green to herbivory	0.000822		same as C4 crops

Table A.1: Input parameters for herbaceous biomass plantations. All flags are boolean (0 if off and 1 if on).

Fraction of carbon from heterotrophic respiration that is emitted to the atmosphere	0.5		same as C4 crops
Life time of leaf litter	820	days	same as C4 grasses
Life time of woody litter	10950.0	days	same as all PFTs
LAI shed constant	0	/days	a value of zero prevents leaf shedding in the absence of favorable growing conditions
Maximum carbon content in woody parts	0	mol(C)/m^2	*Miscanthus* and *Panicum* do not contain wood
Reserve carbon to leaf carbon ratio	4		same as all grasses, pastures and crops
Maximum LAI	9	m^2/m^2	Heaton et al. 2008
Stem area	0	m^2/m^2	same as all grasses, pastures and crops
Specific leaf area of carbon	0.451	m^2(leaf)/mol(C)	same as all grasses, pastures and crops
Clumpiness factor	2		same as grasses
Canopy albedo in the visible range	0.08		same as all grasses, pastures and crops
Canopy albedo in the near infrared range	0.33		
Minimum snow albedo in the visible range	0.52		

Table A.1: Input parameters for herbaceous biomass plantations. All flags are boolean (0 if off and 1 if on).

Maximum snow albedo in the visible range	0.9		same as all grasses, pastures and crops
Minimum snow albedo in the near infrared range	0.3		same as all grasses, pastures and crops
Maximum snow albedo in the near infrared range	0.65		
Minimum snow albedo	0.4		same as all grasses, pastures and crops
Maximum snow albedo	0.8		same as all grasses, pastures and crops
Dynamic PFT flag	0		*Miscanthus* and *Panicum* are controlled by land-use not by dynamical vegetation
Woody PFT flag	0		*Miscanthus* and *Panicum* are not woody types
Pasture PFT flag	0		*Miscanthus* and *Panicum* are not pastures
PFT-specific minimum coldest monthly mean temperature	-40	°C	same value as in LPJ, Tim Beringer and Vera Heck, personal communication
PFT-specific maximum coldest monthly mean temperature	1000	°C	default value for non-dynamic types
PFT-specific maximum warmest monthly mean temperature	1000	°C	default value for non-dynamic types
PFT-specific 20-year average min warmest - coldest month temperature range	-1000	°C	default value for non-dynamic types

Table A.1: Input parameters for herbaceous biomass plantations. All flags are boolean (0 if off and 1 if on).

PFT-specific minimum growing degree days	0		default value for non-dynamic types
PFT-specific GDD base	5		same as all grasses, pastures and crops
PFT-specific upper limit of warmest-month temperature	0		same as all grasses, pastures and crops
Time scale of the pfts	0		same as all grasses, pastures and crops

References

Acaroğlu, M. and Aksoy, A. (1998). Third year growing results of C4 energy plant *Miscanthus sinensis* in producing energy from biomass. In *Biomass for Energy and the Environment: Proceedings of the 10th European Bioenergy Conference*, pages 1700–1703.

Acaroğlu, M. and Şemi Aksoy, A. (2005). The cultivation and energy balance of *Miscanthus* × *giganteus* production in Turkey. *Biomass and Bioenergy*, 29(1):42 – 48.

Adler, Paul R.and Sanderson, M. A., Boateng, A. A., Weimer, P. J., and Jung, H.-J. G. (2006). Biomass yield and biofuel quality of switchgrass harvested in fall or spring. *Agronomy Journal*, 98(6):1518–1525.

Adler, P. R., Del Grosso, S. J., and Parton, W. J. (2007). Life-cycle assessment of net greenhouse-gase flux for bioenergy cropping systems. *Ecological Applications*, 17(3):675–691.

Andrea, M., Tieppo, R., Gimeney, L., Povh, F., Katsman, T., and Romanelli, T. (2014). Energy demand in agricultural biomass production in Parana state, Brazil. *Agric. Eng. Int.: CIGR Journal*, Special issue:42–51.

Angelini, L. G., Ceccarini, L., o Di Nasso, N. N., and Bonari, E. (2009). Comparison of *Arundo donax* L. and *Miscanthus* × *giganteus* in a long-term field experiment in Central Italy: Analysis of productive characteristics and energy balance. *Biomass and Bioenergy*, 33(4):635 – 643.

Aravindhakshan, S. C., Epplin, F. M., and Taliaferro, C. M. (2010). Economics of switchgrass and *Miscanthus* relative to coal as feedstock for generating electricity. *Biomass and Bioenergy*, 34:1375–1383.

Arora, V. K. and Boer, G. J. (2010). Uncertainties in the 20th century carbon budget associated with land use change. *Global Change Biology*, 16(12):3327–3348.

Arundale, R. (2012). *The higher productivity of the bioenergy feedstock Miscanthus* × *giganteus relative to Panicum virgatum is seen both into the long term and beyond Illinois*. PhD thesis, University of Illinois at Urbana-Champaign.

Bathiany, S., Claussen, M., Brovkin, V., Raddatz, T., and Gayler, V. (2010). Combined biogeophysical and biogeochemical effects of large-scale forest cover changes in the mpi earth system model. *Biogeosciences*, 7:13831399.

Beale, C., Bint, D., and Long, S. (1996). Leaf photosynthesis in the C4-grass *Miscanthus* × *giganteus*, growing in the cool temperate climate of southern England. *Journal of Experimental Botany*, 47(295):267–273.

Beale, C. and Long, S. (1997). Seasonal dynamics of nutrient accumulation and partitioning in the perennial C4-grasses *Miscanthus* × *giganteus* and *Spartina cynosuroides*. *Biomass and Bioenergy*, 12(6):419 – 428.

Beringer, T., Lucht, W., and Schaphoff, S. (2011). Bioenergy production potential of global biomass plantations under environmental and agricultural constraints. *Bioenergy*, 3:299–312.

Betts, R. A. (2001). Biogeophysical impacts of land use on present-day climate: Near-surface temperature change and radiative forcing. *Atmospheric Science Letters*, 2(1-4):39–51.

Betts, R. A., Falloon, P. D., Goldewijk, K. K., and Ramankutty, N. (2007). Biogeophysical effects of land use on climate: Model simulations of radiative forcing and large-scale temperature change. *Agricultural and Forest Meteorology*, 142(24):216 – 233. The Contribution of Agriculture to the State of Climate.

Betts, R. A., Jones, C. D., Knight, J. R., Keeling, R. F., and Kennedy, J. J. (2016). El Niño and a record CO_2 rise. *Nature Climate Change*.

Bonan, G. (2002). *Ecological Climatology, 678 pp.* Cambridge Univ. Press, New York.

Bonan, G. B. (2008). Forests and climate change: forcings, feedbacks, and the climate benefits of forests. *Science*, 320:1444–1449.

Boysen, L. R. (2016). *Potentials, consequences and trade-offs of terrestrial carbon dioxide removal - strategies for climate engineering and their limitations*. PhD thesis, Mathematisch-Naturwissenschaftliche Fakultät der Humbolt-Universitt zu Berlin.

Brosse, N., Dufour, A., Meng, X., Sun, Q., and Ragauskas, A. (2012). *Miscanthus*: A fast-growing crop for biofuels and chemicals production. *Biofuels, Bioproducts and Biorefining*, 6:580–598.

Brovkin, V., Boysen, L., Arora, V. K., Boisier, J., Cadule, P., Chini, L., Claussen, M., Friedlingstein, P., Gayler, V., van den Hurk, B., Hurtt, G., Jones, C., E., K., de Noblet-Ducoudré, N., Pacifico, F., Pongratz, J., and Weiss, M. (2013). Effect of anthropogenic land-use and land-cover changes on climate and land carbon storage in CMIP5 projections for the twenty-first century. *Journal of Climate*, 26:6859–6881.

Brovkin, V., Claussen, M., Driesschaert, E., Fichefet, T., Kicklighter, D., Loutre, M., Matthews, H., Ramankutty, N., Schaeffer, M., and Skolov, A. (2006). Biogeophysical effects of historical land cover changes simulated by six Earth system models of intermediate complexity. *Climate Dynamics*, 26:587600.

Brovkin, V., Raddatz, T., Reick, C. H., Claussen, M., and Gayler, V. (2009). Global biogeophysical interactions between forest and climate. *Geophysical Research Letters*, 36.

Cadoux, S., Riche, A. B., Yates, N. E., and Machet, J.-M. (2012). Nutrient requirements of *Miscanthus* × *giganteus*: Conclusions from a review of published studies. *Biomass and Bioenergy*, 38:14 – 22. Overcoming Barriers to Bioenergy: Outcomes of the Bioenergy Network of Excellence 2003 2009.

Cannell, M. G. (2003). Carbon sequestration and biomass energy offset: theoretical, potential and achievable capacities globally, inEurope and the UK. *Biomass and Bioenergy*, 24(2):97 – 116.

Chase, T. N., Pielke, R. A., Kittel, T. G., Nemani, R., and Running, S. W. (1996). Sensitivity of a general circulation model to global changes in leaf area index. *Journal of Geophysical Research. D. Atmospheres*, 101:7393–7408.

Cherubini, F. (2010). GHG balances of bioenergy systems — Overview of key steps in the production chain and methodological concerns. *Renewable Energy*, 35(7):1565–1573.

Christian, D., Riche, A., and Yates, N. (2008). Growth, yield and mineral content of *Miscanthus* × *giganteus* grown as a biofuel for 14 successive harvests. *Industrial Crops and Products*, 28:320327.

Christian, D., Yates, N., and Riche, A. (2005). Establishing *Miscanthus sinensis* from seed using conventional sowing methods. *Industrial Crops and Products*, 21(1):109 – 111.

Chung, J.-H. and Kim, D.-S. (2012). *Miscanthus* as a potential bioenergy crop in East Asia. *Journal of Crop Science and Biotechnology*, 15(2):65–77.

Ciais, P., Sabine, C., Bala, G., Brovkin, V., Canadell, A., Chhabra, A., DeFries, R., Galloway, J., Heinemann, M., Jones, C., Le Quéré, C., Myneni, R. B., Piao, S., and Thornton, P. (2013). Carbon and Other Biogeochemical Cycles. In Climate Change 2013: The Physical Science Basis. Contribution of Working Group 1 to the Fifth Assessment Report on Climate Change. In *Climate Change 2013: The Physical Science Basis*, chapter 6, pages 486–494. Cambridge University Press, Cambridge, United Kingdom and New York, NY, USA.

Claussen, M., Brovkin, V., and Ganopolski, A. (2001). Biogeophysical versus biogeochemical feedbacks of largerscale land cover change. *Geophysical Research Letters*, 28(6):1011–1014.

Clifton-Brown, J. and Lewandowski, I. (2000). Water use effciency and biomass partitioning of three different *Miscanthus* genotypes with limited and unlimited water supply. *Annals of Botany*, 86:191200.

Clifton-Brown, J.-C., Breuer, J., and Jones, M. B. (2007). Carbon mitigation by the energy crop, *Miscanthus*. *Global Change Biology*, 13(11):2296–2307.

Clifton-Brown, J. C., Lewandowski, I., Andersson, B., Basch, G., Christian, D. G., Kjeldsen, J. B., Jørgensen, U., Mortensen, J. V., Riche, A. B., Schwarz, K.-U., Tayebi, K., and Teixeira, F. (2001). Performance of 15 *Miscanthus* genotypes at five sites in Europe. *Agron. J.*, 93:10131019.

Clifton-Brown, J. C., Stampfl, P. F., and Jones, M. B. (2004). *Miscanthus* biomass production for energy in Europe and its potential contribution to decreasing fossil fuel carbon emissions. *Global change biology*, 10(4):509–518.

Cosentino, S. L., Patanè, C., Sanzone, E., Copani, V., and Foti, S. (2007). Effects of soil water content and nitrogen supply on the productivity of *Miscanthus* × *giganteus* Greef et Deu. in a Mediterranean environment. *Industrial Crops and Products*, 25:75–88.

Dalmonech, D. and Zaehle, S. (2013). Towards a more objective evaluation of modelled land-carbon trends using atmospheric CO_2 and satellite-based vegetation activity observations. *Biogeosciences*, 10(6):4189–4210.

Danalatos, N. G., Archontoulis, S. V., and Mitsios, I. (2007). Potential growth and biomass productivity of *Miscanthus* × *giganteus* as affected by plant density and N-fertilization in central Greece. *Biomass and Bioenergy*, 31:145 152.

Dass, P. (2013). *The role of bioenergy production in the terrestrial carbon cycle and energy balance*. PhD thesis, International Max Planck Research School on Earth System Modelling.

Dohleman, F. G., Heaton, E., Leakey, A., and Long, S. (2009). Does greater leaf-level photosynthesis explain the larger solar energy conversion efficiency of *Miscanthus* relative to switchgrass? *Plant, Cell and Environment*, 32:15251537.

Dohleman, F. G. and Long, S. P. (2009). More productive than maize in the midwest: How does *Miscanthus* do it? *Plant Physiology*, 150:2104–2115.

Dougherty, R. F., Quinn, L. D., Endres, A. B., Voigt, T. B., and Barney, J. N. (2014). Natural history survey of the ornamental grass *Miscanthus sinensis* in the introduced range. *Invasive Plant Science and Management*, 7(1):113–120.

Dufossé, K., Drewer, J., Gabrielle, B., and Drouet, J.-L. (2014). Effects of a 20-year old *Miscanthus* × *giganteus* stand and its removal on soil characteristics and greenhouse gas emissions. *Biomass and Bioenergy*, 69:198 – 210.

Ehleringer, J. R. and Cerling, T. E. (2002). C3 and C4 photosynthesis. In *Encyclopedia of Global Environmental Change, The Earth system: Biological and ecological dimensions of global environmental change*, volume 2, pages 186–190.

Ercoli, L., Mariotti, M., Masoni, A., and Bonari, E. (1999). Effect of irrigation and nitrogen fertilization on biomass yield and efficiency of energy use in crop production of *Miscanthus*. *Field Crops Research*, 63(1):3 – 11.

Fales, S., Moore, K. J., and Kilborn, D. (2008). Variation in biomass yield of switchgrass grown for biofuel.

Frühwirth, P., Graf, A., Humer, M., Hunger, F., Köppl, H., Liebhard, P., and Thumfart, K. (2006). *Miscanthus sinensis "Giganteus" — Chinaschilf als nachwachsender Rohstoff*, volume 72. Landwirtschaftskammer Österreich, Ländliches Fortbildungsinstitut, Wien.

Gallagher, E. (2008). *The Gallagher review of the indirect effects of biofuels production*. Renewable Fuels Agency.

Gasser, T., Guivarch, C., Tachiiri, K., Jones, C., and Ciais, P. (2015). Negative emissions physically needed to keep global warming below 2°C. *Nature communications*, 6.

Gauder, M., Graeff-Hönninger, S., Lewandowski, I., and Claupein, W. (2012). Long-term yield and performance of 15 different *Miscanthus* genotypes in southwest Germany. *Annals of Applied Biology*, 160(2):126–136.

Gelfand, I., Sahajpal, R., Zhang, X., Izaurralde, R. C., Gross, K. L., and Robertson, G. P. (2013). Sustainable bioenergy production from marginal lands in the US Midwest. *Nature*, 493(7433):514–517.

Gennari, P., Heyman, A., and Kainu, M. (2015). FAO Statistical Pocketbook — World food and agriculture. In *FAO Statistical Pocketbook*. Food and Agriculture Organization of the United Nations.

Georgescu, M., Lobell, D. B., and Field, C. B. (2011). Direct climate effects of perennial bioenergy crops in the United States. *Proceedings of the National Academy of Sciences*, 108(11):4307–4312.

Ghannoum, O., Caemmerer, S. V., Ziska, L. H., and Conroy, J. P. (2000). The growth response of C4 plants to rising atmospheric CO_2 partial pressure: A reassessment. *Plant, Cell & Environment*, 23(9):931–942.

Giorgetta, M. A., Jungclaus, J., Reick, C. H., Legutke, S., Bader, J., Bttinger, M., Brovkin, V., Crueger, T., Esch, M., Fieg, K., Gulshak, K., Gayler, V., Haak, H., Hollweg, H.-D., Ilyina, T., Kinne, S., Kornblueh, L., Matei, D., Mauritsen, T., Mikolajewicz, U., Mueller, W., Notz, D., Pithan, F., Raddatz, T., Rast, S., Redler, R., Roeckner, E., Schmidt, H., Schnur, R., Segschneider, J., Six, K. D., Stockhause, M., Timmreck, C., Wegner, J., Widmann, H., Wieners, K.-H., Claussen, M., Marotzke, J., and Stevens, B. (2013). Climate and carbon cycle changes from 1850 to 2100 in MPI-ESM simulations for the Coupled Model Intercomparison Project phase 5. *Journal of Advances in Modeling Earth Systems*, 5:1–26.

Hallgren, W., Schlosser, A., and Monier, E. (2012). Impacts of land use and biofuels policy on climate: Temperature and localized impacts.

Hallgren, W., Schlosser, C. A., Monier, E., Kicklighter, D., Sokolov, A., and Melillo, J. (2013). Climate impacts of a large-scale biofuels expansion. *Geophysical Research Letters*, 40(8):1624–1630.

Hansen, E., Christensen, B., Jensen, L., and Kristensen, K. (2004). Carbon sequestration in soil beneath long-term *Miscanthus* plantations as determined by ^{13}C abundance. *Biomass and Bioenergy*, 26(2):97 – 105.

Hansen, J., Sato, M., Ruedy, R., Schmidt, G. A., and Lo, K. (2016). Global temperature in 2015. *Climate Science, Awareness and Solutions*.

Hartmann, D., Tank, A. K., Rusticucci, M., Alexander, L., Brönnimann, Charabi, Y., Dentener, F., Dlugokencky, E., Easterling, D., Kaplan, A., Soden, B., Thorne, P., Wild, W., and Zhai, P. (2013). Observations: Atmosphere and Surface In Climate Change 2013: The Physical Science Basis. Contribution of Working Group I to the Fifth Assessment Report of the Intergovernmental Panel on Climate Change. In Stocker, T., Quin, D., Plattner, G.-K., Tignor, M., Allen, S., Boschung, J., Nauels, A., Xia, Y., Bex, V., and Midgley, P., editors, *Climate Change 2013: The Physical Science Basis*, chapter 2, page 159254. Cambridge University Press, Cambridge, United Kingdom and New York, NY, USA.

Harvey, C. A., Chacón, M., Donatti, C. I., Garen, E., Hannah, L., Andrade, A., Bede, L., Brown, D., Calle, A., Chará, J., Clement, C., Gray, E., Hoang, M. H., Minang, P., Rodrguez, A. M., Seeberg-Elverfeldt, C., Semroc, B., Shames, S., Smukler, S., Somarriba, E., Torquebiau, E., van Etten, J., and Wollenberg, E. (2014). Climate-smart landscapes: Opportunities and challenges for integrating adaptation and mitigation in tropical agriculture. *Conservation Letters*, 7(2):77–90.

Heaton, E. A., Dohleman, F. G., and Long, S. P. (2008). Meeting US biofuel goals with less land: the potential of *Miscanthus*. *Global Change Biology*, 14(9):2000–2014.

Heck, V., Gerten, D., Lucht, W., and Boysen, L. R. (2016). Is extensive terrestrial carbon dioxide removal a 'green' form of geoengineering? A global modelling study. *Global and Planetary Change*, 137:123 – 130.

Hickman, G. C., Vanlooke, A., Dohleman, F. G., and Bernacchi, C. J. (2010). A comparison of canopy evapotranspiration for maize and two perennial grasses identified as potential bioenergy crops. *GCB Bioenergy*, 2(4):157–168.

Himken, M., Lammel, J., Neukirchen, D., Czypionka-Krause, U., and Olfs, H.-W. (1997). Cultivation of *Miscanthus* under West European conditions: Seasonal changes in dry matter production, nutrient uptake and remobilization. *Plant and Soil*, 189(1):117–126.

Hong, C., Fang, J., Jin, A., Cai, J., Guo, H., Ren, J., Shao, Q., and Zheng, B. (2011). Comparative growth, biomass production and fuel properties among different perennial plants, bamboo and *Miscanthus*. *The Botanical Review*, 77(3):197–207.

Houghton, R. A. and Nassikas, A. A. (2017). Global and regional fluxes of carbon from land use and land cover change 18502015. *Global Biogeochemical Cycles*, pages n/a–n/a. 2016GB005546.

Hughes, J. K., Lloyd, A. J., Huntingford, C., Finch, J. W., and Harding, R. J. (2010). The impact of extensive planting of *Miscanthus* as an energy crop on future CO_2 atmospheric concentrations. *GCB Bioenergy*, 2(2):79–88.

Humpenöder, F., Popp, A., Dietrich, J. P., Klein, D., Lotze-Campen, H., Bonsch, M., Bodirsky, B. L., Weindl, I., Stevanovic, M., and Müller, C. (2014). Investigating afforestation and bioenergy CCS as climate change mitigation strategies. *Environmental Research Letters*, 9(6):064029.

Hurtt, G., Chini, L., Frolking, S., Betts, R., Feddema, J., Fischer, G., Fisk, J., Hibbard, K., Houghton, R., Janetos, A., Jones, C., Kindermann, G., Kinoshita, T., Klein Goldewijk, K., Riahi, K., Shevliakova, E., Smith, S., Stehfest, E., Thomson, A., Thornton, P., van Vuuren, D., and Wang, Y. (2011). Harmonization of land-use scenarios for the period 1500-2100: 600years of global gridded annual land-use transitions, wood harvest, and resulting secondary lands. *Climatic Change*, 109(1-2):117–161.

Ilyina, T., Six, K. D., Segschneider, J., Maier-Reimer, E., Li, H., and Núñez Riboni, I. (2013). Global ocean biogeochemistry model HAMOCC: Model architecture and performance as component of the MPI-Earth system model in different CMIP5 experimental realizations. *Journal of Advances in Modeling Earth Systems*, 5(2):287–315.

Jørgensen, U. (1997). Genotypic variation in dry matter accumulation and content of N, K and Cl in *Miscanthus* in Denmark. *Biomass and Bioenergy*, 12(3):155 – 169. Biomass Quality for Power Production.

Jungclaus, J. H., Fischer, N., Haak, H., Lohmann, K., Marotzke, J., Matei, D., Mikolajewicz, U., Notz, D., and von Storch, J. S. (2013). Characteristics of the ocean simulations in the Max Planck Institute Ocean Model (MPIOM) the ocean component of the MPI-Earth system model. *Journal of Advances in Modeling Earth Systems*, 5(2):422–446.

Kering, M., Butler, T., Biermacher, J., and Guretzky, J. (2012). Biomass yield and nutrient removal rates of perennial grasses under nitrogen fertilization. *BioEnergy Research*, 5(1):61–70.

Kuemmel, B. (2003). Theoretical investigation of the effects of field margin and hedges on crop yields. *Agriculture, Ecosystems & Environment*, 95(1):387 – 392.

Lal, R. (2004). Soil carbon sequestration impacts on global climate change and food security. *Science*, 304(5677):1623–1627.

Larsen, S. U., Jørgensen, U., Kjeldsen, J. B., and Lærke, P. E. (2014). Long-term *Miscanthus* yields influenced by location, genotype, row distance, fertilization and harvest season. *BioEnergy Research*, 7(2):620–635.

Le, P. V. V., Kumar, P., and Drewry, D. T. (2011). Implications for the hydrologic cycle under climate change due to the expansion of bioenergy crops in the Midwestern United States. *Proceedings of the National Academy of Sciences*, 108(37):15085–15090.

Lemus, R., Brummer, E., Moore, K. J., Molstad, N. E., Burras, C., and Barker, M. F. (2002). Biomass yield and quality of 20 switchgrass populations in southern Iowa, USA. *Biomass and Bioenergy*, 23(6):433 – 442.

Lemus, R. W. (2004). *Switchgrass as an energy crop: Fertilization, cultivar, and cutting management*. PhD thesis, Virginia Polytechnic Institute and State University.

Lenton, T. M. and Vaughan, N. E. (2009). The radiative forcing potential of different climate geoengineering options. *Atmospheric Chemistry and Physics*, 9(15):5539–5561.

Lewandowski, I., Clifton-Brown, J., Scurlock, J., and Huisman, W. (2000). *Miscanthus*: European experience with a novel energy crop. *Biomass and Bioenergy*, 19(4):209 – 227.

Lim, S.-H., Yook, M. J., Kim, J.-W., Song, J.-S., Zhang, C.-J., Nah, G., and Kim, D.-S. (2014). Genetic diversity in agronomic traits associated with the biomass production of *Miscanthus* species collected in Northeast Asia. *Plant Genetic Resources*, 12:S137–S140.

Lima, M. A., Gomez, L. D., Steele-King, C. G., Simister, R., Bernardinelli, O. D., Carvalho, M. A., Rezende, C. A., Labate, C. A., McQueen-Mason, S. J., Polikarpov, I., et al. (2014). Evaluating the composition and processing potential of novel sources of Brazilian biomass for sustainable biorenewables production. *Biotechnology for biofuels*, 7(1):10.

Liu, W. and Sang, T. (2013). Potential productivity of the *Miscanthus* energy crop in the Loess Plateau of China under climate change. *Environmental Research Letters*, 8(4):044003.

López-Díaz, M., Benítez, R., and Moreno, G. (2017). How do management techniques affect carbon stock in intensive hardwood plantations? *Forest Ecology and Management*, 389:228 – 239.

Masson-Delmotte, V., Schulz, M., Abe-Ouchi, A., Beer, J., Ganopolski, A., González Rouco, J., Jansen, E., Lambeck, K., Luterbacher, J., Naish, T., et al. (2013). Information from Paleoclimate Archives. In Climate Change 2013: The Physical Science Basis. Contribution of Working Group 1 to the Fifth Assessment Report on Climate Change. In *Climate Change 2013: The Physical Science Basis*, volume 383464, chapter 5, page 2013. Cambridge University Press.

Matson, P. A., Parton, W. J., Power, A. G., and Swift, M. J. (1997). Agricultural intensification and ecosystem properties. *Science*, 277(5325):504–509.

McKendry, P. (2002a). Energy production from biomass (part 1): Overview of biomass. *Bioresource Technology*, 83(1):37 – 46. Reviews Issue.

McKendry, P. (2002b). Energy production from biomass (part 2): Conversion technologies. *Bioresource Technology*, 83(1):47 – 54. Reviews Issue.

McKendry, P. (2002c). Energy production from biomass (part 3): Gasification technologies. *Bioresource Technology*, 83(1):55 – 63. Reviews Issue.

Meinshausen, M., Smith, S. J., Calvin, K., Daniel, J. S., Kainuma, M. L. T., Lamarque, J.-F., Matsumoto, K., Montzka, S. A., Raper, S. C. B., Riahi, K., Thomson, A., Velders, G. J. M., and van Vuuren, D. P. (2011). The RCP greenhouse gas concentrations and their extensions from 1765 to 2300. *Climatic Change*, 109(1):213–241.

Melillo, J. M., Reilly, J. M., Kicklighter, D. W., Gurgel, A. C., Cronin, T. W., Paltsev, S., Felzer, B. S., Wang, X., Sokolov, A. P., and Schlosser, C. A. (2009). Indirect emissions from biofuels: How important? *Science*, 326(5958):1397–1399.

Meyer, M. H., Paul, J., and Anderson, N. O. (2010). Competive ability of invasive *Miscanthus* biotypes with aggressive switchgrass. *Biological Invasions*, 12(11):3809–3816.

Miguez, F. E., Villamil, M. B., Long, S. P., and Bollero, G. A. (2008). Meta-analysis of the effects of management factors on *Miscanthus* × *giganteus* growth and biomass production. *Agricultural and Forest Meteorology*, 148(89):1280 – 1292.

Miller, J. N., VanLoocke, A., Gomez-Casanovas, N., and Bernacchi, C. J. (2015). Candidate perennial bioenergy grasses have a higher albedo than annual row crops. *GCB Bioenergy*.

Mooney, D. F., Roberts, R. K., English, B. C., Tyler, D. D., and Larson, J. A. (2009). Yield and breakeven price of alamo switchgrass for biofuels in Tennessee. *Agronomy Journal*, 101(5):1234–1242.

Mulkey, V., Owens, V., and Lee, D. (2006). Management of switchgrass-dominated conservation reserve program lands for biomass production in South Dakota. *Crop Science*, 46(2):712–720.

Mulkey, V., Owens, V., and Lee, D. (2008). Management of warm-season grass mixtures for biomass production in South Dakota USA. *Bioresource Technology*, 99(3):609 – 617.

Naidu, S. and Long, S. (2004). Potential mechanisms of low-temperature tolerance of C4 photosynthesis in *Miscanthus* × *giganteus*: an in vivo analysis. *Planta*, 220(1):145–155.

Nass, L. L., Pereira, P. A. A., and Ellis, D. (2007). Biofuels in Brazil: An overview. *Crop science*, 47(6):2228–2237.

Niles, J. O., Brown, S., Pretty, J., Ball, A. S., and Fay, J. (2002). Potential carbon mitigation and income in developing countries from changes in use and management of agricultural and forest lands. *Philosophical Transactions of the Royal Society of London A: Mathematical, Physical and Engineering Sciences*, 360(1797):1621–1639.

Nussbaumer, T. (2003). Combustion and co-combustion of biomass: Fundamentals, technologies, and primary measures for emission reduction. *Energy & fuels*, 17(6):1510–1521.

Nyawira, S. S., Nabel, J. E., Axel, D., Brovkin, V., and Pongratz, J. (2016). Soil carbon response to land-use change: evaluation of a global vegetation model using observational meta-analyses. *Biogeosciences*, 13(19):5661.

Palmer, I. E., Gehl, R. J., Ranney, T. G., Touchell, D., and George, N. (2014). Biomass yield, nitrogen response, and nutrient uptake of perennial bioenergy grasses in North Carolina. *Biomass and Bioenergy*, 63:218 – 228.

Parikka, M. (2004). Global biomass fuel resources. *Biomass and Bioenergy*, 27(6):613 – 620. Pellets 2002. The first world conference on pellets.

Pimm, S. L. and Joppa, L. N. (2015). How many plant species are there, where are they, and at what rate are they going extinct? *Annals of the Missouri Botanical Garden*, 100(3):170–176.

Pongratz, J., Raddatz, T., Reick, C. H., Esch, M., and Claussen, M. (2009a). Radiative forcing from anthropogenic land cover change since A.D. 800. *Geophysical Research Letters*, 36(2):n/a–n/a. L02709.

Pongratz, J., Reick, C. H., Raddatz, T., and Claussen, M. (2009b). Effects of anthropogenic land cover change on the carbon cycle of the last millennium. *Global Biogeochemical Cycles*, 23(4):n/a–n/a. GB4001.

Pongratz, J., Reick, C. H., Raddatz, T., and Claussen, M. (2010). Biogeophysical versus biogeochemical climate response to historical anthropogenic land cover change. *Geophysical Research Letters*, 37(8):n/a–n/a. L08702.

Popp, A., Krause, M., Dietrich, J. P., Lotze-Campen, H., Leimbach, M., Beringer, T., and Bauer, N. (2012). Additional CO_2 emissions from land use change — Forest conservation as a precondition for sustainable production of second generation bioenergy. *Ecological Economics*, 74:64 – 70.

Rechid, D., Raddatz, T. J., and Jacob, D. (2009). Parameterization of snow-free land surface albedo as a function of vegetation phenology based on MODIS data and applied in climate modelling. *Theoretical and applied Climatology*, 95(3-4):245–255.

Reick, C., Raddatz, T., Brovkin, V., and Gayler, V. (2013). Representation of natural and anthropogenic land cover change in MPI-ESM. *Journal of Advances in Modeling Earth Systems*, 5(3):459–482.

Riahi, K., Krey, V., Rao, S., Chirkov, V., Fischer, G., Kolp, P., Kindermann, G., Nakicenovic, N., and Rafai, P. (2011). RCP8.5: Exploring the consequence of high emission trajectories. *Climatic Change. doi*, 10:1007.

Sabine, C. L., Feely, R. A., Gruber, N., Key, R. M., Lee, K., Bullister, J. L., Wanninkhof, R., Wong, C., Wallace, D. W., Tilbrook, B., et al. (2004). The oceanic sink for anthropogenic CO_2. *Science*, 305(5682):367–371.

Sanderson, M., Reed, R., Ocumpaugh, W., Hussey, M., Esbroeck, G. V., Read, J., Tischler, C., and Hons, F. (1999). Switchgrass cultivars and germplasm for biomass feedstock production in Texas. *Bioresource Technology*, 67(3):209 – 219.

Sanderson, M. A. (2008). Upland switchgrass yield, nutritive value, and soil carbon changes under grazing and clipping. *Agronomy Journal*, 100(3):510–516.

Schaaf, C. B., Gao, F., Strahler, A. H., Lucht, W., Li, X., Tsang, T., Strugnell, N. C., Zhang, X., Jin, Y., Muller, J.-P., Lewis, P., Barnsley, M., Hobson, P., Disney, M., Roberts, G., Dunderdale, M., Doll, C., d'Entremont, R. P., Hu, B., Liang,

S., Privette, J. L., and Roy, D. (2002). First operational BRDF, albedo nadir reflectance products from MODIS. *Remote Sensing of Environment*, 83(12):135 – 148. The Moderate Resolution Imaging Spectroradiometer (MODIS): a new generation of Land Surface Monitoring.

Schaeffer, M., Eickhout, B., Hoogwijk, M., Strengers, B., van Vuuren, D., Leemans, R., and Opsteegh, T. (2006). CO_2 and albedo climate impacts of extratropical carbon and biomass plantations. *Global Biogeochemical Cycles*, 20(2):n/a–n/a. GB2020.

Schilling, K. E., Jha, M. K., Zhang, Y.-K., Gassman, P. W., and Wolter, C. F. (2008). Impact of land use and land cover change on the water balance of a large agricultural watershed: Historical effects and future directions. *Water Resources Research*, 44(7):n/a–n/a. W00A09.

Schlegel, S., Kaphengst, T., et al. (2007). European Union policy on bioenergy and the role of sustainability criteria and certification systems. *Journal of Agricultural and Food Industrial Organization*, 5(2):1–17.

Schneck, R., Reick, C. H., and Raddatz, T. (2013). Land contribution to natural CO_2 variability on time scales of centuries. *Journal of Advances in Modeling Earth Systems*, 5(2):354–365.

Schwarz, H. (1993). *Miscanthus sinensis* 'Giganteus' production on several sites in Austria. *Biomass and Bioenergy*, 5(6):413 – 419.

Searchinger, T., Heimlich, R., Houghton, R. A., Dong, F., Elobeid, A., Fabiosa, J., Tokgoz, S., Hayes, D., and Yu, T.-H. (2008). Use of U.S. croplands for biofuels increases greenhouse gases through emissions from land-use change. *Science*, 319(5867):1238–1240.

Seidel, D. J., Fu, Q., Randel, W. J., and Reichler, T. J. (2008). Widening of the tropical belt in a changing climate. *Nature Geoscience*, 1(1):21–24.

Seto, K. C., Güneralp, B., and Hutyra, L. R. (2012). Global forecasts of urban expansion to 2030 and direct impacts on biodiversity and carbon pools. *Proceedings of the National Academy of Sciences*, 109(40):16083–16088.

Sharma, N., Piscioneri, I., and Pignatelli, V. (2003). An evaluation of biomass yield stability of switchgrass (*Panicum virgatum* L.) cultivars. *Energy Conversion and Management*, 44(18):2953 – 2958.

Siregar, M., Yuhaeni, S., Salam, R., and Nulik, J. (1985). Forages in Southeast Asian and South Pacific Agriculture: Forages in Indonesia. pages 80–83. Proceedings of an international workshop held at Cisarua, Indonesia, 19-23 August 1985.

Sladden, S., Bransby, D., and Aiken, G. (1991). Biomass yield, composition and production costs for eight switchgrass varieties in Alabama. *Biomass and Bioenergy*, 1(2):119 – 122.

Söderberg, C. and Eckerberg, K. (2013). Rising policy conflicts in Europe over bioenergy and forestry. *Forest Policy and Economics*, 33:112 – 119. Forest Land Use and Conflict Management: Global Issues and Lessons Learned.

Sonntag, S., Pongratz, J., Reick, C. H., and Schmidt, H. (2016). Reforestation in a high-CO_2 world — Higher mitigation potential than expected, lower adaptation potential than hoped for. *Geophysical Research Letters*, 43(12):6546–6553. 2016GL068824.

Stevens, B., Giorgetta, M., Esch, M., Mauritsen, T., Crueger, T., Rast, S., Salzmann, M., Schmidt, H., Bader, J., Block, K., Brokopf, R., Fast, I., Kinne, S., Kornblueh, L., Lohmann, U., Pincus, R., Reichler, T., and Roeckner, E. (2013). Atmospheric component of the MPI-M Earth System Model: ECHAM6. *Journal of Advances in Modeling Earth Systems*, 5(2):146–172.

Stewart, J., Toma, Y., Fernández, F. G., Nishiwaki, A., Yamada, T., and Bollero, G. (2009). The ecology and agronomy of *Miscanthus sinensis*, a species important to bioenergy crop development, in its native range in Japan: A review. *GCB Bioenergy*, 1(2):126–153.

Subak, S., Raskin, P., and Von Hippel, D. (1993). National greenhouse gas accounts: Current anthropogenic sources and sinks. *Climatic Change*, 25(1):15–58.

Talbot, M., Milner, A. D., Nutkins, M. A. E., and Law, J. R. (1995). Effect of interference between plots on yield performance in crop variety trials. *The Journal of Agricultural Science*, 124(3):335–342.

Thomas, C. D., Franco, A. M., and Hill, J. K. (2006). Range retractions and extinction in the face of climate warming. *Trends in Ecology & Evolution*, 21(8):415–416.

Thomson, A. M., Calvin, K. V., Smith, S. J., Kyle, G. P., Volke, A., Patel, P., Delgado-Arias, S., Bond-Lamberty, B., Wise, M. A., Clarke, L. E., and Edmonds, J. A. (2011). RCP4.5: A pathway for stabilization of radiative forcing by 2100. *Climatic Change*, 109(1):77–94.

Valles, G., Pacini, H., Sanches-Pereira, A., Durleva, M., Kane, M., and Bhutani, A. (2014). The state of the biofuels market. United Nations Conference on Trade and Development.

van Vliet, O. P., Faaij, A. P., and Turkenburg, W. C. (2009). Fischer-Tropsch diesel production in a well-to-wheel perspective: A carbon, energy flow and cost analysis. *Energy Conversion and Management*, 50(4):855 – 876.

van Vuuren, D. P., Edmonds, J., Kainuma, M., Riahi, K., Thomson, A., Hibbard, K., Hurtt, G. C., Kram, T., Krey, V., Lamarque, J.-F., et al. (2011a). The representative concentration pathways: an overview. *Climatic change*, 109:5–31.

van Vuuren, D. P., Stehfest, E., den Elzen, M. G. J., Kram, T., van Vliet, J., Deetman, S., Isaac, M., Klein Goldewijk, K., Hof, A., Mendoza Beltran, A., Oostenrijk, R., and van Ruijven, B. (2011b). RCP2.6: Exploring the possibility to keep global mean temperature increase below 2 °C. *Climatic Change*, 109(1):95–116.

Vanloocke, A., Bernacchi, C. J., and Twine, T. E. (2010). The impacts of *Miscanthus* × *giganteus* production on the Midwest US hydrologic cycle. *GCB Bioenergy*, 2(4):180–191.

Vautard, R., Cattiaux, J., Yiou, P., Thépaut, J.-N., and Ciais, P. (2010). Northern Hemisphere atmospheric stilling partly attributed to an increase in surface roughness. *Nature Geoscience*, 3(11):756–761.

Virgilio, N. D., Monti, A., and Venturi, G. (2007). Spatial variability of switchgrass (*Panicum virgatum* L.) yield as related to soil parameters in a small field. *Field Crops Research*, 101(2):232 – 239.

Yu, L., Ding, G., Huai, Z., and Zhao, H. (2013). Natural variation of biomass yield and nutrient dynamics in *Miscanthus*. *Field Crops Research*, 151:1–8.

Zub, H. W. and Brancourt-Hulmel, M. (2010). Agronomic and physiological performances of different species of *Miscanthus*, a major energy crop. A review. *Agronomy for Sustainable Development*, 30(2):201–214.

Acronyms and Symbols

A.3 Acronyms

AFR	Africa
AUS	Australia
AUT	Austria
AVEM	Avoided emissions
CAM	Central America
CH4	Methane
CHE	Switzerland
CISC	Change in sink capacity
CMIP	Coupled Model Intercomparison Project
CO2	Carbon dioxide
COP21	United Nations Climate Change Conference in 2015
DEU	Germany
DGVM	Dynamic Global Vegetation Model
DNK	Denmark
ECHAM6	Atmosphere component of MPI-ESM
Eff	Effectiveness
ESM	Earth System Model
ET	Evapo-transpiration
EU	European Union
EUR	Europe
FFS	Fossil-fuel substitution
FRA	France
FRST	Forests
GPP	Gross primary production
GRB	United Kingdom
HAMOCC5	Hamburg Ocean Carbon Cycle model
HBPs	Herbaceous biomass plantations
IMAGE2.2	Integrated Model to Assess the Global Environment
IRL	Ireland
ITA	Italy
JSBACH	Jena Scheme for Biosphere-Atmosphere Coupling in Hamburg
LAI	Leaf Area Index

LASC	Loss of additional sink capacity
LPJmL	Lund-Potsdam-Jena managed Land
MPI-ESM	Max-Planck-Institute Earth System Model
MPIOM	Max-Planck-Institute Ocean Model
NAM	North America
NAS	Norther Asia
NIR	Near infrared
NPP	Net primary production
OASIS	Coupler for the MPI-ESM model
PFT	Plant functional type
RCP	Representative Concentration Pathway
SAM	South America
SAS	South Asia
SRES	Special Report on Emissions Scenarios
SWE	Sweden
T	Transpiration
TUR	Turkey
USA	United States of America
VIS	Visible spectrum
WUE	Water use efficiency

A.4 Mathematical Symbols

A	Area (except transition scheme
C	Crops (transition scheme)
C	Carbon (except transition scheme)
$\tilde{c}$	Cover fraction modified by modified transition scheme
c_i	Initial cover fraction of cover type i
c_i'	Cover fraction of cover type i for the next day
F	Forests (transition scheme)
$F(t)$	Radiative forcing at timestep t
G	Grasses (transition scheme)
H	Herbaceous biomass plantations (transition scheme)
P	Pastures (transition scheme)
S	Scaling factor for transition scheme
T	Original transition matrix
$T_{i \to j}$	Transition element, fraction of area transferred from cover type i to cover type j
$\tilde{T}$	Modified transition matrix
Δ	Conversion fraction for transition scheme
$\gamma_{i,j}$	Scaling factor for the radiative forcing
λ	proportionality factor for transition scheme
ρ	Carbon density
ρ_{CO_2}	Concentration of CO_2

List of Figures

List of Tables

Acknowledgements

This thesis would never have succeeded without the tireless toils of many other people. I particularly thank my supervisors Julia Pongratz, Christian Reick and my panel chair Martin Claussen who have invested much time and effort to help me improve both personally and scientifically. I thank Daniela Kracher and Sebastian Sonntag for their help with the model and the science and for providing the data for the afforestation scenario I use as a baseline. I also thank my cooperation partners at the Potsdam Institute for Climate Impact Research, especially Vera Heck and Lena Boysen, for our valuable cooperation and for providing data from the LPJ model.
I would like to thank the directors of the Max Planck Institute for Meteorology and the Executive Committee of the International Max Planck Research School on Earth System Modelling (IMPRS-ESM) for thinking me worthy of joining the school.
Various scientific programmers have supported me and helped solve problems with the model, in particular, Julia Nabel, Thomas Raddatz, Veronika Gayler, Rainer Schnur and Helmuth Haak.
My sister, Veronika Tegetmeyer, provided the two figures in the introduction representing the carbon cycle and land-atmosphere interactions. My parents, Angelika and Matthias Mayer, provided me with numerous comments and suggestions. Both my parents and my sister and her family deserve special mention for their unconditional love and support throughout my PhD and my entire life.
I would also like to thank the many people who have helped me with administrative issues, particularly Antje Weitz, coordinator of the IMPRS-ESM, Wiebke Böhm, Cornelia Kampmann and Michaela Born at the IMPRS-ESM office, and Sylvia Houston, secretary in the land department.
A special thanks goes to the members of the Forest Management group at the Max Planck Institute for Meteorology for their warm welcome, patience and support. The entire land department of the Max Planck Institute for Meteorology deserves mention for their support as well as the cordial working atmosphere. Thank you also to all the members of IMPRS for all the fun and many parties.
This project was part of the Schwerpunktsprogramm (priority program) "Climate Engineering: Risks, Challenges, Opportunities?" funded by the Deutsche Forschungsgemeinschaft (German Research Foundation) and the Max Planck Institute for Meteorology.

Eidesstattliche Versicherung
Declaration on Oath

Hiermit erkläre ich an Eides statt, dass ich die vorliegende Dissertationsschrift selbst verfasst und keine anderen als die angegebenen Quellen und Hilfsmittel benutzt habe.

I hereby declare, on oath, that I have written the present dissertation by myself and have not used other than the acknowledged resources and aids.

Hamburg, den 6. September 2017

Dorothea Mayer